Cyprus University of Technology

Faculty of Engineering and Technology

Doctoral Dissertation

Mathematical and Bayesian Inference Strategies for Optimal Unit Commitment in Modern Power Systems

Pavlos Nikolaidis

Limassol, September 2019

CYPRUS UNIVERSITY OF TECHNOLOGY

FACULTY OF ENGINEERING AND TECHNOLOGY

DEPARTMENT ELECTRICAL ENGINEERING, COMPUTER ENGINEERING AND INFORMATICS

Doctoral Dissertation

Mathematical and Bayesian Inference Strategies for Optimal Unit Commitment in Modern Power Systems

Pavlos Nikolaidis

Limassol, September 2019

Approval Form

Doctoral Dissertation

Mathematical and Bayesian Inference Strategies for Optimal Unit Commitment in Modern Power Systems

Presented by

Pavlos Nikolaidis

Supervisor: Dr. Sotirios Chatzis, Assistant Professor

Signature _____

Member of the committee: Dr. Georgios Ellinas, Professor

Signature _____

Member of the committee: Dr. Anastasios Bakirtzis, Professor

Signature _____

Cyprus University of Technology

Limassol, September 2019

Copyrights

The approval of the dissertation by the Department of Electrical Engineering, Computer Engineering, and Informatics does not imply necessarily the approval by the Department of the views of the writer.

This thesis is dedicated to my family for their endless support and love and to the memory of my uncle who's no longer with us

Acknowledgements

First I would like to kindly thank my supervisor Dr. Sotirios Chatzis for his expert advice and encouragement throughout this project and for giving me the opportunity to work with him and trust me to be part of the Data Analytics and Statistical Inference Research Laboratory at the Cyprus University of Technology. I greatly appreciate Dr. Andreas Poullikkas from Cyprus Energy Regulatory Authority (CERA), for his guidelines, support and the opportunity to be involved in CERA's exciting research projects.

I would also like to thank all my colleagues and friends that I met and collaborated with during my PhD project starting with professors and students throughout the academic and administrative staff of the Department. I enjoyed a wonderful collaboration with you and I appreciate that you were always willing to help me all these years.

Finally, special thanks to my parents, Nikos and Chryso Nikolaidis and to my sister Elena Nikolaidou, for their endless support and love.

Abstract

Global efforts aiming to shift towards de-carbonization give rise to remarkable challenges for power systems and their operators. Modern power systems need to deal with the uncertain and volatile behavior of their components (especially, renewable energy generation); this necessitates the use of increased operating reserves. To ameliorate this expensive requirement, intelligent systems for determining appropriate unit commitment schedules have risen as a promising solution. This is especially the case for weak power systems with low dispatching flexibility and high dependency on imported fossil fuels.

With the fast-paced changing technologies in the context of sustainable development, new approaches and concepts are needed to cope with the variability and uncertainty affecting generation, transmission and load demand. The main challenge remains in developing technologies that can efficiently make use of the available renewable resources. Among them, electrical energy storage constitutes a potential candidate capable of regulating the power generation to match the loads via time-shifting. Optimally planned, such facilities can meet the increasing requirement of reserves to manage the variability and uncertainty of renewable energy sources whilst improving the system operation efficiency and economics.

In this thesis, we present a novel Lagrange Relaxation method with constraints, considering the impact of variable renewable energy sources. Our proposed approach successfully deals with identical generating units found in isolated power systems, enabling the realistic determination of the optimal electricity storage size based on actual data. In addition, we introduce a radically novel paradigm for addressing the optimal unit commitment problem, that is capable of accounting for the largely unaddressed challenge of the uncertain and volatile behavior of modern power systems. Our innovative solution leverages state-of-the-art developments in the field of uncertainty-aware machine learning models, namely Bayesian optimization. This framework enables the effective discovery of the best possible configuration of a volatile system with uncertain and unknown dynamics in the least possible number of trials, and without the need of introducing restrictive prior assumptions.

Developing a deep understanding of the different electricity storage principles and their applications, we develop an innovative model able to distinguish the power-related and energy-related cost components and integrate complex features such as the round-trip

efficiency, depth of discharge, self-discharge rate, etc. We evaluate the impact of intermittent renewable energy sources on total production cost, by making use of annual data regarding the isolated power system of the island of Cyprus. Once electrical energy storage is identified as an approach enhancing flexibility and reliability, we formulate and evaluate the selected facilities via a life-cycle cost analysis, based on the most realistic characteristics and cost metrics found in the literature. The derived simulation results showed that improvements exist in profitable return credits when storage was integrated.

Keywords: *renewable energy generation, weak power systems, electrical energy storage, machine learning models, Bayesian optimization, life-cycle cost analysis.*

Contents

LIST OF TABLES

LIST OF FIGURES

LIST OF ABBREVIATIONS

AA-CAES	Advanced adiabatic compressed-air energy storage
AF	Acquisition function
AFC	Alkaline fuel cell
ARD	Adaptive relevance determination
BO	Bayesian optimization
BOP	Balance of plant
BS	Black-start
CAES	Compressed-air energy storage
CHP	Co-generation of heat and power
CR	Contingency reserve
DoD	Depth of discharge
DP	Dynamic programming
EA	Energy arbitrage
EB	Emergency back-up
ED	Economic dispatch
EDLC	Electrochemical double-layer capacitor
EES	Electrical energy storage
EFC	Electrochemical flow capacitor
ENS	Energy not served
ESM	Energy storage medium
EV	Electric vehicles
FC	Fuel cell
FES	Flywheel energy storage
FHM	Forecast hedging mitigation
FR	Frequency regulation
FS	Fluctuation suppression
GA	Genetic algorithm
GHG	Greenhouse gas emissions
GP	Gaussian process
HFO	Heavy fuel oil
HTSC	High temperature superconducting coil
IPC	Initial project cost
LAES	Liquid-air energy storage
LCC	Life-cycle cost
LCOS	Levelized cost of storage
LF	Load following
Li-ion	Lithium-ion
LL	Load levelling
LTSC	Low temperature superconducting coil
LVRT	Low voltage ride-through

MCFC	Molten carbonate fuel cell
MG	Microgrid
NaNiCl	Sodium nickel chloride
Na-S	Sodium-sulfur
Ni-Cd	Nickel-cadmium
NiMH	Nickel-metal hydride
NPV	Net present value
O&M	Operation and maintenance
OD	Oscillation damping
PAFC	Phosphoric acid fuel cell
Pb-acid	Lead-acid
PCS	Power conversion system
PEMFC	Proton exchange membrane
PHES	Pumped-hydro energy storage
PHEV	Plug-in hybrid electric vehicles
PS	Peak shaving
PSB	Polysulfide bromide
PV	Photovoltaic
RBF	Radial basis function
RDG	Relative duality gap
Reg-FC	Regenerative fuel cell
RES	Renewable energy sources
RG	Renewable generation
RNS	Reserve not served
RS	Reactive support
SDR	Self-discharge rate
SLI	Starting, lighting and ignition
SMES	Superconducting magnetic energy storage
SOFC	Solid oxide fuel cell
SR	Spinning reserve
SS	Seasonal storage
SS-CAES	Small-scale compressed-air energy storage
T&D CR	Transmission and distribution congestion relief
TPC	Total production cost
TSO	Transmission system operator
UC	Unit commitment
UPS	Uninterruptible power supply
VR	Voltage regulation
VRB	Vanadium redox battery
VRES	Variable renewable energy sources
VRLA	Valve-regulated lead acid
Zn-air	Zinc-air
ZnBr	Zinc-bromine

NOMENCLATURE

Sets and Indices

$t \in \mathcal{T}$	Time intervals within the period of assessment $\mathcal{T}$
$i \in \mathcal{N}$	Conventional thermal generating units
$j \in \mathcal{J}$	Identical generating units within group *i*; $\mathcal{J} \subseteq \mathcal{N}$
$c \in \mathcal{C}$	Set of constraints
$x \in \mathcal{X}$	Finite set of input values
$D \in \{x, y\}$	Training data set
$s \in \mathcal{S}$	Electricity storage technologies
$k \in \mathcal{K}$	Electricity storage applications
$y \in \mathcal{L}$	Examined years in life cycle cost analysis
$m \in \mathcal{M}$	Fixed maintenance cost classes $\mathcal{M} = \{\text{Bulk}, \text{Distributed}, \text{Quality}\}$

Parameters

P_{load}^{t}	Load demand at interval *t* (MW)
P_{PV}^{t}	Photovoltaic power output at interval *t* (MW)
P_{wind}^{t}	Wind power output at interval *t* (MW)
$P_{Biomass}^{t}$	Biomass power output at interval *t* (MW)
$P_{i,min}$	Minimum power output of unit *i* (MW)
$P_{i,max}$	Maximum power output of unit *i* (MW)
ε	Power balance tolerance (MW)
$C_{SU\,i}^{t}$	Start-up cost of unit *i* for interval *t* (€/h)
$C_{SD\,i}^{t}$	Shut-down cost of unit *i* for interval *t* (€/h)
a_i, b_i, c_i	Positive fuel cost coefficients of unit *i* (€/MW^{2}h, €/MWh, €/h)
C_{fM_i}	Fixed maintenance cost of unit *i* (€/kW/year)
C_{BM_i}	Based maintenance cost of unit *i* (€/MWh)
C_{IM_i}	Incremental maintenance cost of unit *i* (€/h)
τ_i	Thermal time constant of unit *i* (h)
HSU_i	Hot start-up cost of unit *i* (€)
CSU_i	Cold start-up cost of unit *i* (€)
k_i	Incremental shut-down cost of unit *i* (€/h)
SR^t	Spinning reserve requirements for interval *t* (MW)
P_{loss}^{t}	Transmission losses during the interval *t* (MW)
P_{RES}^{t}	Renewable generation during the interval *t* (MW)
MU_i	Minimum up time of unit *i* (h)
MD_i	Minimum down time of unit *i* (h)
n_s	Round-trip efficiency of EES technology *s* (%)
h_s^k	Storage duration for application *k* (h)

h_d^k	Discharge time for application *k* (h)
C_{ESM}^s	Cost of energy storage medium of EES technology *s* (€/MWh)
C_{PCS}^s	Cost of power conversion system of EES technology *s* (€/MW)
C_{BOP}^s	Balance of plant cost of EES technology *s* (€/MW)
$C_{m,fO\&M}^s$	Fixed maintenance cost of technology *s* and class m (€/MW/year)
$C_{vO\&M}^s$	Variable maintenance cost of technology *s* (€/MWh)
i_R	Discount rate (%)

Variables

P_i^t	Power output of unit *i* for interval *t* (MW)
λ^t	Lagrange Multiplier at interval *t*
F_i^t	Production cost of unit *i* for interval *t* (€/h)
E_i^t	Emission cost of unit *i* for interval *t* (€/h)
$C_{M_i}^t$	Maintenance cost of unit *i* for interval *t* (€/h)
$C_{SU_i}^t$	Start-up cost of unit *i* for interval *t* (€/h)
$C_{SD_i}^t$	Shut-down cost of unit *i* for interval *t* (€/h)
$C_{M_i}^t$	Maintenance cost of unit *i* for interval *t* (€/h)
C_{ENS}^t	Cost of energy not served for interval *t* (€/h)
C_{RNS}^t	Cost of reserve not served for interval *t* (€/h)
U_i^t	Binary variable; equal to 0 (1) if unit *i* is off (on) during interval *t*
$C_{vM_i}^t$	Variable maintenance cost of unit *i* for interval *t* (€/MWh)
J^*	Total cost by relaxed λ values (€)
q^*	Total cost by corrected λ values (€)
η_i^t	Active unit number of each generating group *i* for interval *t*
f	Scalar cost value (€)
u	Expected improvement (€)
L_{ESM}^s	Durability life of ESM for technology *s* (y)
N_R^s	Number of ESM replacements for technology *s*
P_{rated}^*	Optimal rated power for the proposed EES facility (MW)
E_{cap}^*	Optimal energy capacity for the proposed EES facility (MWh)

LIST OF PUBLICATIONS

Journal papers

Nikolaidis, Pavlos, and Andreas Poullikkas. "A comparative overview of hydrogen production processes." *Renewable and sustainable energy reviews* 67 (2017): 597-611.

P. Nikolaidis and A. Poullikkas, “A comparative review of electrical energy storage systems for better sustainability,” *J. Power Technol.*, vol. 97, no. 3, pp. 220–245, 2017.

P. Nikolaidis and A. Poullikkas, “Cost metrics of electrical energy storage technologies in potential power system operations,” *Sustain. Energy Technol. Assessments*, vol. 25, no. August 2017, pp. 43–59, 2018.

P. Nikolaidis, S. Chatzis, and A. Poullikkas, “Renewable energy integration through optimal unit commitment and electricity storage in weak power networks,” *Int. J. Sustain. Energy*, vol. 37, no. 10, pp. 1–17, 2018.

P. Nikolaidis, S. Chatzis, and A. Poullikkas, “Life cycle cost analysis of electricity storage facilities in flexible power systems,” *Int. J. Sustain. Energy*, vol. 38, no. 8, pp. 752–772, 2019.

Nikolaidis, Pavlos, Sotirios Chatzis, and Andreas Poullikkas. "Optimal planning of electricity storage to minimize operating reserve requirements in an isolated island grid." Energy Systems (2019): 1-18.

(accepted on September 2019) P. Nikolaidis and S. P. Chatzis, “Gaussian Process-Based Bayesian Optimization for Data- Driven Unit Commitment,” *IEEE-Transactions Neural Networks Learn. Syst.*, 2019.

Conference papers

Naxakis, I., P. Nikolaidis, and E. Pyrgioti. "Performance of an installed lightning protection system in a photovoltaic park." *2016 IEEE International Conference on High Voltage Engineering and Application (ICHVE)*. IEEE, 2016.

Spanias C., P. Nikolaidis, and I. Lestas. "Techno-Economic Analysis of the Potential Conversion of the Outdated Moni Power Plant to a Large Scale Research Facility." *5th International Conference on Renewable Energy Sources & Energy Efficiency*. 2016.

(accepted on May 2019) Georgiou G., P. Nikolaidis, L. Lazari and P. Christodoulides. " A Genetic Algorithm Driven Linear Programming for Battery Optimal Scheduling in nearly Zero Energy Buildings." *2019 54th International Universities Power Engineering Conference (UPEC)*. IEEE, 2019.

Book chapters

Pavlos Nikolaidis and Andreas Poullikkas, “Secondary battery technologies: a static potential for power,” in *Energy Generation and Efficiency Technologies for Green Residential Buildings*, 2019, pp. 191–207.

1. Introduction and Motivation

The challenge for modern power generation systems is to meet the growing electricity demand, providing uninterruptible and high-quality supply. For several years now, this requirement is fulfilled mostly by using fossil fuels due to them being characterized by two critical advantages. First, their concentrated energy can be transported through various means (rail, road or pipelines) where is to be used, and remains stored as long as needed. The second characteristic has to do with the output of the traditional production methods which is easy to adjust according to the power requirements. However, the introduction of greenhouse gas emissions (GHG) into the atmosphere, due to the continuous burning of fossil fuels, poses a serious threat to the global environment and consequent climate change [1][2]. In addition, the growing energy demand has imposed the increase of conventional fuel prices which are declining, thus exposing national economies which are dependent on their import. To allow for ameliorating climate change over the long-term horizon, while reducing the dependence on the diminishing fossil fuel reserves, energy sources must meet the requirements of being emission-free and renewable in the forthcoming years [3][4][5].

On the contrary, renewable energy sources (RES) turn out to be inadequate for power generation due to their intermittent and unpredictable potential availability. Electricity demand varies seasonally and fluctuates during the day and as a result, the need to increase the share of RES and gradually replace conventional sources remains a formidable challenge. Even the conventional coal or nuclear plants cannot quickly change their power output and in order to co-operate with renewables, significant investment in fast-response gas turbine generation is needed. To deal with such a critical concern, the focus should be turned into alternative sources which increase the flexibility in modern power systems.

Because electric power is consumed the instant it is produced, generation is carefully timed so that it occurs at the same time it is demanded. Traditional storage usually occurs at the fuel level by storing water behind dams, natural gas in fields and pipelines, and in coal piles. Peaks and troughs in demand can be anticipated and satisfied by increasing or decreasing fuel injection at fairly short notice. Systems that can be scheduled and dispatched to contribute in generation are referred to as dispatchable; this is in contrast to renewables which are strictly correlated to imperfectly predictable and uncontrollable weather conditions. Load curves for a typical electricity grid are presented in Figure 1.

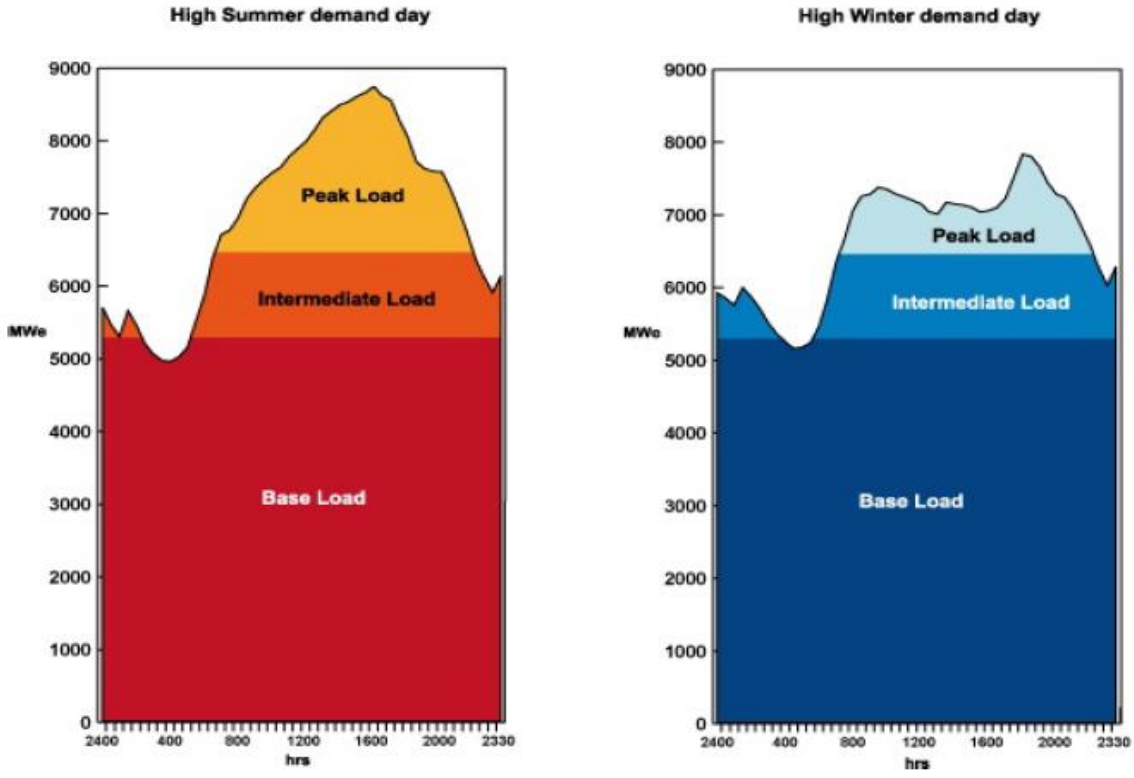

Figure 1: Load curves for typical electricity grid [6]**.**

The demand profile is usually steady and pretty known, following daily, weekly and seasonal patterns. Base load, which represents the amount of energy that is produced at any time, is typically covered by plants possessing long start-up times and relatively low operating and fuel costs (e.g. nuclear, hydroelectric, HFO). Easier to start-up and faster-producing power plants, such as coal, with moderate operating costs are employed for serving the intermediate load. Unexpected increases in electricity demand outside of the daily road-map are accommodated by using peak load plants such as gas turbines power plants which are able of providing faster response in the range of seconds to a few minutes [7].

With high levels of RES penetration in future power systems, there has been a growing need to evaluate their impact on power system operations. Rises in demand do not necessarily correspond to rises in RES generation. Technologies range from the traditional wind turbines, solar panels, hydroelectric, biomass and geothermal systems to emerging tidal

and wave generators, whose stochastic output is reflected to the residual load. Figure 2 illustrates a daily generation stems from wind and solar PV versus demand.

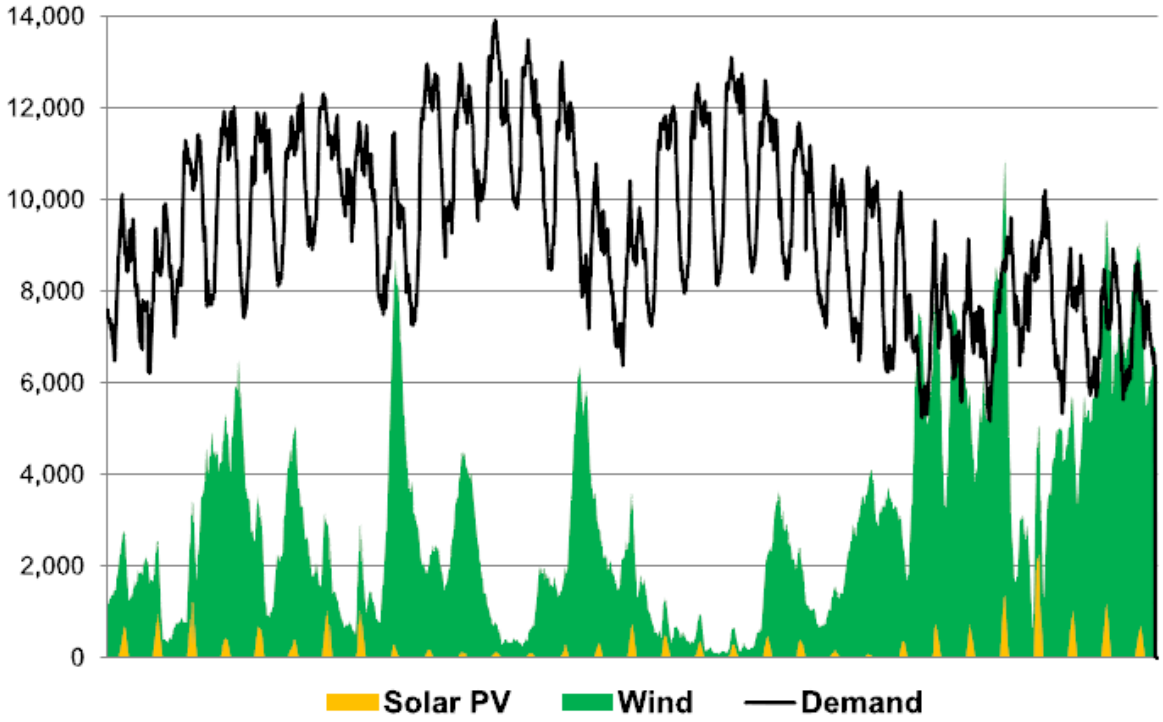

Figure 2: Monthly wind and solar PV generation versus demand [6]**.**

The net or residual load represents the demand that must be supplied by the conventional generation fleet if all the renewable electricity is to be introduced into power network. As a result, the residual load variations may fluctuate far more widely than the demand curve requiring increased flexibility from generation units. Conventional generators have many attributes that affect their relative contribution to meeting net load, the most important of which are:

- Minimum and maximum output ratings
- Capital, fuel, and operation and maintenance (O&M) costs
- Start-up and shut-down costs
- Ramp rate capability
- Minimum up and down times
- Energy conversion efficiency at different output levels (heat rate)
- Inertia or rotating mass

- GHG emissions

The precise balance between generation and demand must be guaranteed throughout the time for the frequency to be maintained within stability levels of 50 or 60Hz, depending on the country's standards. Power generators and auxiliary equipment are designed to operate within specific ratings and thus, deviations higher than ±10% of the nominal value may cause load shedding, a generator to trip or even a whole system collapse. Unit commitment (UC) is one of the key problems of generation scheduling. UC defines a method which determines which generating units to be committed during each interval of a short-term scheduling period of some hours, a day or a week, considering all attributes affecting their operation. The sub-problem which deals with the economic allocation of the total load among the committed generation units is called Economic Dispatch (EC). Further attributes constrained UC are spinning reserve, fuel reserve margins and transmission lines capacity and losses. The optimal UC problem is, thus, defined as the allocation of the power output to the generators to minimize the cost of operating all generators.

A typical hourly loading of units is realized in Figure 3. Based on the aforementioned principles, units 1 and 2 are assigned as base load generators, units 3-5 operate for intermediate load while unit 6 represents a gas turbine power plant intended for meeting the peak variations.

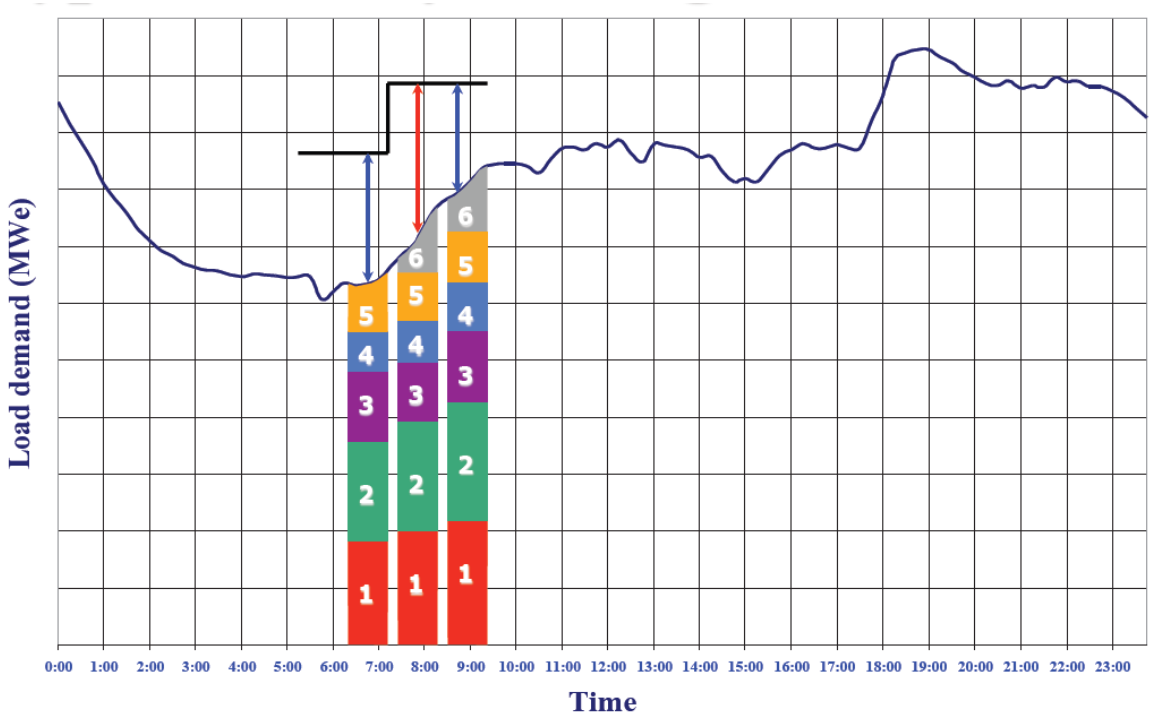

Figure 3: Typical hourly loading of units [6]**.**

Spinning reserve can be provided by operating and synchronized plants. It must be qualified throughout the period considering minimum up and down times, ramp rates and the maximum energy not served in case of a generator lost. For the online generation units, this fraction is estimated by the subtraction of the actual loading of each unit from the maximum-possible output capability. A further problem occurs when high renewable potential is available during low-demand/off-peak periods. The maximum share of RES fed to the grid is constrained by the minimum generation capacity of the conventional units being committed. As the penetration of variable RES increases, it is more than usual for utilities to over-schedule and keep the plants partially loaded, to avoid curtailment. This implies uneconomic dispatch due to increased start-up costs, operation at inefficient output and increases in capital and O&M costs.

Transmission system operators (TSOs) are responsible for ensuring system security and stability against the variability and uncertainty of both generation and demand, while maintaining a satisfactory level of reliability at a reasonable cost. Among the various sources able to provide such flexibility and optionality, a diverse range of electrical energy storage (EES) approaches is available. EES technologies find ready application in various sectors, attracting increasing interest for power grid operations that provide regulation, contingency and management reserves [8]. The term of storage refers to a wide variety of technologies and potential applications and hence, can be confusing as it occasionally acts as increased demand or generator [9][10].

Modern power systems could not exist without the many forms of electricity storage that can be integrated at different levels of the power chain. The value analysis of EES is therefore complicated by the fact that it can provide multiple benefits at one time such as arbitrage, balancing and reserve power sources, voltage and frequency control, investment deferral, cost management and load shaping and levelling. Global efforts aiming to shift towards intermittent renewable sources, reducing gaseous emissions and reliance on fossil fuels, force the whole energy system to dramatic changes. Large-scale RES connected to the grid, highly distributed variable generation, growing penetration of plug-in hybrid electric vehicles (PHEVs) and EVs, and requirements for demand response, constitute some of the most important, opening a wider field of applications which will certainly call for active participation of EES and provide additional value [11][12][13][14]. Of vital importance are also for micro grid (AC or DC) and smart grid systems which are expected to thrive in the

future, opening the pathway of a test environment for EES topology, model and device study [15].

1.1. Thesis Motivation

Since electricity is crucial to the development, progress and overall lifestyle in the global economy, improvements in both renewable and storage technologies are continuously needed for the grid to accommodate the ever-increasing variable sources. However, for increased penetrations, energy storage also for non-renewables may be essential for a transition to a sustainable energy production.

Although much research has been elaborated during the last decades on UC, revolutionizing the existing power system is operated, there has not yet been a comprehensive analysis considering the best strategies for EES integration, also evaluating their impact on future power systems. The majority of the literature has identified the utilization of EES as a source of flexibility and optionality, concentrating on either individual stationary applications or by distinguishing them into categories by scale, time of response or storage duration. None of these research works has considered to form an effective algorithmic suit for enabling the whole range of benefits potentially offered by EES (such as RES integration, emissions avoidance, power plants cost savings, asset deferral, etc.). This is the reason why the subject of this Ph.D. thesis forms an interesting problem for further research. Specifically, this thesis targets the exploration of both conventional mathematical optimization schemes, as well as bleeding-edge, data-driven inference approaches from the field of machine learning, and namely Bayesian optimization. Both these directions constitute an innovative paradigm which holds huge promise for revolutionizing the field.

In the following chapters, we provide some basic theory of Mathematical and Bayesian Optimization as well as the concepts for optimal UC. The different operational and technical constraints of power systems and their influence on the energy sector are also analyzed. Moreover, we present the general concept and idea of robust UC formulation in the presence of renewable generation and a discussion about different studies regarding the design and management of such problems, in terms of energy reliability and production-cost minimization. In addition, we introduce the principles of EES technologies along with the main requirements and conditions of their distinguished applications across the power chain.

Based on the most realistic technical data and cost metrics, we demonstrate our approach performed in a real-world scenario concerning an isolated power system. Finally, we present our findings derived from a life-cycle cost analysis.

1.2. Thesis Outline

This thesis is divided into two distinct research sections which are eventually combined to deliver a comprehensive solution to scientific community. The first consists of four chapters, (Chapters 2-5) with a focus on new methods for solving the constrained problem of unit commitment. The second research area is related to the technological development, application and overall performance of electricity storage systems participating in potential power system operations and contains two chapters, namely Chapter 6 and Chapter 7. Chapter 8 presents the combined solution proposed for a representative isolated power system where both research areas are modelled and explored in detail.

The contents for each of the remaining eight chapters are outlined as follows: **Chapter 2** provides the operating principles relating to electricity generation that will be presented in later chapters of this PhD thesis. All-important attributes are discussed along with their governing equations and theoretical background of each particular aspect. In **Chapter 3**, the introduction to the crucial problem of unit commitment is presented, as well as the most representative research work with valuable examples. Their advantages and disadvantages compared to their contribution as solution approaches to the problem are also summarized. **Chapter 4** presents our innovative work and first reported, regarding the double decomposition approach proposed for a solution to the unit commitment. The chapter concludes that both the performance and overall costs are greatly improved in power systems consisting of identical generating units. A first-ever data-driven for optimal unit commitment, namely Bayesian optimization, is introduced in **Chapter 5**. The experimental results show that Bayesian optimization based on Gaussian Process enables finding better optimal solutions with less computational costs.

The following chapters focus on the main characteristics of the state-of-the-art EES technologies, the requirements and preferences of their most realistic applications and different ways by which they can be modelled. **Chapter 6** deals with electricity storage technologies providing a comprehensive review and guide to the information extensively published in the literature. The most important technologies are discussed along with the

most realistic smart-grid applications found in modern power systems. The chapter provides all necessary metrics for a complete formulation and modelling of electricity storage facilities. **In Chapter 7**, we examine for the first time the decomposition of cost relating to different electricity storage systems to express the energy-related and power-related components. The latter are considered to be very crucial and are ranked on the basis of a novel multi-criteria decision method, which normalizes conventional criteria to account for the selection of the appropriate electrical energy storage system for a specific application. We finally assess the application of electricity storage to replace the deficit of spinning reserve in **Chapter 8**. As an internal optimization task, electrical storage is included in the algorithm developed for a real-world isolated and autonomous power system with high renewable energy contribution. Based on the most realistic characteristics and cost metrics found in the literature, the results showed that improvements (in terms of cost credits and maximum renewable energy penetration) exist through the optimal sizing and operation strategy of the storage medium.

The thesis concludes with **Chapter 9**; remarks regarding the work presented in this thesis are included. In addition, we elaborate on future trends and directions to facilitate forthcoming researchers to deal with our topics.

2. Power system optimization principles

Before we start to review and discuss the literature it is necessary to develop a deep understanding of the methodologies that are further mentioned in this dissertation. This chapter introduces techniques of power system optimisation. Specifically, topics to be addressed include power generation characteristics, economic dispatch and methods of solution, the unit commitment problem and optimization with constraints [16].

2.1. Power generation characteristics

Power systems are networks consisting of devices that generate, transmit and distribute electricity to consuming centers such as industry, commerce, households and so on. Power plants usually tend to be located at sites with access to water for cooling purposes and where noise and emissions are not disturbing issues. Once it is produced, electrical power is transported to the loads via electrical grids. Such grids consist of high voltage transmission lines and network coupling and voltage transformation substations. A simplified configuration of a power system is shown in Figure 4.

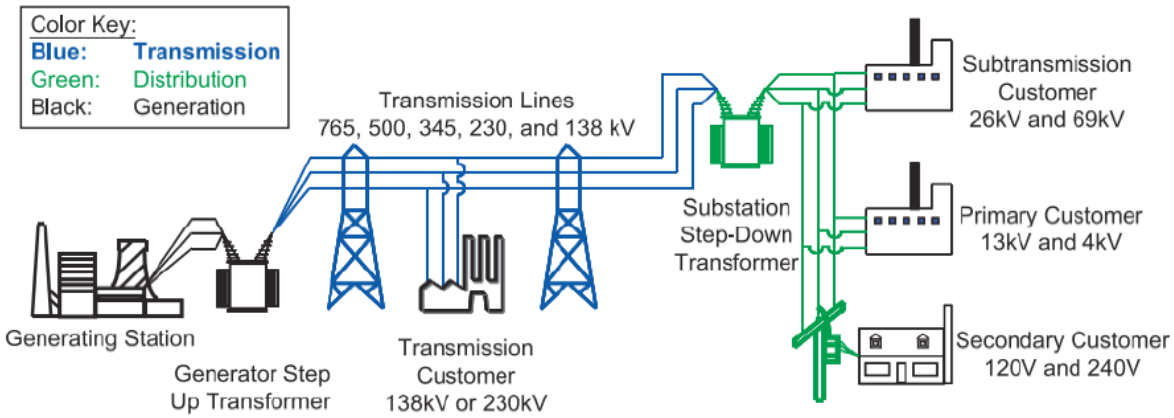

Figure 4: A simplified configuration of a power system [6]**.**

To reduce the energy losses over long distances, various transmission grid types exist, utilizing different voltage levels. The voltage generated is transformed into higher levels (110, 132, 138, 220, 345, 400, 500 or 750kV) via generator step-up transformers. Near urban

areas the medium voltage (between 1 and 100kV) is converted in transmission substations to carry the electrical energy to primary customers or to distribution transformers in order to be further decreased and supply secondary customers at low voltage in the range of 120-400V.

In contrast to radial low-voltage portion, the medium-voltage part of distribution networks usually has a weakly meshed network structure, though it is radially operated. This type of operation provides possibilities for network reconfiguration; consists in modifying the network topology by operating remotely controlled sectionalizing switches to close normally open and/or open normally closed lines, whilst retaining the radial operation of the network. Such reconfigurations can be done for different purposes, like to redirect the power flows or to improve other performance indices [17]. In the case of high voltage, the transmission networks are designed to form a ring in order to offer the above merits and qualify the N-1 criterion. In such cases, it is more than usual to consider a single-bus model for generation scheduling purposes.

The efficient and optimum economic operation and planning of electric power generation systems have always occupied an important position in the electric power industry. Fundamental to the economic operating problem is the set of input–output characteristics of a thermal power generation unit. The typical configuration of a boiler-turbine-generator unit sketched in Figure 5 reveals the terms of gross and net output.

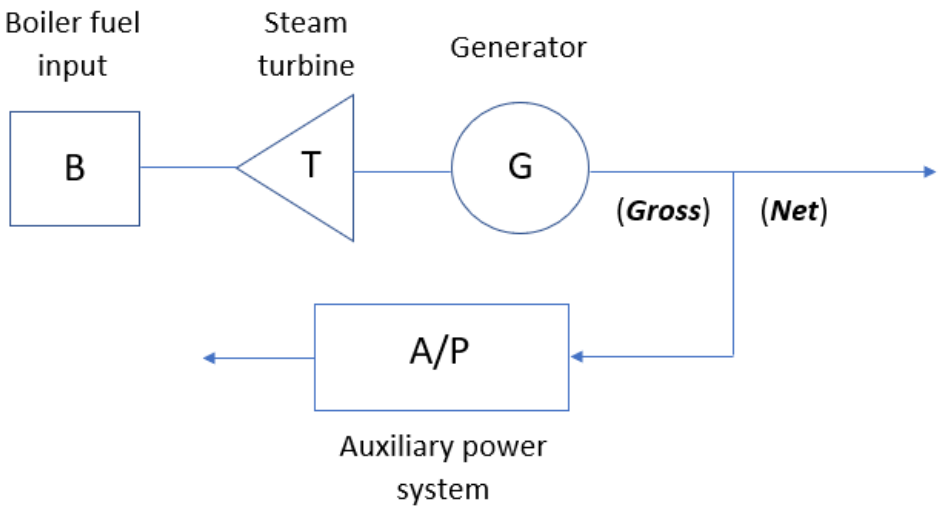

Figure 5: A typical configuration of a boiler-turbine-generator unit [16].

As can be observed, the electrical output of each chain set is connected not only to the electric power network, but also to the auxiliary power system which consumes a fraction of the gross output for the auxiliary requirements of boiler feed pumps, fans, condenser circulating water pumps, and so on. Gross input represents the heat (H) or cost (F) rate usually measured in million Btu per hour (MBtu/h) or dollars per hour ($/h) respectively, whereas the net output is the electrical power output available to the electric utility system (P) measured in MW. These data may be obtained from either design calculations or heat rate tests. Figure 6 shows the input-output characteristic of a generating unit.

Minimum load limitations are generally caused by fuel combustion stability and inherent design constraints. The data obtained, can be fitted by polynomial curves. A characteristic widely used in economic dispatching of a unit is the incremental heat or cost rate depending on the input. Heat rate function can be converted into the cost function (F) by multiplying it by the equivalent fuel cost (f_c) in terms of $/Btu. The slope (or derivative) of the resulting curve ($\Delta F/\Delta P$) will be then the incremental cost.

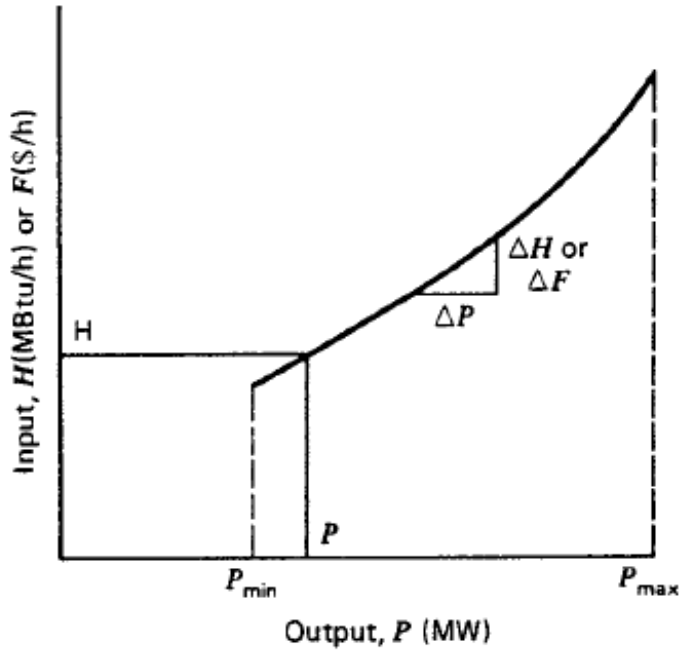

Figure 6: Input-output curve of a generating unit [16]**.**

The last important characteristic of a thermal unit is the unit net heat rate which is evaluated by dividing H with P. It is inversely proportional to efficiency and represents the heat input needed for a kilowatt-hour of output produced. The net heat rate of H/P versus P for a steam turbine generator is depicted in Figure 7.

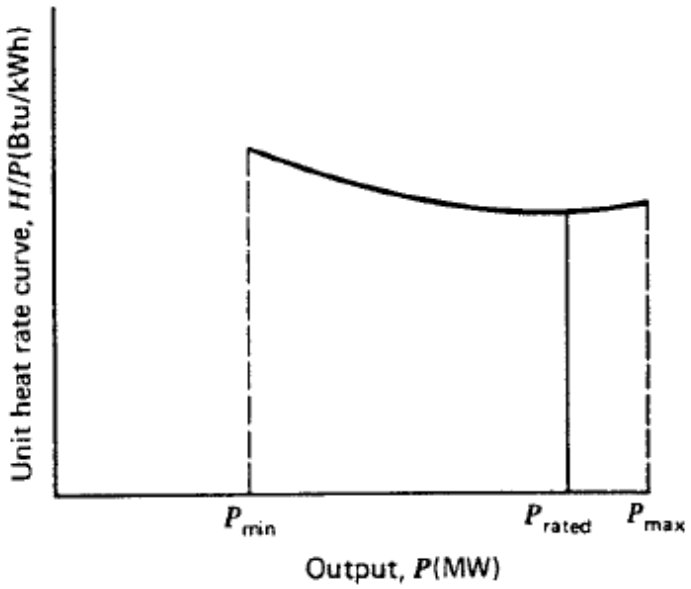

Figure 7: Net heat rate characteristic of a steam turbine generator unit [16]**.**

Generally, the strategies pursued in most power system optimization tasks require this model to function similarly for all types of thermal generating units. These include steam generators, gas turbines, combined cycle and internal combustion engines. Based on *Rankine Cycle*, a steam turbine consists of the following components: 1) The boiler where the combustion is realized by heating the water until it is steamed, 2) The turbine which is driven by the exhaust of the steam which is then liquefied, and 3) The condenser which leads the hot water to the boiler for reheating and vaporization. On the other hand, gas turbine is comprised by a burner where the combustion takes place and the exhaust gases are conducted to the turbine. After being exhausted driving the turbine, the super-heated gases are released into the atmosphere completing a *Brayton Cycle*.

Combined-cycle generating units differ in that they must take into account the heat-rate curves of both individual gas-turbines and the boiler, according to the operation mode (e.g. 1+1, 2+1, …, N+1). Such an arrangement can be realized based on the following Figure where a 4+4+1 configuration is illustrated. G/T refers to the gas turbine, HRSG is used to represent each individual heat-recovery steam generator whereas T defines the steam turbine of the plant. It is apparent that the plant efficiency characteristics depend on the number of G/Ts in operation.

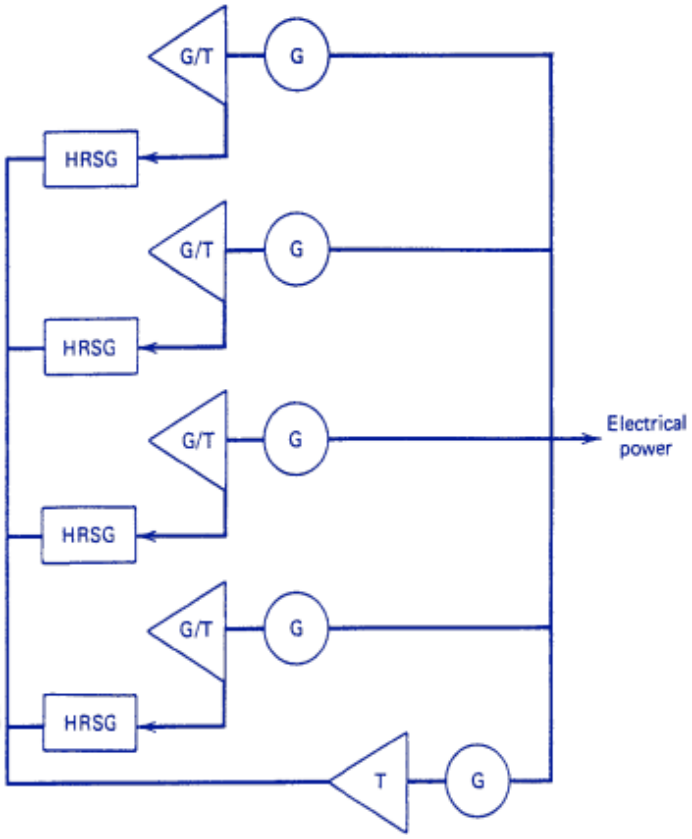

Figure 8: Combined cycle configuration [16]**.**

2.2. The Economic Dispatch problem

For a complete understanding of the economic dispatch problem formulation, a system of N thermal-generating units is assumed to be connected to a single bus serving a received electrical load P_{load} in MW. F_{i} represents the cost rate input to each unit in \$/h while P_{i} is the electrical power output generated by that particular unit in MW. The essential constraint on the operation of this system is that the sum of the power outputs must equal to the load demand. The problem is to minimize F_{T} subject to this constraint.

Objective function:

Minimize

$$F_T = F_1 + F_2 + \cdots + F_N = \sum_{i=1}^{N} F_i(P_i) \tag{2.1}$$

subject to

$$\Phi = 0 = P_{load} - \sum_{i=1}^{N} P_i \tag{2.2}$$

Adding the constraint function to the objective after multiplying the first by an undetermined multiplier λ, we obtain *Lagrange Function* shown in Equation 2.3.

$$\mathcal{L} = F_T + \lambda\Phi \tag{2.3}$$

By taking the first derivative of Equation 2.3 and setting the derivatives equal to 0 results in:

$$\frac{\partial \mathcal{L}}{\partial P_i} = \frac{dF_i(P_i)}{dP_i} - \lambda = 0 \tag{2.4}$$

Consequently, the necessary condition for the existence of a minimum cost of operation for the thermal power system is that all the unit incremental cost rates must be equal to the undetermined value λ.

2.2.1 Mathematical statements

To incorporate the thermal constraints of minimum and maximum power output of each generating unit, the following conditions must be qualified:

$$\begin{cases} \dfrac{dF_i}{dP_i} = \lambda & for \quad P_{i,min} \le P_i \le P_{i,max} \\ \dfrac{dF_i}{dP_i} \le \lambda & for \quad P_i = P_{i,max} \\ \dfrac{dF_i}{dP_i} \ge \lambda & for \quad P_i = P_{i,min} \end{cases} \tag{2.5}$$

Solving the Equation 2.4 subject to constraint of Equation 2.2, a value for Lagrange Multiplier λ is defined. The problem must be reformulated in case where one or more units are not within limits. The power output of these units is set to the maximum and minimum accordingly and new values of λ must be defined. This method follows a continuous procedure of finding new λ until the mathematical statements of Equation 2.5 are satisfied. The procedure becomes much less useable when there are many generators because of the need of finding the exact combination of units at upper and lower limits to get the final solution.

2.2.2 Lambda iteration method

Lambda iteration is another approach to accomplish the same objective as done with mathematical statements. It is based on the development of an analytical function for the power output as a function of the incremental cost rate which is stored and used to establish the output of each individual unit. The value of λ is adjusted up/down until the sum of the generator output meets the load to be supplied. In contrast to other constraint satisfaction problems where a stopping criterion could be the counting of iterations and stopping when a maximum number is exceeded, in the presence of coupled constraints the only appropriate rule is to find a proper operating point within a specified power balance tolerance, $|\varepsilon|$. A flow diagram explaining the concept of lambda iteration method is shown in Figure 9.

At the first iteration λ is arbitrarily set to a value. The power outputs are calculated and set according to their minimum and maximum operating limits. Then they are summed up and if the total power is too low λ must be increased whereas if the total power is too high λ must be decreased. This procedure converges very rapidly for this specific type of optimization problems and guarantees a global optimum when dealing with convex unit cost functions (marginal cost functions non-decreasing).

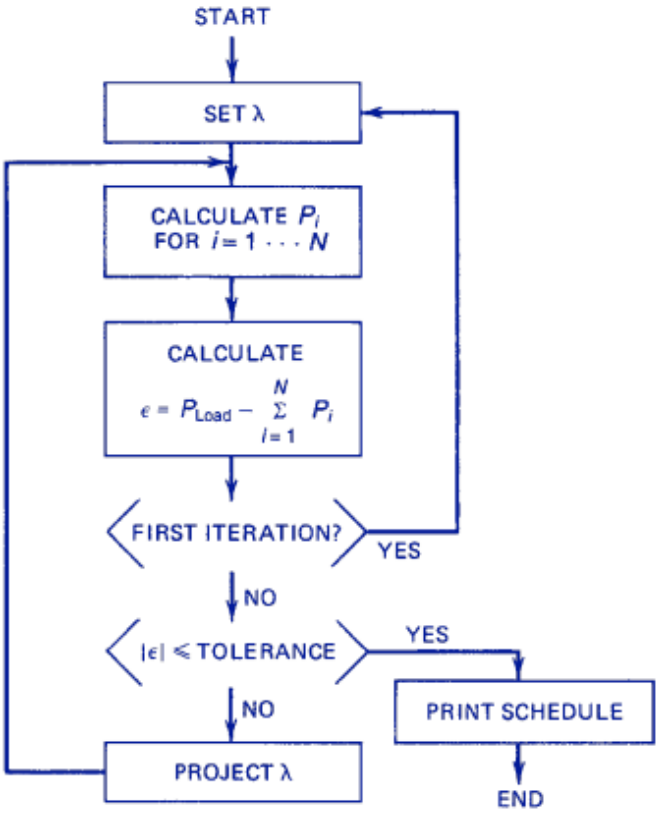

Figure 9: Economic dispatch by the lambda iteration method [16].

2.2.3 Binary search

This is another useful lambda iteration algorithm which avoids oscillations and always succeeds in finding the optimum economic dispatch. First, the incremental cost at the minimum and maximum output for each generator must be calculated. Next λ_{min} and λ_{max} are defined as follows:

$$\lambda_{\min} = \min\left(\lambda_{1,\min} + \lambda_{2,\min} + \cdots + \lambda_{N,\min}\right) \tag{2.6}$$

$$\lambda_{\max} = \max\left(\lambda_{1,\max} + \lambda_{2,\max} + \cdots + \lambda_{N,\max}\right) \tag{2.7}$$

The procedure starts with $\lambda = \lambda_{min}$ and continuous with binary search of λ values using Equations 2.8 and 2.9, and the statements formed below.

$$\Delta\lambda = \frac{\lambda_{max} - \lambda_{min}}{2} \tag{2.8}$$

$$\lambda_i = \lambda_{min} + \Delta\lambda \tag{2.9}$$

Table 1. Mathematical statements for the binary search method.

- If $\sum_{i=1}^{N} P_i > P_{load}$	lambda must be reduced:
	$\Delta\lambda = \frac{\Delta\lambda}{2}$ $\lambda_{i+1} = \lambda_i - \Delta\lambda$
- If $\sum_{i=1}^{N} P_i < P_{load}$	lambda must be increased:
	$\Delta\lambda = \frac{\Delta\lambda}{2}$ $\lambda_{i+1} = \lambda_i + \Delta\lambda$
- If $abs\left\{\sum_{i=1}^{N} P_i - P_{load}\right\} \leq$ tolerance	algorithm is converged.

Note that when the generator outputs are calculated for a specific λ value and diverged from limits, they are just set to their maximum or minimum value accordingly.

2.2.4 Dynamic programming

Equal incremental cost methodologies examined previously, cannot be used when non-convex input-output curves are to be used. The reason can be explained through the help of the following figure. As can be observed from Figure 10, there are multiple values of power output for any given value of incremental cost. Dynamic programming gives a solution to economic dispatch as an allocation problem, an approach that generates a set of outputs at discrete points for an entire range of load values rather than calculate a single optimum set of power outputs for a specific total load demanded.

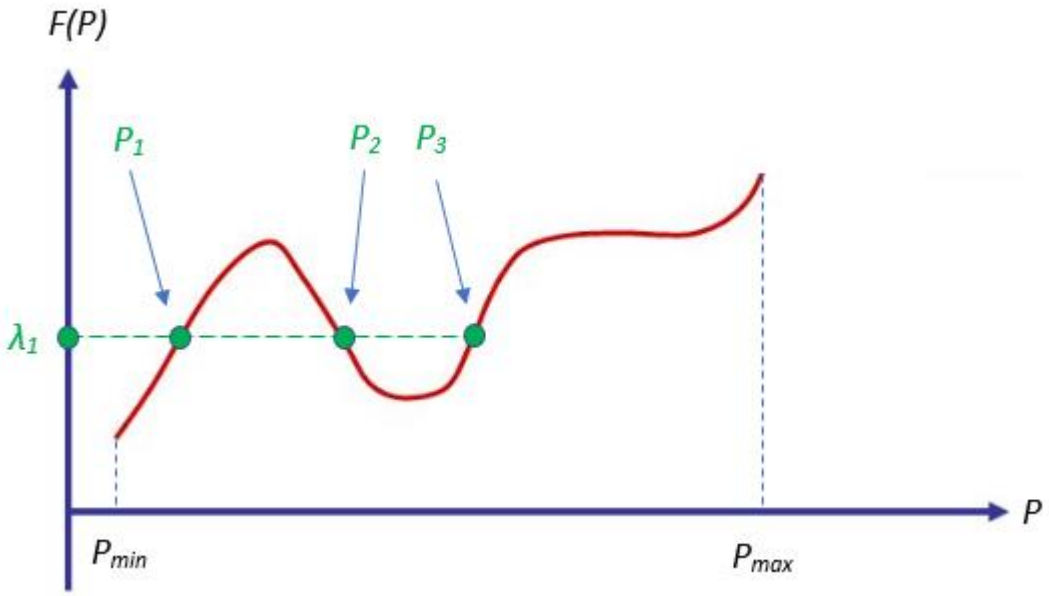

Figure 10: A typical example of a non-convex input-output curve [6]**.**

As can be observed from Figure 10, there are multiple values of power output for any given value of incremental cost. Dynamic programming gives a solution to economic dispatch as an allocation problem, an approach that generates a set of outputs at discrete points for an entire range of load values rather than calculate a single optimum set of power outputs for a specific total load demanded.

The procedure starts by scheduling the first two units. The objective is to minimize a new cost function developed (Equation 2.10) while moving from $P_{2,\,min}$ to $P_{2,\,max}$ with constant step.

$$f_2 = F_1(D - P_2) + F_2(P_2) \tag{2.10}$$

Variable *D* represents the load to be supplied by scheduled units and varies similarly in the same step (e.g. 25MW) with P_2. The cost for serving each value of *D* (minimum f_2) need to be saved along with *D* and power output of unit 2 (P_2) for each load level. The next step involves the minimization of a new cost function derived as follows:

$$f_3 = f_2(D - P_3) + F_3(P_3) \tag{2.11}$$

Similarly, the next unit is scheduled on-line and moving from $P_{3,\,min}$ to $P_{3,\,max}$ a new function is developed using the values of minimized f_2 stored before. The new data set (f_3, *D*, P_3) is saved and the process is repeated until the last unit is scheduled in supply. The final function to be minimized will be then:

$$f_N = F_{N-1}(D - P_N) + F_N(P_N) \tag{2.12}$$

2.2.5 Composite cost function

Composite cost function constitutes a useful approach in studying problems dealt with large numbers of generating units. The idea of grouping is quite important especially in power systems that consist of several generating units which are identical for security and maintenance purposes. Additionally, this technique facilitates power plants that developed to meet common needs such as the same type of loads (base, intermediate or peak load).

Scope of this method is to pre-allocate the supposed load to a single generator, in which the characteristics concerning all individual units that compose it, have been integrated, to form a composite cost curve. After the development of an analytical function for each generator as a function of the incremental cost rate, the total fuel consumption and total power output from all units are calculated based on the following equations.

$$P_S = P_1 + P_2 + \cdots + P_N \tag{2.13}$$

$$F_S(P_S) = F_1(P_1) + F_2(P_2) + \cdots + F_N(P_N) \tag{2.14}$$

The increment λ is adjusted from the specified λ_{min} to λ_{max} defined in Equations 2.6 and 2.7 respectively, and the power outputs are set according to the limits. The overall concept of composite generator unit is depicted in Figure 11.

Although the minimum cost is achieved for each load demand, the utilization of composite functions entails the loss of useful information about the individual units.

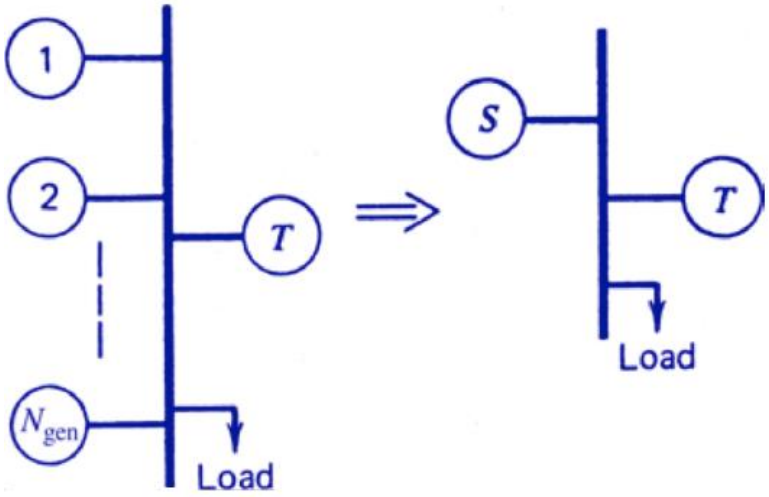

Figure 11: Composite generator unit [16]**.**

2.2.6 Base point and participation factors

Aiming to move the generators from one economically optimum schedule to another without running a completely new economic dispatch, this method assumes that each generator "participates" with a proportional fraction in reasonably small load changes. Base point represents the given optimum schedule of power outputs denoted as $P_{base\text{-}i}$. To examine the participation factors (the change in load) for each unit, let's refer to the incremental cost curve illustrated in Figure 12. A small change of ΔP_i in power output P_i implies a variation from λ to λ+Δλ which can be approached by the second derivative as follows:

$$\Delta\lambda_i \cong F_i'' \Delta P_i \tag{2.15}$$

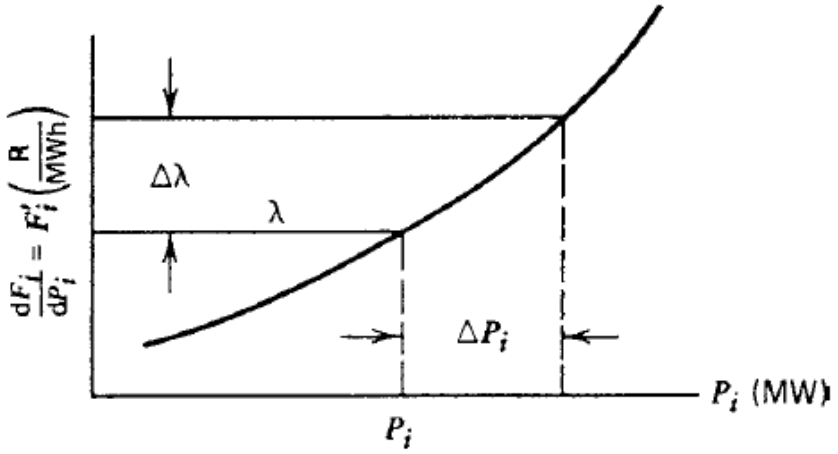

Figure 12: Incremental cost curve example [16]**.**

As a result, for a total change in generation of ΔP_D the participation factor for each generating unit can be found from Equation 2.17.

$$\Delta P_D = \Delta P_1 + \Delta P_2 + \cdots + \Delta P_N \tag{2.16}$$

$$\left(\frac{\Delta P_i}{\Delta P_D}\right) = \frac{(1/F_i'')}{\sum(F_i'')} \tag{2.17}$$

The new optimal schedule is given using Equation 2.18. This scheme is extremely useful in computer implementations where the execution time for the economic dispatch is short.

$$P_{new-i} = P_{base-i} + \left(\frac{\Delta P_i}{\Delta P_D}\right)\Delta P_D \tag{2.18}$$

2.3. The principles of Unit Commitment

Unit commitment is one of the key and high-priority problems of generation and production scheduling systems. It determines both the combination of available generating units to be committed and scheduling of their respective power output to meet the forecasted demand, dealing with the operating, transmission, fuel, security and environmental constraints during each interval of a short-term scheduling period (from 24h of a day to 168h of a week). In contrast to economic dispatch where it is assumed that all units are already connected to the system, unit commitment assumes that the generating units are available, and the appropriate

subsets must be selected in order to provide the minimum operating cost. UC is more difficult to solve mathematically since it involves integer variables (generating units being either on or off) constituting a more complex procedure which considers the ED as a subproblem to the solution.

Several solution methods have been proposed during the last decades and classified into heuristic and mathematical programming. Most methods have been improved and more recently, metaheuristic approaches have been widely used. However, to achieve a spherical view of UC decision problem the selected methods to be further investigated in this chapter regard priority-list schemes and dynamic programming. The rest of the methods adding value to the literature will be discussed in Chapter 3.3 of literature review.

2.3.1 Priority list

The simplest method consists of creating a priority list of units to determine which generators to first drop or start as a function of a system load with the load varying throughout the time. The need to obtain a start-up (or shutdown) rule is addressed by making use of incremental cost of each generating unit. This numeric value coincides at the point of minimum average cost, i.e. close to full load. As a result, it can be expressed based on the full-load average production cost. Once λ_i values are defined, the generators are put in an ascending order according to their incremental cost λ. By simply incorporating the upper and lower bounds of the generating units the priority list is developed as shown in the following Table:

Table 2. Typical formulation of the priority-list approach.

λ_i	λ_{i*}	$P_{i*,\,min}$	$P_{i*,\,max}$	Combination
λ_1	λ_{1*}	$P_{1*,\,min}$	$P_{1*,\,max}$	1
λ_2	λ_{2*}	$P_{1*,\,min}+ P_{2*,\,min}$	$P_{1*,\,max}+ P_{2*,\,max}$	1 + 2
.	.	$P_{1*,\,min}+ P_{2*,\,min}+ \ldots$	$P_{1*,\,max}+ P_{2*,\,max}+ \ldots$	1 + 2 + ...
λ_N	λ_{N*}	$P_{1*,\,min}+ P_{2*,\,min}+ \ldots+ P_{N*,\,min}$	$P_{1*,\,max}+ P_{2*,\,max}+ \ldots+ P_{N*,\,max}$	1 + 2 + ... + *N*

The values of λ-star correspond to the ascending units from the most economical to the worst (λ_{1*} is the smallest value and λ_{N*} is the largest value). As the load goes up within the limits listed in columns 3 and 4, the appropriated units will be committed or continue running whereas they will be de-committed when the load goes back down following the same order.

Although this scheme ignores the constraints of minimum up/down time, start-up cost, ramp rates and others, various enhancements can be made by grouping of units to ensure a reliable operation via dynamic programming.

2.3.2 Dynamic programming

The dynamic programming in general involves the search over several commitment states that must be tested in each time interval. For *N* available generators and *M* time-periods there are $(2^N\text{-}1)^M$ possible combinations. Although some of these combinations are rejected instantly because they are found infeasible, a large number of feasible states will always exist even for an average size utility. Hence, many hybrid methods have been proposed to give some sort of simplification.

As an example, priority-based dynamic programming, allows the units to be committed by priority considering the constraints of ramp-rates, minimum up/down times, start-up costs and so on. Decomposing the problem into sub-problems, the optimal solution is given recursively, step-by-step. A simplified diagram of dynamic programming steps for a single unit is shown in Figure 13.

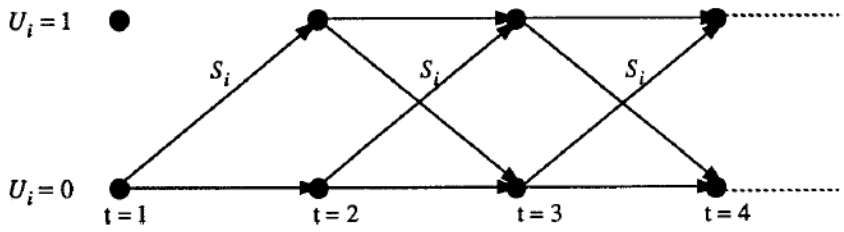

Figure 13: DP steps for a single unit [16]**.**

3. Literature on Unit Commitment

Day-ahead scheduling of electricity generation is a crucial and challenging optimization problem in current power systems. Variability and uncertainty in net load caused by increasing penetration of renewable generation (RG) have motivated the study of alternative approaches that increase flexibility without affecting the stable operation of conventional power plants [18].

The UC problem is a large-scale, complex, dynamic and restricted non-linear mathematical optimization problem with both integer and continuous variables. Load curve serves as an input data to the problem while the output is the commitment status and generation dispatch of various generating units satisfying system-wide and unit-specific constraints defined below [19]. Due to the non-convex nature of the UC objective, the exact solution can be obtained only by complete enumeration, leading research endeavours in search of efficient, near-optimal solutions with decreased computation time requirements [20].

3.1. Unit Commitment: Objective

Besides achieving minimum total production cost, the generation schedule must satisfy a large set of different technical and operational constraints. The total production cost (TPC) of a power system consisting of traditional thermal units is mainly the cost of fuel (C_F) [21][22], start-up (C_{SU}) and shut-down (C_{SD}) costs [23][24][25], maintenance cost (C_M) [26], emission cost (C_E) [27], and cost of energy not served (C_{ENS}) [28]. By denoting the number of generating units with N and the number of periods with T, a formulation for the UC problem is as follows:

$$\min \sum_{t=1}^{T} \{ \sum_{i=1}^{N} \{ \left[F_i\left(P_i^t\right) + E_i\left(P_i^t\right) + C_{M_i}^t + \left(1 - U_i^{t-1}\right) C_{SU_i}^t \right] U_i^t + \left(1 - U_i^t\right) C_{SD_i}^t U_i^{t-1} \} + C_{ENS}^t \} \quad (3.1)$$

The discrete variable U_i^t, determines the on-off states of generating units, taking the value "1" if the i^{th} unit is on-line at the particular time t or "0" if the unit is off-line according to Equation 3.2.

$$U_i^t \in \{1,0\} \quad (3.2)$$

The thermal fuel cost $F_i(P_i^t)$ depends on the production level of each unit and is expressed by a second order (quadratic) function as follows:

$$F_i(P_i^t) = a_i + b_i.P_i^t + c_i.(P_i^t)^2 \tag{3.3}$$

where, a_i, b_i and c_i are positive fuel cost coefficients derived from the processing of the specific fuel cost and heat rate curve of each generating unit [21][22]. The maintenance costs that do not change as a function of plant output are expressed via fixed costs (C_{fM}) per kW-month or kW-year unit, while the variable costs (C_{vM}) represent the maintenance costs that change as a function of energy output (measured per unit of MWh) [26]. The variable maintenance cost consists of two components, namely the base (C_{BM}) and incremental maintenance cost (C_{IM}), formulated by the next equation.

$$C_{vM_i}^t = C_{BM_i} + C_{IM_i}.P_i^t \tag{3.4}$$

The formulation of the start-up cost can be represented by Equation 3.5.

$$C_{SU_i}^t = \alpha_i + \beta_i.(1 - e^{-\frac{T}{\tau_i}}) \tag{3.5}$$

where α_i represents a fixed cost including crew and maintenance expenses, β_i is the equivalent cold-start cost, τ_i is the unit thermal time constant while T refers to the duration in hours the unit was cooled. The start-up cost is warmth-dependent, corresponding to the hot, warm or cold condition of each generating unit, defined by the time that the unit has been off-loaded until start up [23]. Consequently, it can vary from a small value if the unit was only turned off recently to a maximum "cold-start" value.

$$C_{SU_i}^t = \begin{cases} HSU_i & ,if\ MD_i \le T_i \le MD_i + t_{i,cold} \\ CSU_i & ,if\ T_i > MD_i + t_{i,cold} \end{cases} \tag{3.6}$$

where $t_{i,cold}$ is the cold start time of the *ith* unit and MD_i is the minimum down time of the *ith* unit which is explained below.

On the contrary, the shut-down cost is usually a constant or at least time-independent value for each thermal unit, and thus it is usually considered 0 for all generating units and

excluded from the objective function. Otherwise, it could be described as a function of power output by Equation 3.7 (where k_i is the incremental shut-down cost).

$$C_{SD_i}^{\ t} = k_i . P_i^t \tag{3.7}$$

In addition, since the conventional thermal units assumed for generation are coal-fired, a quadratic function can be considered for the emission curve as follows:

$$E_i(P_i^t) = \alpha_{ci} + \beta_{ci} . P_i^t + \gamma_{ci} . (P_i^t)^2 \tag{3.8}$$

where α_{ci}, β_{ci} and γ_{ci} are the CO_2 emission coefficients of unit i processed to define the emission cost $E_i(P_i^t)$. Since these coefficients may contradict with the fuel cost coefficients, in problems where they appear together their objectives are typically weighted such that:

$$\min \sum_{t=1}^{T} \sum_{i=1}^{N} \left[w_F F_i\left(P_i^t\right) + w_E E_i\left(P_i^t\right) \right] \tag{3.9}$$

subject to

$$w_F + w_E = 1 \tag{3.10}$$

In this case, the optimization task is able to treat dependent objectives as independent scalar values which are normalized in each class to add up to 1. Finally, the energy not served parameter consists of two cost components. From the reliability perspective, the first component has to do with the unbalance between production and demand. From the security perspective, a second component is defined to penalize for the reserve not served. The mentioned components are represented by Equations (3.11) and (3.12) respectively.

$$C_{ENS}^t = c_{ens} \left\{ P_{load}^t - \sum_{i=1}^{N} P_i^t \right\} \tag{3.11}$$

$$C_{RNS}^t = c_{rns} \left\{ SR^t - \left[\sum_{i=1}^{N} P_{i,max}^t - P_{load}^t \right] \right\} \tag{3.12}$$

Where $P^t_{i,max}$ denotes the maximum possible output of each generator being synchronized, P^t_{load} is the load demand to be satisfied and SR^t constitutes the spinning reserve requirements for system security purposes. (Note that: the component that must be considered less by the

objective function is weighted with a greater w_x, whereas a more preferable component is multiplied by a smaller weight).

3.2. Unit Commitment: Constraints

The constraints that must be satisfied throughout the optimization process of the UC problem are:

1. System power balance. Considering the contribution of renewable generation (P^t_{RES}) normally treated as negative load, the sum of the power produced from all committed units must meet the net load demand (P^t_{netD}) along with transmission loss (P^t_{loss}) at each time-interval.

$$\sum_{i=1}^{N} P_i^t = P_{netD}^t + P_{loss}^t \tag{3.13}$$

$$P_{netD}^t = P_D^t - P_{RES}^t \tag{3.14}$$

Transmission loss depends on line parameters, bus voltages and power flow, requiring complex computations to be determined [29]. To consider the shape and characteristics of the transmission network, three levels of approximation do exist. The single bus model entirely disregards the network aspects, considering the demand satisfied as soon as the total production is approximately equal to the total consumption. Using a simplified version of Kirchhoff law, the DC model takes into account the network structure including the capacity of transmission links, whereas highly nonlinear and nonconvex constraints stem from the full version of Kirchhoff law used in AC models [29].

2. Spinning reserve. The power margins must be guaranteed based on the maximum ramping capacity ($P^t_{i,max\text{-}cap}$) of each unit rather than the maximum operating limit ($P^t_{i,max}$).

$$\sum_{i=1}^{N} P_{i,\max\_cap}^t \geq P_{netD}^t + SR^t \tag{3.15}$$

3. Generator capacity limits. The maximal and minimal rated power that force the generating units to operate within their boundaries.

$$P_{i,\min}^{t}.U_i^t \le P_i^t \le P_{i,\max}^{t}.U_i^t \tag{3.16}$$

4. Minimum up (MU_i) and down times (MD_i). The predefined minimum amount of time needed before a generator can change its status. If t_u and t_d represent the time a unit has started-up or shut-down respectively, then it can change its status satisfying the following conditions.

$$U_i^t = 0 \rightarrow 1 \quad if \quad \sum_{t=td}^{t-1} U_i^t \ge MD_i \tag{3.17}$$

$$U_i^t = 1 \rightarrow 0 \quad if \quad \sum_{t=tu}^{t-1} U_i^t \ge MU_i \tag{3.18}$$

5. Ramp up/down rates. For each generating unit, the change of its power output between adjacent hours is restricted by the ramp-up (RU_i) and ramp-down (RD_i) rates according to Equations (14) and (15) respectively [30].

$$P_i^t - P_i^{t-1} \le RU_i, \quad if\ generation\ increases \tag{3.19}$$

$$P_i^{t-1} - P_i^t \le RD_i, \quad if\ generation\ decreases \tag{3.20}$$

6. Unit status restrictions. Three possible states can be observed in this category, namely the must-run, must-out and run at fixed-MW output units. Must-run units are committed online during certain interval of operation on the basis of operating reliability and/or economic considerations. Must-out characterizes the units which are unavailable for commitment, subjected to forced outages, maintenance or other unforeseen problems [22]. Finally, some units may be subject to technical or other constraints (e.g. limited fuel), that require them to operate at a specified, fixed power output.

$$\forall t \in \mathcal{T} \begin{cases} U_j^t = 1 \ \ , if\ j^{th}\ unit\ must\ run \\ U_j^t = 0 \ \ , if\ j^{th}\ unit\ must\ out \\ P_j^t = \begin{cases} 0 & if\ U_j^t = 0 \\ P_{j,const.} & if\ U_j^t = 1 \end{cases} , if\ j^{th}\ unit\ must\ run\ at\ fixed - MW \end{cases} \tag{3.21}$$

7. Initial unit states. At the beginning of the scheduling period, the initial unit conditions must be properly considered. These may include the on-off status of each generator unit, the real-valued power output, the time duration from the last up or down and so on. Otherwise, the optimization procedure may lead to wrong decisions regarding the on-off status of the generating units. This constitutes a usual phenomenon especially observed at the beginning of a forward-programming approach which typically forces the units with the lowest start-up cost to get on-line. Once the load demand during the first time-slot is quite low (e.g. at 00:00), the power output of each proposed to be committed unit is proportionally low enough such that its start-up cost (SU_i) to be comparable with its operating cost ($F(P_i)$). In some cases, the parameters of MU and MD are set to negative integer values to prevent such units from getting online.

8. Plant crew constraints. Apart from the minimum up and down times needed, crew size (number of operators available) is another feature restricting the actions to be performed in a specific plant. Crew constraints pertain the number of units that can simultaneously start-up or shut-down [21]. A further constraint pertaining the simultaneous start-up of multiple generators is the maximum steam generation which is strictly dependent on the maximum ratings of water feed-pumps supplying the boilers.

9. Transmission constraints. The thermal rate and contingency limitations affect the maximum transmission capacity of individual transmission tie lines connecting power plants situated at different places and consumers [30].

3.3. Unit Commitment: Related work

In recent years, extensive research is made around the concept of optimal UC exploring the efficacy of deterministic and stochastic programming. In this chapter, the scientific work related to the problem stated for this Ph.D. thesis is presented. Some recent approaches are discussed, and some comparisons are made regarding their performance and weaknesses.

The UC problem has commonly been formulated as a non-convex, nonlinear and mixed-integer optimization problem with constraints. In [31], a detailed explanation and comparison of the methods broadly used is presented. A more realistic view of the wide range of UC techniques is provided in [32], where the methods are classified into heuristic, mathematical and meta-heuristic, while an introduction to hybrid approaches is also included. The selected examples are representative in relation to the year they were published, illustrating the progress around the UC optimization task and the embedded constraints imposed by the continuous evolution of power systems.

Tao Li and Mohammad Shahidehpour [33], provided a price-based UC via Lagrangian Relaxation and Mixed Integer Programming. The contribution of combined-cycle units was considered for the first time along with 54 thermal units and cascaded-hydro plants. Although a globally optimal solution was guaranteed at reasonable computational time and memory requirement, the constraints incorporated were limited to thermal and load balance, and no transmission constraints were taken into account. In [34], the transmission constraints are included and addressed together with the constraints relating to co-generation of heat and power (CHP) plants. The scheduling and planning coordination are addressed via a dynamic programming-based algorithm with the assumption that large-scale RES are used to satisfy heat demand. Therefore, heat, power and demand must be considered simultaneously, and thus more sophisticated methods must be developed.

Aiming to offer the flexibility needed in the presence of variable energy sources, the authors in [35] proposed to control the demand by electric water heaters incorporating a physically based aggregate model of the population in the day-ahead UC. Peak load shifting in municipal utilities has been achieved through a large controllable temperature range. The related work may be extended to consider other electric loads with energy storage such as electric vehicles, space heating and cooling loads. The approach in [35] considered no uncertainty and variability of RES participation. A similar work found in [36], proposes a daily UC that utilizes interruptible load to deal with the increased uncertainty due to wind power. Both load and wind are treated as uncertainty sources and are assumed to follow normal distribution and the UC problem is effectively solved by the adoption of a hybrid Lagrange Relaxation-Dynamic Programming algorithm. The interruptible load is not considered in the objective function and thus, if a lack of spinning reserve occurs, the reliability of the system may be at risk.

Ilia G. Marneris et al. [37], introduce the terms of deterministic and stochastic unit commitment, with focus on the determination, allocation and deployment of reserves. The UC model formulated constitutes a Mixed Integer Linear Programming approach and is divided into two stages. The first stage involves the day-ahead scheduling (hourly deterministic unit commitment) and the second is based on real-time dispatch and UC which addresses the intra-hourly forecast errors (uncertainty) and system ramping requirements (variability). Although several constraints have been included (start-up and –down costs, load shedding and wind spillage cost, ramp rates along with the minimum up/down times) the transmission network constraints are neglected. Once the proposed approach deals with real-time estimates, the development of decomposition techniques is essential to help reducing the execution times of UC solution.

A new co-evolutionary paradigm of multi-agent systems is presented in [27]. The uncertainties of load, solar and wind power are taken into account and assumed subject to the normal distribution. A 10-unit system with standard input data of power plants, emission coefficients and load demand, considering plug-in hybrid electric vehicles (PHEVs), wind and solar, is tested by adaptive decomposition and compared with Genetic Algorithm and Lagrangian Relaxation. According to the results, the operational cost and emission under the proposed cooperative co-evolution algorithm are the lowest. However, the investigation assumes that PHEVs utilize the maximum amount of RES. In this work neither the EES devices used in vehicles nor their main attributes (such as cycle efficiency, depth of discharge, self-discharge rate, etc.) are mentioned.

In a similar work [38], the researchers proposed a new computational framework to integrate the scenario based on renewable generation and flexible charging and discharging of plug-in electric vehicles (PEV). A new multi-zone sampling approach was proposed to generate scenarios of intermittent renewable generation and the problem was solved through a hybrid topology of combined particle swarm optimization, self-adaptive differential evolution and lambda iteration method. According to the results, the charging/discharging scenario of PEVs has shown to be capable of significantly reducing the total and average power cost comparing with no PEVs or PEVs charging only case. Nevertheless, the information regarding the kind of EES technology used in vehicles was not included.

Among the state-of-the-art approaches for solving constrained, NP-hard optimization problems are also Genetic Algorithms (GAs). A solution to the UC problem via GA is

proposed in [39]. Relying on natural selection processes that imitates biological evolution, GA produces a population of points and recommends the best point as an optimal solution to the next iteration. In contrast to classical algorithms which generate a single point at each iteration and select the next point based on deterministic computation, GA repeatedly modifies a population of solutions to progressively lead to an optimal solution using random number generators. Hence, it constitutes a heuristic technique for optimization capable of minimizing the burden of computational time as well as the number of function evaluations needed.

The main steps comprising the optimization process include the initial population generation, its evaluation, selection of the best candidate, crossover and mutation. This procedure is repeated until convergence. The general criterion for convergence is 'a no change in the solution for *n* generations' [40]. Thus, the exploitation of best solutions via the exploration of new regions guarantees a large search space which heuristically provides a high-quality solution. Although GA allows for the constraints to be easily integrated, the randomness with which the transitions are made add concerns about the quality of solution. In addition, according to the type of random number generators used, these algorithms may converge to different values at the end of each optimization season.

Finally, a very recent work found in [41], studies the unit commitment problem considering pumped storage and renewable energy via a novel heuristic algorithm called the Binary Artificial Sheep Algorithm (BASA). The proposed BASA performs better than traditional metaheuristics in solving UC and the results demonstrate that the equivalent increase in load fluctuation and operating costs of thermal units, due to increased RES forecast error, can effectively be counterbalanced by the deployment of pumped-hydro energy storage. Although several scenarios of forecast error levels in combination with different system constraints are investigated, EES is not properly addressed. It is well-known that PHES requires special site conditions the most essential of which are the availability of technically suitable locations with access to water. Thus, it cannot be considered as a viable option able to deal with the flexibility needed in modern power systems. Moreover, other special features regarding the storage losses are missing from the simulation. Finally, for the optimal EES size to be determined, larger representative periods are needed (e.g., yearly simulation).

Recent expansion of intermittent RG and price-responsive demand participation posed new challenges to the UC formulation and solution, and hence the application of stochastic programming has been widely reported. The various approaches broadly used can be divided into mathematical, heuristic, meta-heuristic and hybrid. Ranging from classical mathematical to hybrid meta-heuristic, the most important methods are categorized as: Dynamic Programming, Priority List, Lagrangian Relaxation, Mixed-Integer Linear Programming, Quadratic Programming, Stochastic Programming, Branch-and-Bound, Simulated Annealing, Genetic Algorithm, Tabu Search, Ant Colony, Particle Swarm Optimization, Fuzzy Logic, Artificial Neural Network, Decision Tree and other hybrid techniques [41][42]. Despite numerous research efforts to improve the UC process, a perfect method guaranteeing a global optimum has not existed yet.

In general, heuristic methods are non-rigorous, empirical methods that make UC decisions based on pre-calculated priority list and incorporate the operating constraints heuristically. Although they are flexible (allowing practical operating constraints to be integrated) and require moderate computational memory and running time, the optimal solution cannot be guaranteed especially in large-scale power systems where even the magnitude of their sub-optimality cannot be estimated. Aiming to employ more rigorous methods generating more economical solutions, meta-heuristic approaches have been proposed in the expense of large computational efforts requirement. Both categories require great experience relating to the whole power system´s behaviour for their confident design and implementation. However, they include randomness and use stochastic approach in moving from one solution to another, compared to mathematical techniques which follow deterministic transition rules.

3.4. Unit Commitment: Open challenges

As presented in the previous chapter, lot of research has been performed on the problem of minimizing the costs associated with electricity production, whilst increasing the contribution of variable RES. Most works are focused on alternative approaches to enhance the penetration of RES through mathematical optimization or rule-based algorithms. Such techniques showed that different appliances can be scheduled in different times and the load

can be shifted with the aid of storage, based on both the renewable generation and load demand profiles.

Despite these advances, the vast majority of the existing approaches rely on heuristic or rules-based systems, which suffer from glaring drawbacks, as outlined in the previous chapters. Most importantly, their limited scalability to large systems, their unacceptable reliance on heuristic thresholds, which are both close to impossible to correctly determine and of limited generalization value, and their reliance on strong and hard to update assumptions, undermine their effectiveness in anything more serious than simplistic simulation environments.

Mathematical optimization constitutes a more promising approach allowing the constraints to easily be added. Priority-list schemes are fast and rely on committing generation-units based on the order of increasing operating cost. Dynamic programming suffers from the curse of dimensionality calling for some simplification techniques and opening a special field of hybridization. Due to its ability to overcome the difficulty of non-convexity and non-linearity of large-scale systems, a global optimum (if any exists) can be achieved. Lagrangian relaxation can be easily modified to model characteristics of specific utilities. It is capable of incorporating unit constraints separately and coupling constraints by just defining a respective Lagrangian multiplier which is adjoined into the objective function of the relaxed problem. Although it may be the most attractive for large systems, only a near optimal feasible solution can be expected. Another weakness regards the sensitivity problem which may cause unnecessary commitments of some units.

However, the lack of a single model able to, simultaneously, minimize the production cost based on fossil fuel prices and the energy grid congestion, maximize the share of RES, the overall efficiency and reliability, remains a challenge. Consequently, one major priority of this thesis concentrates on devising a mathematical optimization technique able to achieve the above-mentioned targets using actual or forecasted generation inputs from variable RES and responsive load demand.

This research direction is both novel and with the potential of reaping important benefits for future power systems, while utilizing a paradigm of proven feasibility, namely mathematical optimization. However, it is also the case that this conventional paradigm suffers from a set of limitations; these include: 1) They require that the practitioners postulate specific assumptions regarding the functional form of the initial unit states, the predefined

power output for the committed plants and the priority-based order of starting-ups. Apparently, under such a paradigm, the effectiveness of the optimization method unacceptably relies heavily on the quality of these assumptions. 2) They are well-known for their proneness to get trapped into poor local optima, also depending on the adopted initialization strategy. This renders coming up with a good initialization strategy a major burden to the practitioners.

Based on this motivation, this thesis also considers an alternative, ground-breaking research direction that may open new research avenues in the field. Specifically, we explore whether the bleeding-edge advances in data-driven inference and machine learning can be exploited so as to attack the shortcomings of currently used mathematical optimization paradigms. We posit that appropriate exploitation of carefully selected and crafted inference techniques may represent the needed innovative component for achieving a leap-forward in the performance of UC in the power systems of the future.

Our considered solution relies on the framework of Bayesian optimization (BO) [43]. This is a machine learning-driven optimization paradigm that uniquely allows to obviate the need of simulating the stochastic behavior of UC components, especially renewable generation (RG) systems, by relying on coarse, heuristic, and therefore approximate assumptions of the underlying distributions. This way, it holds huge promise in the effort of generating reliable estimates of the magnitude of their expected variation; this is achieved by using a data-driven Bayesian regression technique that allows for uncertainty-aware prediction, namely Gaussian processes (GPs) [44]. Crucially, BO uses the GP-derived uncertainty estimates to guide an indicate iterative optimization process, which aims at obtaining the globally optimal UC setup in the least possible number of iterations (trials). We elaborate on the main principles of BO in Chapter 4.

Finally, it is our strong belief that for our research to be completed, a methodology is needed for evaluating and comparing EES technologies with different cost structures in potential grid applications, distinguishing their power-related and capacity-related costs. Aiming to apply the same evaluation method to all cases, we seek for an algorithm which incorporates the initial project cost, storage replacement cost, fixed and variable O&M costs over the life of an EES facility. Once the costs of the subsystems comprising the whole facility are defined, the calculation of life-cycle cost ascribed to the present value in terms of the power rating ($/kW) will constitute a quick and useful metric for EES facility owners to compare between technologies that may possess different characteristics.

In the following, we elaborate on the envisaged methodological solution that we will adopt in the context of both the research directions outlined in this chapter. We will commence with a detailed account of the proposed mathematical optimization solution. Subsequently, we will proceed to introduce the main principles and rationale of BO and we will further provide the main innovative components that constitute our ground-breaking solution.

4. Mathematical optimization solution

In contrast to economic dispatch (ED) where it is assumed that all units are already connected to the system, UC assumes that the generating units are available and appropriate subsets must be selected to provide the minimum operating cost. While integer variables are involved, UC is more difficult to solve mathematically as it constitutes a more complex procedure which considers the ED as a subproblem to the solution. In the following, we present the framework of a mathematical approach based on dual optimization, the so-called Lagrange Relaxation (LR). Initially, we demonstrate a traditional formulation and assess its performance on a power system consisting of 18 generating units. Then, we compare it with our novel version and evaluate its ability to deal with identical generating units.

4.1. Mathematical framework of Lagrange Relaxation

By utilizing dual optimization, Lagrange Relaxation becomes advantageous over dynamic programming-based approaches where all generating units are examined in the same time interval. This disturbs the coupling constraints since an action to one unit affects what will happen on the others. Through the dual optimization procedure, the UC problem is solved by "relaxing" (or temporarily ignoring) the coupling constraints as if they did not exist, so that other primal constraints can easily be added to the problem [45].

The method starts by defining the fundamental constraints and the objective function.

Minimize:

$$F(P_i^t, U_i^t) = \sum_{t=1}^{T} \sum_{i=1}^{N} \left[F_i(P_i^t) + C_{SU_i}^t \right] U_i^t \tag{4.1}$$

subject to loading constraints,

$$P_{netD} - \sum_{i=1}^{N} P_i = 0 \quad \forall\, t \in \mathcal{T} \tag{4.2}$$

and unit constraints.

$$U_i^t P_{i,min}^t \leq P_i^t \leq U_i^t P_{i,max}^t \quad \forall\, i \in \mathcal{N}\,, \forall\, t \in \mathcal{T} \tag{4.3}$$

Adding the constraint function (4.2) to the objective (4.1) after multiplying the first by an undetermined multiplier λ, we obtain *Lagrange Function* shown in Equation 5.4.

$$\mathcal{L}(P,U,\lambda) = F(P_i^t, U_i^t) + \sum_{t=1}^{T} \lambda^t \left(P_{netD}^t - \sum_{i=1}^{N} P_i^t U_i^t \right) \tag{4.4}$$

The first derivative gives the necessary condition for the existence of a minimum cost. When the Lagrangian is rewritten as:

$$\mathcal{L} = \sum_{t=1}^{T} \sum_{i=1}^{N} \left[F_i(P_i^t) + C_{SU_i}^t \right] U_i^t + \sum_{t=1}^{T} \lambda^t P_{load}^t - \sum_{t=1}^{T} \sum_{i=1}^{N} \lambda^t P_i^t U_i^t \tag{4.5}$$

it is observed that the second term is constant and can be neglected to reach the form of Equation 4.6.

$$\mathcal{L} = \sum_{i=1}^{N} \left(\sum_{t=1}^{T} \left\{ \left[F_i(P_i^t) + C_{SU_i}^t \right] U_i^t - \lambda^t P_i^t U_i^t \right\} \right) \tag{4.6}$$

This way, we achieve unit separation and the term inside the outer brackets can now be solved separately for each generating unit. The minimum of the final function for each unit over all time periods is found by the first derivative and makes sense only when $U_i^t = 1$. The necessary condition for the existence of a minimum cost of operation for the thermal power system is that all the unit incremental cost rates must be equal to the undetermined value λ^t over all time periods according to:

$$\frac{d}{dP_i^t} \left[F_i(P_i^t) - \lambda^t P_i^t \right] = \frac{d}{dP_i^t} F_i(P_i^t) - \lambda^t = 0 \tag{4.7}$$

To incorporate the thermal constraints of minimum and maximum power output of each generating unit, the following conditions must be qualified:

$$min\left[F_i(P_i^t) - \lambda^t P_i^t \right] = \begin{cases} F_i(P_i^{opt}) - \lambda^t P_i^{opt} & for\ P_i^{min} \le P_i^{opt} \le P_i^{max} \\ F_i(P_i^{min}) - \lambda^t P_i^{min} & for\ P_i^{opt} \le P_i^{min} \\ F_i(P_i^{max}) - \lambda^t P_i^{max} & for\ P_i^{opt} \ge P_i^{max} \end{cases} \tag{4.8}$$

Finally, since the objective is to minimize $[F_i(P_i^t) - \lambda^t P_i^t]$ at each stage and as this value goes to 0 only when $U_i^t = 0$, the only way to get a lower value is to achieve:

$$[F_i(P_i^t) - \lambda^t P_i^t] < 0 \tag{4.9}$$

While the solution is given for each generating unit independently, the remaining constraints can easily be integrated. Specifically, for each time-interval the independent generating units are allowed to change their status (or check if they satisfy Equation 4.9) based on Equations (3.17) and (3.18). At the same time, their minimum and maximum capacity are limited according to Equations (3.19) and (3.20). The dimensionality problems affecting dynamic programming have been avoided and a way remains to be found adjusting λ^t values for the coupling constraints of load balance, spinning reserve, etc. Such an example is presented by Equation (4.10).

$$\lambda^{k+1} = \lambda^k + \left[\frac{d}{d\lambda} q(\lambda)\right] a \tag{4.10}$$

The function q(λ) represents the *Lagrangian Function* and its derivative results in:

$$\frac{d}{d\lambda} q(\lambda) = \sum_{t=1}^{T} \left(P_{load}^t - \sum_{i=1}^{N} P_i^t U_i^t \right) \tag{4.11}$$

To avoid oscillations the values of α must be distinguished according to derivative's sign so that:

$$a = \begin{cases} c & if \ \frac{d}{d\lambda} q(\lambda) < 0 \\ \frac{c}{2} & if \ \frac{d}{d\lambda} q(\lambda) > 0 \end{cases} \tag{4.12}$$

A measure of the closeness to the solution is referred to as relative duality gap (RDG) and is given by the following Equation.

$$RDG = \frac{J^* - q^*}{q^*} \tag{4.13}$$

In this equation, J^* represents the total cost (for the N generating units during the T time periods) estimated by the relaxed λ while q^* is the total cost given by the corrected λ values used in ED. In some cases, the process may fall into oscillations due to unnecessary commitments and de-commitments of identical units. This is reflected as overload or underload conditions violating the power balance constraints. To deal with such a sensitivity problem, the identical units j can be grouped to form a composite cost function and an alternative process is utilized to optimally define the active unit number (η_i^t) of each group i based on the following mathematical statements [46]:

$$\eta_{i,min}^t \leq \eta_i^t \leq \eta_{i,max}^t \tag{4.14}$$

$$\eta_{i,min}^t . P_{ij,min}^t \leq \eta_i^t . P_{ij}^t \leq \eta_{i,max}^t . P_{ij,max}^t \tag{4.15}$$

As we observe, the solution of the above problem comprises the computation of 3-dimensional matrices. In contrast to conventional LR formulations where each variable could be represented by processing $\mathcal{N}x\mathcal{T}$ (2-dimensional) matrices, the composition of groups to accommodate identical units requires a further dimension. This is needed, for example, to define a variable's value for a generating unit i classified in group j for the interval t. As this procedure is computationally cumbersome, this thesis will examine an innovative method that performs the commitment of identical units in two further stages regarding the dual and primal problem for grouped (i) and individually included (j) generating units [47]. This way, the contribution of each generating group is reformulated, by making use of dual variable constraints. To overcome oscillations and achieve the convergence, we propose that such variables are needed to detect which group was last-up, to set the time duration that each distinguished (un-grouped) unit has been on-line or off-line at the end of interval t, and to identify if the unit was started-up at the beginning of this interval. The dual and relaxed problems will be alternatively resolved until the optimal Lagrange multiplier vector is found iteratively.

4.2. A demonstration of Lagrangian Relaxation

Based on the previously presented framework, a model has been developed and assessed in two test-cases. We consider the IEEE Reliability Test System which consists of 18 generating units depicted below.

Table 3. Characteristics of IEEE Reliability Test System.

GU	P_{min} (MW)	P_{max} (MW)	a ($/h)	b ($/MWh)	c ($/MW^{2}h)	SU ($)	MU (hr)	MD (hr)	Initial Operating hours
1	100	800	5	4	0.001	10000	8	8	8
2	100	800	5	6	0.002	10000	8	8	8
3	80	400	20	8	0.0025	8000	4	4	4
4	80	400	20	10	0.0025	8000	4	4	4
5	60	300	30	10	0.002	6000	3	3	3
6	60	300	30	12	0.002	6000	3	3	3
7	50	200	40	14	0.0015	5000	2	2	2
8	50	200	40	16	0.0015	5000	2	2	2
9	25	100	55	15	0.0012	2500	1	1	1
10	25	100	55	17	0.0012	2500	1	1	1
11	25	100	55	17	0.0012	2500	1	1	1
12	60	300	30	10	0.002	6000	3	3	3
13	60	300	30	12	0.002	6000	3	3	3
14	50	200	40	14	0.0015	5000	2	2	2
15	50	200	40	16	0.0015	5000	2	2	2
16	25	100	55	15	0.0012	2500	1	1	1
17	25	100	55	17	0.0012	2500	1	1	1
18	25	100	55	17	0.0012	2500	1	1	1

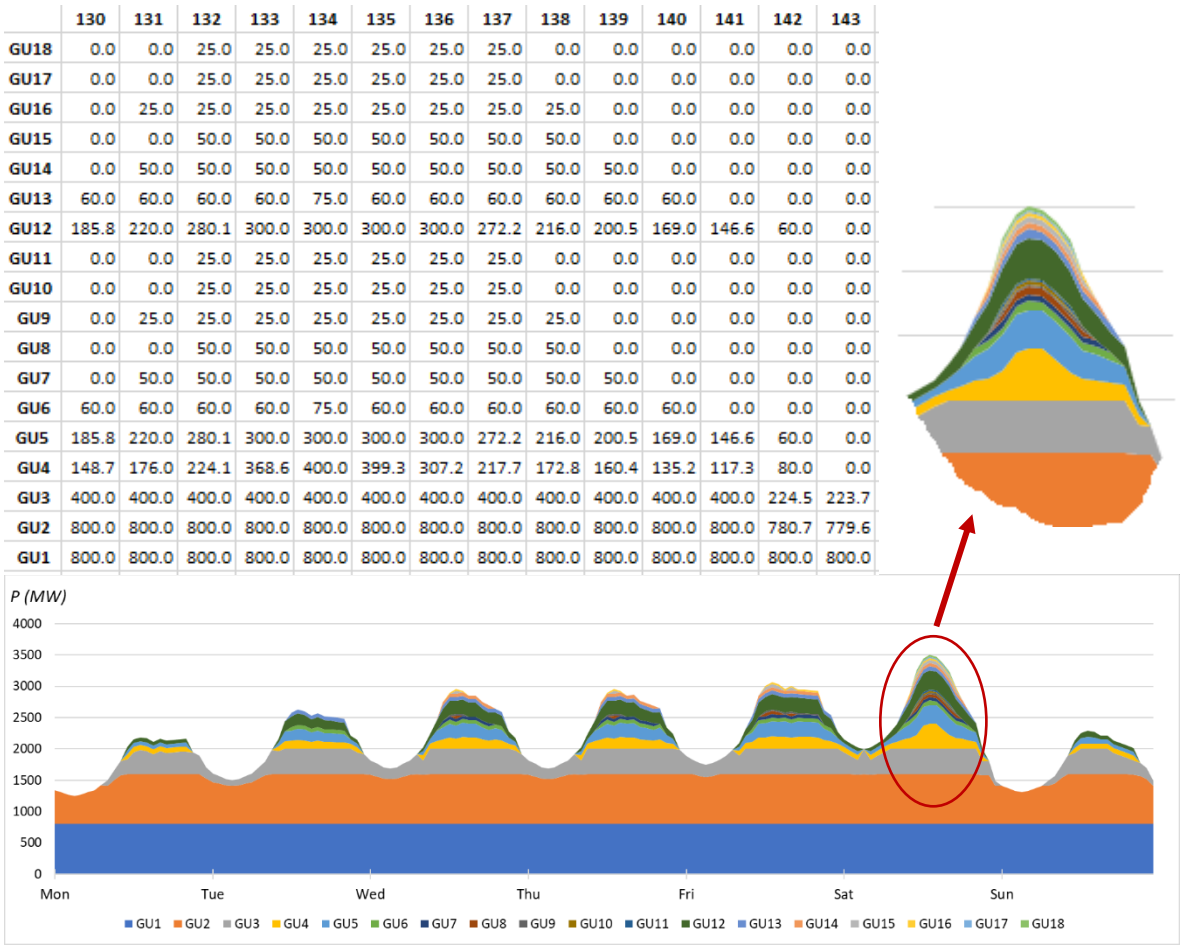

Figure 14. Optimal UC based on traditional Lagrange formulation.

To evaluate the performance of our algorithm, we first use a Lagrangian Relaxation method based on the traditional formulation. Figure 14 illustrates the optimal UC schedule achieved for a weekly load demand variation and spinning reserve requirement of 10%.

Apart from the power balance and spinning reserve, minimum-up and minimum-down times are also included. Other constraints such as unit status restrictions and crew constraints are not integrated into the UC formulation, to allow for reaching a comprehensive overview of the optimization procedure. Furthermore, we completely ignore the ramp limitations since they are found adequate for the respective hourly demand. Finally, all start-up costs are calculated based on a fixed cost including crew and maintenance expenses a_i (Equation 3.5).

As can be observed, traditional UC algorithms relying on mathematical optimization such as Lagrange Relaxation, present a sensitivity regarding the identical generating units. Specifically, the generating units that possess identical or even similar cost coefficients (*a*, *b* and *c*) and start-up costs (*SU*) are selected to get online according to mathematical statement (4.9). As a result, the generation is over-scheduled leading to increased start-up and production costs. When more constraints are taken into account, the committed units force the optimization into oscillations providing consecutive over-load and under-load solutions.

As stated in the previous chapter, to overcome this weakness we propose a double-decomposition approach capable of accounting for the identical units and treating them as individual composite groups. Compared to the models proposed in the framework of LR, the Lagrangian dual function is separable into sub-problems regarding both each group of identical units and each single unit individually. As a result, LR proceeds with a four-stage procedure instead of the classical approaches which converge in two stages of dual and primal problem solutions. Aiming to optimally define the active unit number, n_i^t, which satisfies system power balance and spinning reserve requirements, whilst minimizing the total production cost, a suitable modification can be explained through the main steps of the procedure given below.

1. Initialization: All unit characteristics, cost coefficients and load are imported.
2. Grouping: The identical as per cost coefficients and status units are identified and grouped together to form a composite cost function.

3. Generate the possible binary combinations for each time interval subject to group specific constraints.
4. Economic dispatch: Using the proposed commitment schedule calculate the total generation for those time intervals during which the power balance and spinning reserve constraints are satisfied.
5. Un-grouping: For the rest of time intervals (during which the inequalities are over-constrained), un-group and evaluate the generation of the last-up (costliest) group, updating the dual variables of active unit number of the particular group and last-up, off-line duration and start-up time of each individual unit of the corresponding group.
6. Calculate the total production cost for each time interval and based on the fitness function update λ for each combination.
7. Algorithm update: Regroup the units based on the new parameters constraining their contribution and go back to the step 3 until the maximum iteration number is achieved.

Utilizing dual variable constraints, we reformulated the contribution of each generating group based on mathematical statements (4.14) and (4.15). The quadratic, pricewise cost function is processed in its nominal form for both stages of either grouped or individually included units [48]. Once the appropriate groups are decided to change their status, two possible conditions may occur alternately, namely overload or underload and hence, three extra variables are required to overcome oscillations and achieve the convergence. These include integer variables to detect which group was last-up and to set the time duration that each distinguished (un-grouped) unit has been on-line or off-line at the end of interval *t*, and binary 0/1 variables equal to "1" if the unit is started-up at the beginning of interval *t*. Improvements in the number of committed units to satisfy the same load demand are achieved.

Applying our proposed technique to the same power system configuration, the improvements in UC schedule can be observed in the following scheme. The significance of our proposed approach when identical generating units are utilized for electricity production can be observed through the Figure 15, where the cost difference of the weekly simulations concerning the two test-cases are presented. As can be seen, the unnecessary commitment

of identical generators leads to increased start-up costs and uneconomic dispatch of the partially loaded units.

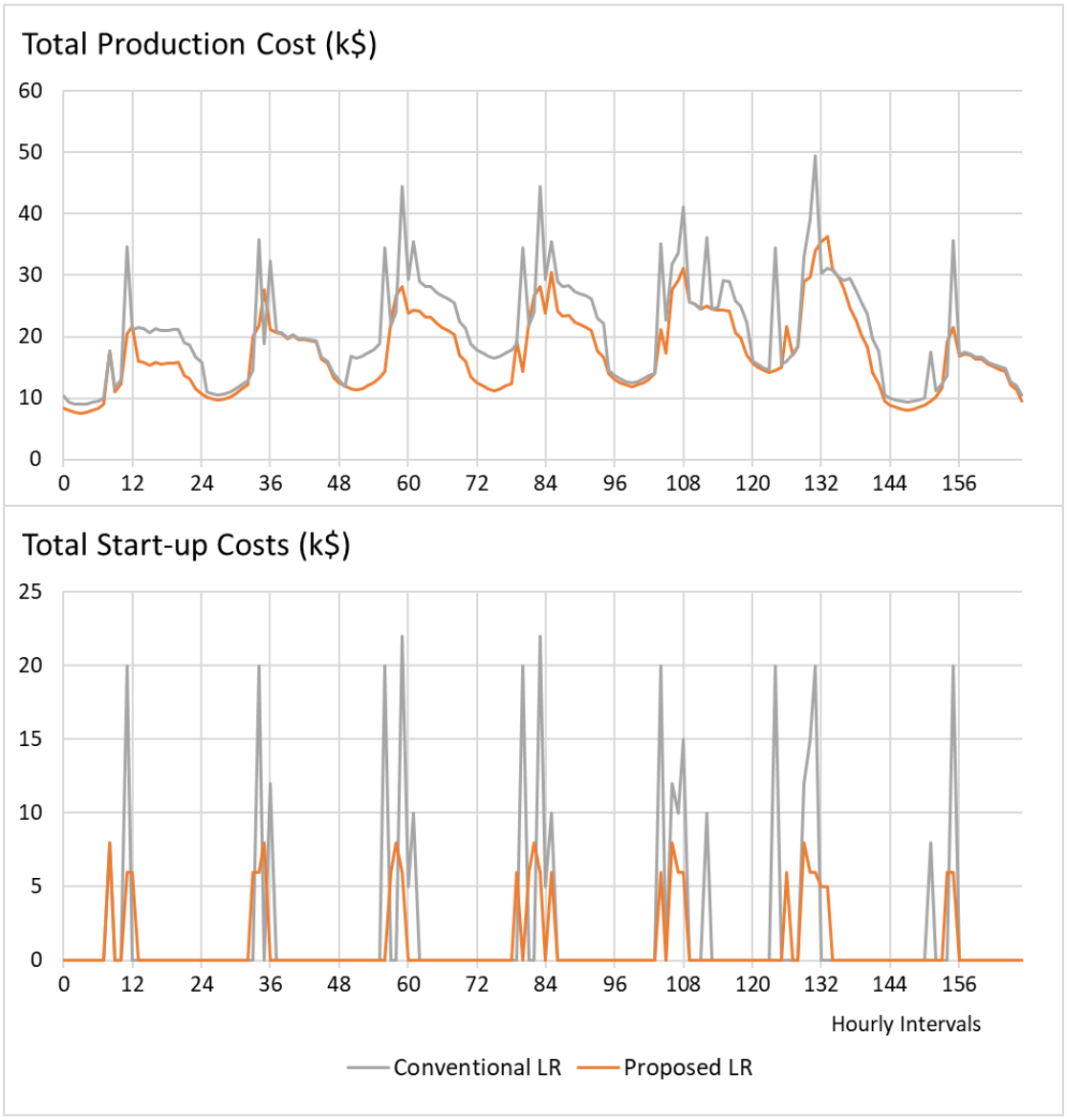

Figure 15. Weekly total production and start-up costs.

The estimated cost difference reaches a total of up to $550,000 which constitutes a 18% increase compared to our novel LR solution. Finally, exploiting the innovative concept of double-decomposition, improvements also for the convergence performance do exist. The optimal UC schedule for the week under consideration is presented in Figure 16. Figure 17 illustrates this performance in terms of duality gap across the required iterations of the conventional and proposed LR optimization processes.

	130	131	132	133	134	135	136	137	138	139	140	141	142	143
GU18	0.0	0.0	0.0	0.0	0.0	0.0	0.0	0.0	0.0	0.0	0.0	0.0	0.0	0.0
GU17	0.0	0.0	0.0	0.0	0.0	0.0	0.0	0.0	0.0	0.0	0.0	0.0	0.0	0.0
GU16	0.0	0.0	0.0	0.0	0.0	0.0	0.0	0.0	0.0	0.0	0.0	0.0	0.0	0.0
GU15	0.0	0.0	0.0	0.0	0.0	0.0	0.0	0.0	0.0	0.0	0.0	0.0	0.0	0.0
GU14	0.0	0.0	0.0	0.0	50.0	50.0	0.0	0.0	0.0	0.0	0.0	0.0	0.0	0.0
GU13	0.0	0.0	127.2	194.3	200.0	184.6	163.6	91.0	0.0	0.0	0.0	0.0	0.0	0.0
GU12	300.0	300.0	300.0	300.0	300.0	300.0	300.0	300.0	300.0	300.0	256.7	165.3	0.0	0.0
GU11	0.0	0.0	0.0	0.0	0.0	0.0	0.0	0.0	0.0	0.0	0.0	0.0	0.0	0.0
GU10	0.0	0.0	0.0	0.0	0.0	0.0	0.0	0.0	0.0	0.0	0.0	0.0	0.0	0.0
GU9	0.0	0.0	0.0	0.0	0.0	0.0	0.0	0.0	0.0	0.0	0.0	0.0	0.0	0.0
GU8	0.0	0.0	0.0	0.0	0.0	0.0	0.0	0.0	0.0	0.0	0.0	0.0	0.0	0.0
GU7	0.0	0.0	0.0	50.0	50.0	50.0	50.0	50.0	0.0	0.0	0.0	0.0	0.0	0.0
GU6	0.0	60.0	127.2	194.3	200.0	184.6	163.6	91.0	60.0	101.4	0.0	0.0	0.0	0.0
GU5	300.0	300.0	300.0	300.0	300.0	300.0	300.0	300.0	300.0	300.0	256.7	165.3	60.0	60.0
GU4	40.4	226.0	400.0	400.0	400.0	400.0	400.0	400.0	314.7	80.0	80.0	80.0	0.0	0.0
GU3	400.0	400.0	400.0	400.0	400.0	400.0	400.0	400.0	400.0	400.0	400.0	400.0	345.2	143.2
GU2	800.0	800.0	800.0	800.0	800.0	800.0	800.0	800.0	800.0	800.0	800.0	800.0	800.0	800.0
GU1	800.0	800.0	800.0	800.0	800.0	800.0	800.0	800.0	800.0	800.0	800.0	800.0	800.0	800.0

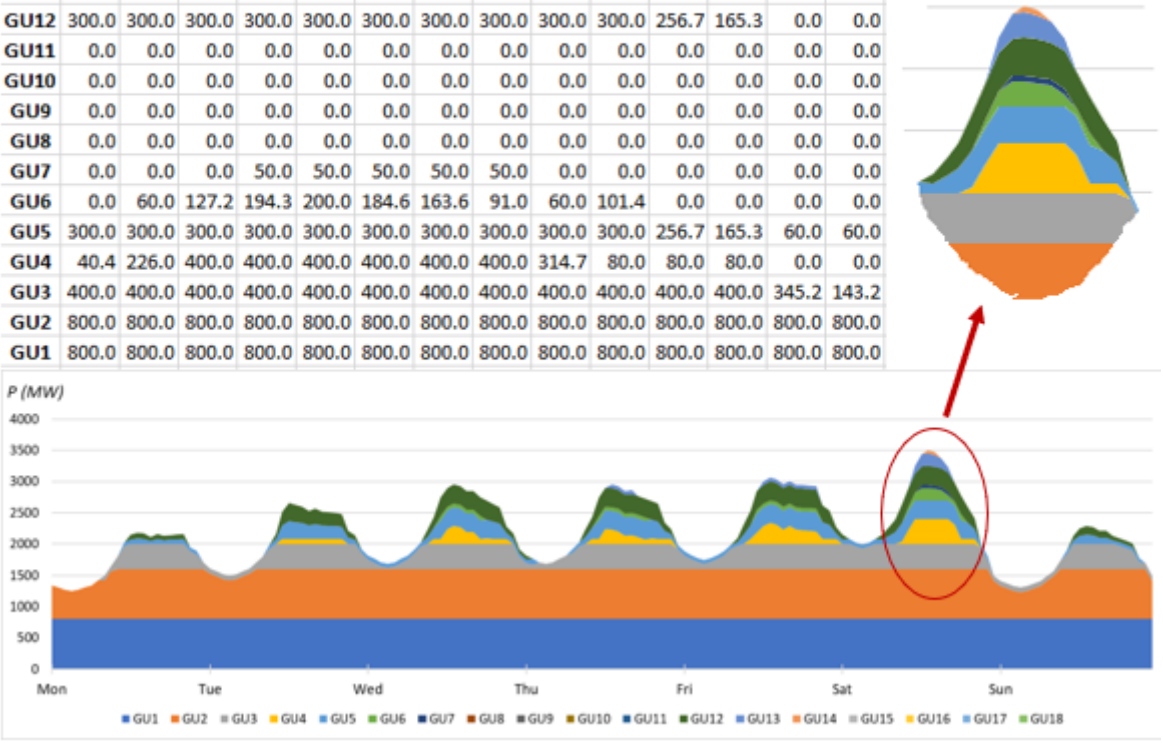

Figure 16. Optimal UC based on novel Lagrange formulation.

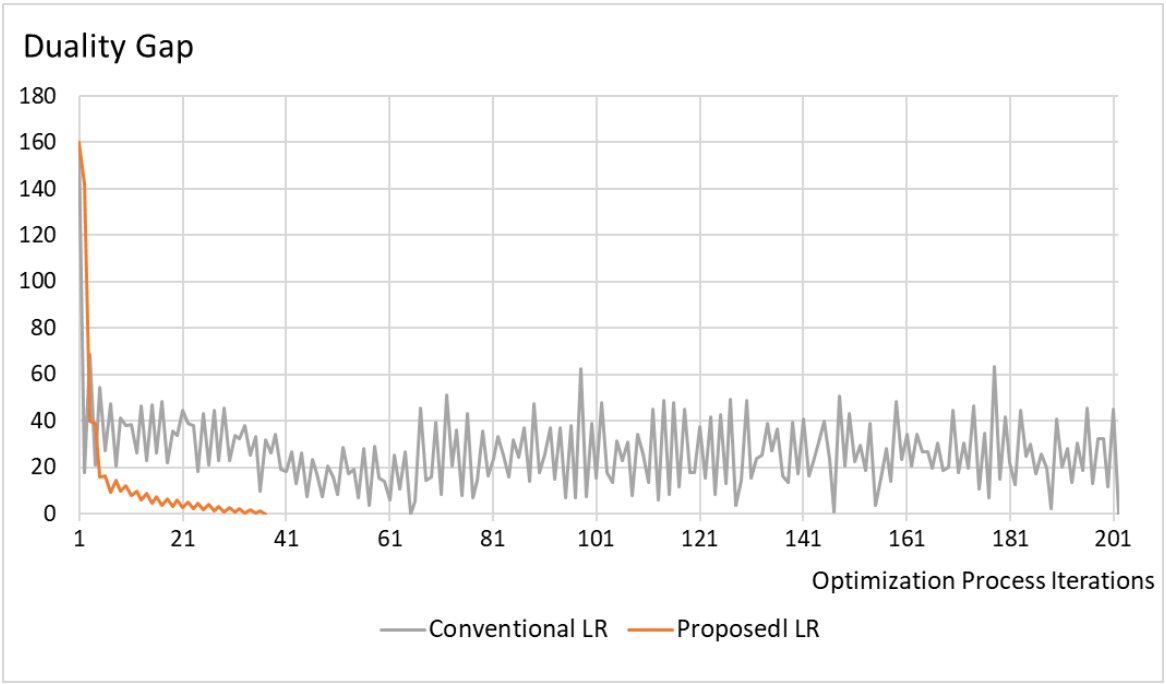

Figure 17. Optimization process LR duality gap.

5. Bayesian optimization solution

In previous chapter, we elaborated on mathematical optimization and we found that it undeniably offers a high-performance/low-cost UC solution technique. Specifically, Lagrange Relaxation framework is easily modified to model characteristics of different utilities, surpassing the sensitivity it might have experienced in managing identical units. However, despite its ability to overcome non-convexity and non-linearity of large-scale systems, only a near-optimal feasible solution can be expected. In addition, LR methods constitute mainly deterministic approaches unable to include the stochastic behaviour of modern power systems into their objectives. They rely, instead, on simulated scenarios weighted with a probability of occurrence. Finally, the number of function evaluations needed increases by increasing generating units and integrated (especially coupled) constraints.

To ameliorate this expensive requirement, intelligent systems for determining appropriate UC schedules have risen as a promising solution. This is especially the case for weak power systems with low dispatching flexibility and high dependency on imported fossil fuels. In this chapter, we introduce a radically novel paradigm for addressing the optimal UC problem, that is capable of accounting for the largely unaddressed challenge of the uncertain and volatile behavior of modern generation. In the following, we first introduce the paradigm of BO. Further, we elaborate on our suggested solution, leveraging BO arguments to revolutionize the UC in power systems.

5.1. A Bayesian optimization primer

We consider the problem of finding the global minimizer $x_\star$ of a scalar objective function $f(x)$ over some bounded domain, typically $\mathcal{X} \subset \mathbb{R}^D$, subject to a set of K constraints $c_1, c_2, \dots, c_K$ as defined previously.

$$x_* = \underset{x \in X}{\operatorname{argmin}} f(x)$$
$$s.t. \qquad c_1(x) \leq 0, \dots, c_K(x) \leq 0 \tag{5.1}$$

BO introduces the fundamental assumption that the functional form of the scalar objective $f(x)$ is unknown and it cannot be determined with certainty. On the contrary, it

constitutes a stochastic function of the input x, which can only be modelled as a random process. On the basis of this assumption, BO infers a Bayesian predictive model for $f(x)$, by making use of previous function evaluations. The predictive model typically used is a GP, which operates as a relatively inexpensive surrogate to guide the optimization algorithm towards regions that are promising (low GP mean) and/or unknown (high GP uncertainty). This procedure is performed on the basis of a local optimization rule which relies on a properly defined acquisition function [49].

Let us consider an existing set of measurement pairs $\{x_i, y_i\}$; this constitutes both the observed data points and the corresponding measured values of the sought stochastic function *f*. BO uses this set as the training data D of an underlying GP model used for predictive inference purposes. GP inference consists in assigning a prior, $p(f)$, over the function $f(x)$ and, combining it with the evidence from the data D, formulated under a likelihood assumption, $p(D|f)$, to get a posterior distribution, $p(f|D)$, over $f(x)$ according to Bayes' theorem.

$$p(f|D) = \frac{p(D|f)p(f)}{p(D)}$$

$$or$$

$$posterior = \frac{likelihood * prior}{marginal\ likelihood} \tag{5.2}$$

In more detail, given any finite collection of *n* points $\boldsymbol{X} = \{x_i \in \mathcal{X} | i = 1,2, \dots, n\}$, the value of f at these points is assumed to be jointly Gaussian with mean m:X↦ℝ, where $m = \big(\mu(x_1), \mu(x_2), \dots, \mu(x_n)\big)^T$ and covariance matrix K:X×X↦ℝ, where $\boldsymbol{K}_{ij} = \boldsymbol{k}\big(x_i, x_j\big)$ for $i \geq 1$, $j \leq n$. The implications of this assumption establish that the sum of the number of independent and identically distributed i.i.d. random variables, $\boldsymbol{X}$, with finite variances will tend to a normal distribution, *f*, which is able to describe any set of their correlated, real values [50]. This is expressed in the form of the postulated prior imposed over $f(x)$ which yields $f \sim \mathcal{N}(m, K)$. In order for neither positive nor negative values to be privileged, the mean is typically taken as zero, yielding:

$$f|X \sim \mathcal{N}(0, K)$$

or

$$\log p(f|X) = -\frac{1}{2} f^T K^{-1} f - \frac{1}{2}\log|K| - \frac{n}{2}\log 2\pi \tag{5.3}$$

Turning to the selection of the covariance function, we typically utilize kernel functions that ensure its positive semi-definiteness. There is a large variety of alternatives that are typically used, including the radial basis function (RBF) kernel, as well as Matern class kernels [51]. For instance, in this work we will make use of the adaptive relevance determination (ARD) Matern 5/2 kernel, which reads:

$$k(x_i, x_j) = \sigma_f^2 \left(1 + \sqrt{5}r + \frac{5}{3}r^2\right) exp\left(-\sqrt{5}r\right) \tag{5.4}$$

$$r = \sqrt{\sum_{m=1}^{D} \frac{\left(x_{im} - x_{jm}\right)^2}{\sigma_m^2}} \tag{5.5}$$

The benefit of this type of kernel lies both on its highly non-Gaussian form, as well as the fact that it puts different trainable weights, σ_m^2, on the components of the observed vectors x. This way, it learns which observed features are the most important for modelling purposes.

On the other hand, to allow for realistic modelling, we take into account that the GP model can only generate noisy predictions, f(x), of the dependent variable y. To encapsulate this assumption, we postulate an additive independent identically distributed Gaussian noise model, ε, with zero mean and variance σ_n^2. Under this formulation, we obtain a likelihood function for the model which reads $y|f \sim \mathcal{N}(f, \sigma_n^2 I)$.

Based on the introduced prior and likelihood assumptions, and using Bayes' rule, it can be shown that the marginal likelihood of the model reads:

$$\log p(y|X) = -\frac{1}{2} y^T (K + \sigma_n^2 I)^{-1} y - \frac{1}{2}\log|K + \sigma_n^2 I| - \frac{n}{2}\log 2\pi \tag{5.6}$$

or

$$y|X \sim \mathcal{N}(0, K + \sigma_n^2 I) \tag{5.7}$$

Optimization of this expression can be performed to estimate the appropriate values of the trainable hyperparameters of the employed kernel functions, for instance the set of σ_m^2 hyperparameters of the ARD Matern 5/2 kernel, as well as the noise variance hyperparameter σ_n^2 of the likelihood of the model.

Once model training by optimizing the marginal likelihood (5.6) is performed, using a data set $D_t = \{x_{1:t}, y_{1:t}\}$, BO employs an acquisition function $u(x|D_t)$ to decide what point x_{t+1} to consider next, as it seeks to find the global optimum of the modelled stochastic function *f(x)*. Considering a minimization setup for *f(x)*, a point x_{t+1} yielding a high acquisition value should correspond to low posterior expected values of *f(x)* inferred by the trained GP, or predictions with high uncertainty, as expressed in the form of the obtained predictive posterior variance.

The notion of expected-improvement offers the most typically used formulation of the acquisition function. We consider [52]:

$$x_{t+1} = \underset{x_t \in x_{1:t}}{\operatorname{argmin}}\, u(x) \tag{5.8}$$

such that

$$\begin{aligned} x_{t+1} &= \underset{x_t \in x_{1:t}}{\operatorname{argmin}}\, \mathbb{E}(\|f_{t+1}(x) - f(x_*)\| | D_t) \\ &= \underset{x_t \in x_{1:t}}{\operatorname{argmin}} \int \|f_{t+1}(x) - f(x_*)\| p(f_{t+1}|D_t)\, df_{t+1} \end{aligned} \tag{5.9}$$

In this expression, the predictive posterior $p(f_{t+1}|D_t)$ is obtained by making use of Bayes' rule and the likelihood and prior assumptions of the employed GP model. Specifically, the joint distribution of the observed target values and the function values $f_{t+1} = f(x_{t+1})$ at the test location x_{t+1} under the prior can be written as:

$$\begin{bmatrix} y_{1:t} \\ f_{t+1} \end{bmatrix} \sim \mathcal{N}\left(0, \begin{bmatrix} \boldsymbol{K} + \sigma_n^2 \boldsymbol{I} & \boldsymbol{k} \\ \boldsymbol{k}^T & k(x_{t+1}, x_{t+1}) \end{bmatrix}\right) \tag{5.10}$$

where

$$\boldsymbol{K} = \begin{bmatrix} k(x_1, x_1) & \cdots & k(x_1, x_t) \\ \vdots & \ddots & \vdots \\ k(x_t, x_1) & \cdots & k(x_t, x_t) \end{bmatrix} \tag{5.11}$$

$$\boldsymbol{k} = [k(x_{t+1}, x_1) \quad k(x_{t+1}, x_2) \quad \cdots \quad k(x_{t+1}, x_t)] \tag{5.12}$$

This yields the predictive distribution:

$$p(f_{t+1}|D_{1:t}, x_{t+1}) \sim \mathcal{N}(m_t(x_{t+1}), \sigma_t^2(x_{t+1}) + \sigma_n^2) \tag{5.13}$$

and the sufficient statistics:

$$m_t(x_{t+1}) = \boldsymbol{k}^T [\boldsymbol{K} + \sigma_n^2 \boldsymbol{I}]^{-1} y_{1:t} \tag{5.14}$$

$$\sigma_t^2(x_{t+1}) = k(x_{t+1}, x_{t+1}) - \boldsymbol{k}^T [\boldsymbol{K} + \sigma_n^2 \boldsymbol{I}]^{-1} \boldsymbol{k} \tag{5.15}$$

Finally, in most practical optimization problems, the observation space does not cover the whole domain of real numbers; some parts of it are excluded due to imposed constraints. Therefore, the BO algorithm must be prohibited from picking such points when applying the expected improvement rule. To ensure this, we can modify the original expected improvement rule, weighting it with the probability of the constraints being satisfied [53][54].

$$u_C(x|D_t) = u(x|D_t) \prod_{k=1}^{K} p(c_k(x) \leq 0|D_t) \tag{5.16}$$

Once observing the output of each query of the objective, the model is updated to produce a more informative posterior over the space of objective functions, the acquisition is recomputed, and a new input is chosen for evaluation. After *n* queries, the algorithm makes a final recommendation x_{n*}, providing the algorithm's best estimate and completing the Bayesian optimization loop [55].

5.2. A Bayesian optimization approach

Our proposed approach utilizes the latest advances in Bayesian inference under prespecified constraints [54]. This represents a data-driven inferential framework for solving combinatorial problems, namely UC and ED. The entailed modelling procedure starts with the definition of the independent variables, the optimizable variables, and the functional

form of the dependent variables, as well as constraints definition, both at the individual unit level and the system level.

We aim to consider two types of optimizable variables, namely a) the power output at unit level, which is a real number and b) the unit status which is integer. Under this scheme, it is easy to ensure satisfaction of the status restrictions, for instance by excluding from the optimization the state variables of the units that must run, the power output variables of the units that run at a fixed-MW output and both variables for those which must be out. In addition to the predefined unit bounds which are, by nature, expressed by the specification of the optimizable variable domain, we intend to also introduce coupled constraints. These include the power balance constraint, as well as the spinning reserve requirements.

Moreover, our investigation may be further improved by considering a third category of constraints that are of deterministic nature. One such a deterministic constraint is the plant crew constraint as defined in Chapter 3. Further, the also previously defined MU/MD and RU/RD constraints can also be treated as conditional constraints since if the optimization enforces certain values to some variables, other variables have to be set to given, feasible values under certain conditions.

5.2.1 Methodology

Inspired from the previously described state-of-the-art advances, in this chapter we propose a radically novel paradigm for addressing the UC challenge. Our vision is: 1) to ameliorate the need of heuristically specifying a functional form for the fuel cost function, which constitutes a core part of the optimized objective function in conventional formulations of the UC problem, and may undermine the obtained outcome if it deviates from reality; and 2) allow to discover quality solutions to the UC problem after only a limited number of function evaluations, which is of utmost importance in real-world settings where scheduling decisions may need to be made within extremely limited time-windows.

To this end, our proposed approach utilizes the latest advances in Bayesian optimization under prespecified constraints, summarized in the previous chapter. Specifically, we formulate the UC problem as a BO task whereby the stochastic dependent variable, y, represents the total production cost of the system, while the independent variables, $\mathbf{x}$, comprise: 1) the exogenous variable that must be satisfied, namely the net load

demand; 2) the optimizable variables that the algorithm needs to specify, namely the status of each unit and the power output of each generating unit. Further, we impose a number of proper constraints to ensure the feasibility of the discovered solutions, both at the individual unit level and the system level. This way, we establish a novel inferential paradigm, which operates in a completely data-driven fashion to discover the system dynamics and utilizes this outcome to effect the optimization task.

In our setup, the power output at unit level is treated as a real number. On the other hand, the unit status constitutes an integer. Under this scheme, it is easy to ensure satisfaction of the imposed status restrictions, for instance by excluding from the optimization the state variables of the units that *must run*, the power output variables of the units that run at a *fixed-MW output*, as well as both these two types of variables in cases of units that must be out. Turning to the specification of the imposed constraints, we consider: 1) the predefined unit bounds; 2) a set of coupled constraints, which include the power balance constraint, as well as the spinning reserve requirements; 3) the plant crew constraint, defined in Equation 3.8; and 4) the MU/MD and RU/RD constraints, given by Equations 3.17-3.18 and 3.19-3.20, respectively. Start-up costs are calculated based on a fixed cost including crew and maintenance expenses a_i (Equation 3.5).

In our realization of the BO pipeline, the functional form of the total production cost is inferred by means of a GP regression model. The postulated GP is presented with historical data, as well as observations fed back to the model during the optimization process and enables efficient prediction of how the dependent variable fluctuates when we modify the values of the independent/optimizable variables. Each time the BO algorithm modifies the value of an optimizable/independent variable, it records the resulting value of the measured dependent variable, namely total production cost, and retrains the postulated GP regression model on the augmented data of independent and corresponding dependent variable values. This way, it allows to process the load demand without requiring hourly measurements and ensures exploration of global solutions to achieve optimality.

Turning to the optimizable variable selection strategy, we rely on an appropriately defined *acquisition function*, pertinent to the addressed problem. The rationale underlying our selection can be summarized under the following objectives: 1) The optimizable variables must be modified in a way that maximally improves the expected dependent variable value, according to the predictions generated by the postulated GP model, 2) The number of modifications performed until the BO algorithm finds the globally optimal

selection for the optimizable variables must be the least possible. Specifically, we utilize the expected improvement function, defined in Equation 5.16, combined with a properly selected threshold for timely detecting BO convergence; we set this at 0.5% iteration-to-iteration improvement, which constitutes a less than marginal cost improvement according to the related practice. Hence, the condition of $f(x_*) < f(x), \forall x \neq x_*$ is retained and optimality is guaranteed.

5.2.2 Experimental evaluation

In the following, we perform a thorough experimental assessment of our proposed approach, adopting a common experimental setup, described for instance in [56]. We consider a power system with 10 generators, the properties of which are summarized in Table 4. In our study, we treat the power demand as an input variable defined over daily horizons of 24-hourly intervals, as depicted in Table 5.

We have implemented our novel paradigm in MATLAB 2018a [57]. To initialize the Bayesian optimization algorithm, we generate an initial guess of the independent variable values in x_0. These comprise an initialization of the UC, selected by considering that generating units 1 and 2 operate at their mean power output. This initialization strategy essentially reflects a simplistic UC policy, commonly used by transmission system operators that have not assimilated sophisticated optimization know-how. Moreover, the operating hours of each generating unit at the first time slot are included in the last column of Table 4.

Table 4. Characteristics of thermal generating units.

Unit *i*	Pmin (MW)	Pmax (MW)	a ($/h)	b ($/MWh)	c ($/MW^{2}h)	RU & RD (MW/hr)	MU/MD (hr)	SU ($)	Oper. hours
1*	225	455	1000	16.19	0.00048	405	8	4500	8
2	225	455	970	17.26	0.00031	405	8	5000	8
3	30	195	700	16.60	0.00200	54	5	550	0
4	30	195	680	16.50	0.00211	54	5	560	0
5	37.5	243	450	19.70	0.00398	67.5	6	900	0
6	30	120	370	22.26	0.00712	54	3	170	0
7	37.5	127.5	480	27.74	0.00079	67.5	3	260	0
8	15	82.5	660	25.92	0.00413	27	1	30	0
9	15	82.5	665	27.27	0.00222	27	1	30	0
10	15	82.5	670	27.79	0.00173	27	1	30	0

* Generating Unit 1 is constantly in must-run mode.

To render our experimental setup more realistic, we introduce an additional constraint which is of major importance for system operators, but is omitted from the experimental setup of [56]: We consider a spinning reserve requirement, and set it at 50MW, which is a standard practice in Cyprus. Figure 18 illustrates the outcome of the objective function evaluations at the determined candidate solutions over the performed algorithm iterations. For exposition purposes, we depict the solutions pertaining to 24-hours along with a colormap, to give a more effective insight into results. As we observe, for each hourly interval, the adopted BO process converges consistently.

Characteristically, the first solutions, obtained through algorithm initialization, yield poor values; however, performance improves fast as the BO algorithm proceeds.

Table 5. Net load demand (MW) for 24 hours.

Hour	Load	Hour	Load	Hour	Load
1	700	9	1300	17	1000
2	750	10	1400	18	1100
3	800	11	1450	19	1200
4	850	12	1500	20	1400
5	950	13	1400	21	1300
6	1000	14	1300	22	1100
7	1150	15	1200	23	900
8	1200	16	1050	24	800

Further, to obtain some comparative results, we also evaluate some state-of-the-art alternatives under the same experimental scenario. Specifically, we consider: 1) Dynamic Programming, which constitutes a standard solution in the related literature [41][42]; 2) the Lagrange Relaxation-based approach, presented in [47]; and 3) a standard Genetic Algorithm implementation, as provided in the GA toolbox of MATLAB [58].

The obtained results are provided in Table 6. Specifically, in this Table we provide the comparative results pertaining to the two key aspects that characterize an optimization process: 1) the number of attempts (function evaluations) required for the algorithm to converge (converge to a minimum); 2) the eventually obtained optimal (cost) value.

Table 6. Comparative results.

Method	Number of Function Evaluations	Minimum TPC achieved
Proposed Approach	7840	567178.5
Lagrangian Relaxation	11520	588217.2
Genetic Algorithm	24000	596217.3
Dynamic Programming	24552	587512.9

* TPC = Total Production Cost ($)

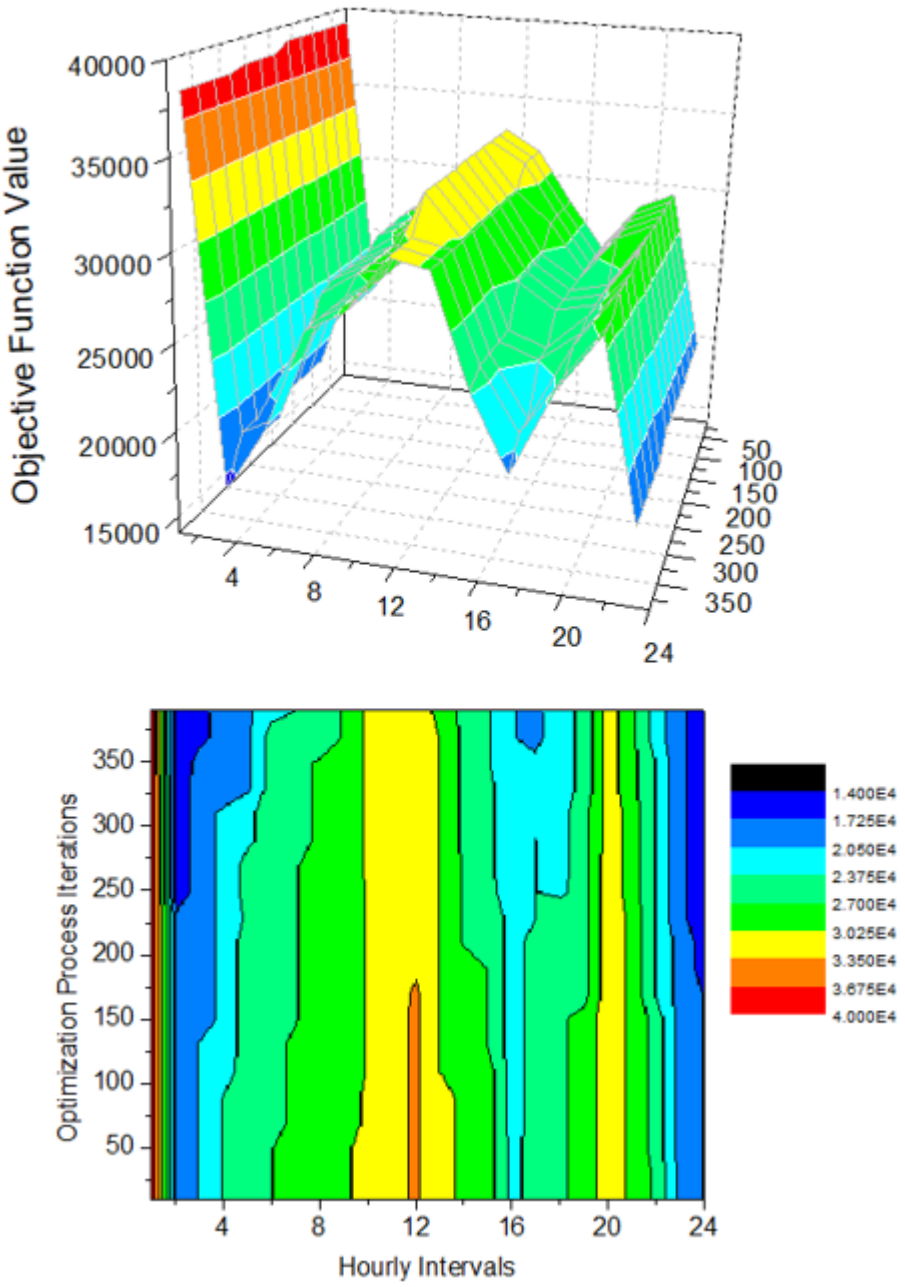

Figure 18. Function evaluations of our proposed approach pertaining to the 24-hourly intervals.

As we observe, our proposed approach yields the best optimal solution, which decreases the minimum achieved TPC by a whopping \$30K. This is an unprecedented improvement over the examined alternatives. It corroborates our claims on how the need of existing solutions to postulate specific functional forms for the cost functions undermines the optimization process. In addition, it offers strong empirical evidence that the proposed data-driven paradigm brings significant merit and benefits to the design of successful UC systems.

Further, our results indicate that our proposed solution constitutes the absolute leader in terms of the required number of function evaluations; it outperforms Dynamic Programming, which yields the second-best optimal cost, by more than three times the total required number of function evaluations. This outcome strongly vouches for the capacity of the employed GP model to effectively learn the underlying cost dynamics given only a limited number of training data. It also provides strong support to the adopted acquisition function, namely the expected improvement.

Finally, for completeness sake, in Figure 19 we illustrate the optimal scheduling results of our approach over all the generating units, for the 24-hourly intervals. In addition, we provide the real-valued, optimal power output of each generating unit in tabular form for the daily satisfaction of electricity demand.

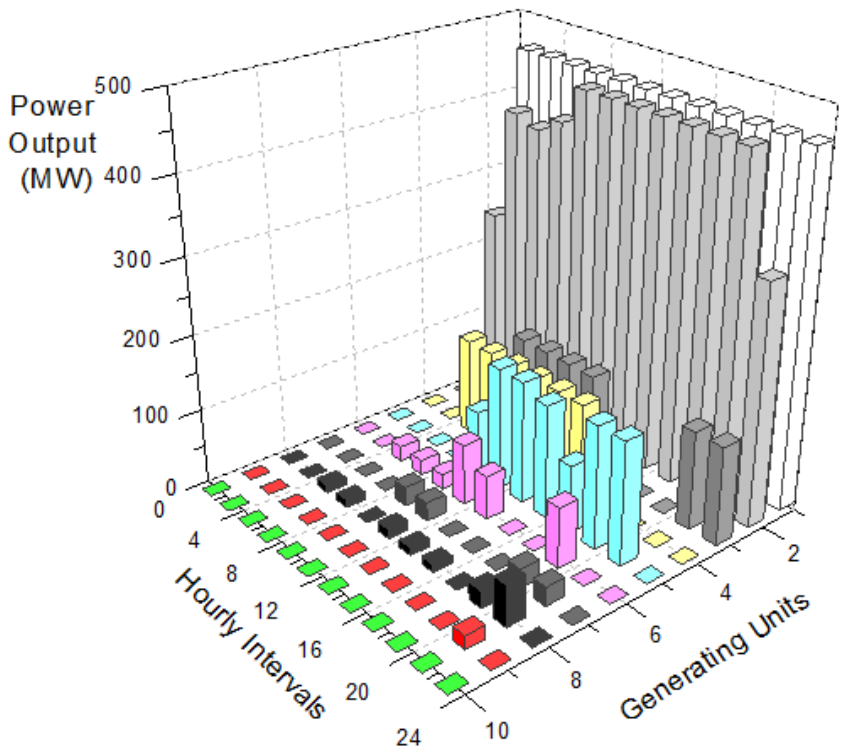

Figure 19. Optimal UC schedule obtained by our approach.

Table 7. Optimal power output (MW) for 24-hours load demand.

t	P1	P2	P3	P4	P5	P6	P7	P8	P9	P10
0	250	250	0	0	0	0	0	0	0	0
1	455	245	0	0	0	0	0	0	0	0
2	455	295	0	0	0	0	0	0	0	0
3	455	395	0	0	0	0	0	0	0	0
4	455	455	0	0	0	30	0	10	0	0
5	455	385	0	130	0	20	0	10	0	0
6	455	455	0	130	0	50	0	10	0	0
7	455	405	130	130	0	20	0	10	0	0
8	455	455	130	130	0	30	0	0	0	0
9	455	455	130	130	85	20	25	0	0	0
10	455	455	130	130	162	43	25	0	0	0
11	455	455	130	130	162	80	25	13	0	0
12	455	455	130	130	162	80	33	55	0	0
13	455	455	130	130	162	58	0	10	0	0
14	455	455	130	130	110	20	0	0	0	0
15	455	455	0	130	150	0	0	10	0	0
16	455	440	0	130	25	0	0	0	0	0
17	455	455	0	0	90	0	0	0	0	0
18	455	455	0	0	162	28	0	0	0	0
19	455	455	0	0	162	80	25	23	0	0
20	455	455	130	0	162	80	25	55	38	0
21	455	455	130	0	162	0	25	55	18	0
22	455	455	130	0	60	0	0	0	0	0
23	455	315	130	0	0	0	0	0	0	0
24	455	215	130	0	0	0	0	0	0	0

5.2.3 Concluding Remarks

Our proposed solution was based on an effective GP algorithm for enabling data-driven inference of the functional form of the underlying cost function, as well as the utilization of a state-of-the-art scheme for selecting the next function evaluation, namely an expected improvement-based acquisition function.

We provided an experimental evaluation of our approach under a standard benchmark scenario, and we compared with state-of-the-art alternatives. As we observed, our proposed approach outperforms the alternatives in terms of the ultimate system costs, as well as the number of required function evaluations. These findings strongly corroborate our theoretical claims motivating this work.

As for future directions for research, we indicate the consolidation of several consecutive hours into one stage. More extended works may also involve multi-bus

formulations introducing the real power network losses and transmission constraints into the UC task. We expect that by increasing the formulation complexity our novel approach might allow for even higher optimization performance.

6. The challenge of Electrical Energy Storage

So far, we have shown how to optimally plan-ahead the thermal generation subject to technical, operational and security constraints. The optimal storage planning constitutes a second, internal optimization problem and differs according to each stakeholder's objectives. Conventional approaches concentrate in either individual applications with common cost metrics or assume several storage techniques participating in a single operation without considering the degradation due to the round-trip efficiency, depth of discharge, self-discharge rate, cycle and life times [59][60][61]. In addition, none of these studies has conducted storage as an optimization problem and if they did so, they omitted to take into account different components for power-related and energy-related costs [62][63][64]. Therefore, the following chapters focus on the main characteristics of the state-of-the-art EES technologies, the requirements and preferences of their most realistic applications and different ways by which they can be modelled.

EES technologies find ready application in a diverse range of sectors including portable electronics, automotive vehicles and stationary systems, providing traction and propulsion, the ubiquitous automotive starting, lighting and ignition (SLI), standby power, remote area power supply, etc [65]. Improvements in both renewable and storage technologies are continuously needed, in order for the grid to accommodate the ever-increasing variable sources.

For several years now, EES is attracting increasing interest for power grid applications that provide regulation, contingency and management reserves [8]. The term of storage refers to a wide variety of technologies and potential applications across the power chain and hence, can be confusing as it occasionally acts as increased demand or generator [9][10]. Until 2017, the storage was limited to 176GW accounting for less than 2% of total electric power production capacity and more than 98% stemmed from pumped hydro. As can be observed from Figure 20, this is followed by lithium-ion batteries and flywheels with a contribution of 1120MW and 930MW respectively, while the rest of 1112MW is held by compressed air (640MW), sodium-based batteries (220MW), lead-acid (80MW), capacitors (80MW), flow batteries (47MW), nickel-based (30MW) and hydrogen-fuel cell (15MW) [66][67][68][69].

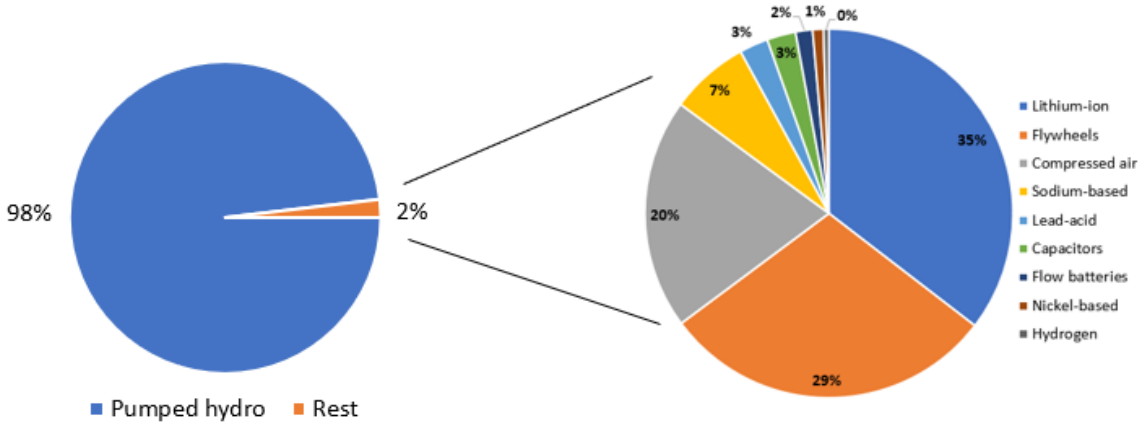

Figure 20: Global EES capacity by technology.

In this chapter a comprehensive overview of the existing and emerging EES systems is carried out, to provide an updated summary and guide to the information extensively published in the literature. The operating principles together with the critical technical and operational features concerning each technology are analyzed. Following, the potential applications that provide support and management in existing and future power system operations are reviewed. Developing a deep understanding of the individual requirements and preferences of the various applications across the power chain, an assessment is conducted in Chapter 7 in order for the appropriate applications to be matched with the best-fit EES option.

6.1. Characteristics of EES

According to the application that the storage devices are intended for use, they are presented favorable or unfavorable as to some performance characteristics. The most essentials include: response time, storage duration, power rating and energy capacity, investment and whole life cost, power and energy density, technical maturity, self-discharge rate, cycle and chronological life, round-trip efficiency, etc. All this information regarding the technical and operational characteristics of each EES technology is included in Tables 8, 9 and 10, 11, respectively.

Table 8. Technical characteristics of EES [70]**.**

Technology	Power Density (kW/m^3)	Energy Density (kWh/m^3)	Specific Power (W/kg)	Specific Energy (Wh/kg)	Power Rating (MW)
PHES	0.01-0.12	0.5-.133	0.01-0.12	0.5-1.5	100-5000
CAES	0.04-10	0.4-20	2.2-24	10-30	5-300
SS-CAES	>10	>20	-	140	0.003-3
LAES	-	80-120	-	214	10-200
Flywheel	40-2000	0.25-424	1000	5-100	0-0.25
Lead-acid	10-400	25-90	180	30-50	0-20
NiCd	38-141	15-150	140-180	35-60	0-40
NiMH	8-588	39-300	220	50-75	0.01-3
Zn-air	10-208	22-1673	60-225	450-650	0-0.01
NaS	1.3-50	150-345	150-240	120	0.05-8
ZEBRA	54.2-300	108-190	174	120	0-0.3
Li-ion	56-800	94-500	500-2000	100-200	0-0.1
VRB	2.5-33.4	10-33	80-150	30-50	0.03-3
ZnBr	3-8.5	5.2-70	100	75-85	0.05-2
PSB	1.35-4.16	10.8-60	-	15-30	1-15
Reg-FC	1-300	25-770	5-50	200-1200	0-50
Capacitor	15-4500	less than SC	10^5	0.01-0.1	0-0.05
EDLC	15-4500	1-35	500-5000	2.5-15	0-0.3
SMES	300-4000	0.2-13.8	500-2000	0.5-5	0.1-10

Table 9. More technical characteristics of EES [70]**.**

Technology	Energy Capacity (MWh)	Power Capital cost ($/kW)	Energy Capital cost ($/kWh)	Technical Maturity
PHES	500-8000	600-2000	5-100	Mature
CAES	<1000	400-800	2-50	Commercialized
SS-CAES	<0.008	1400-1550	200-250	Commercializing
LAES	2.5	900-1900	260-530	Developing
Flywheel	0.75	250-350	1000-5000	Commercializing
Lead-acid	0.001-40	300-600	200-400	Mature
NiCd	6.75	500-1500	800-1500	Commercialized
NiMH	-	270-530	200-730	Mature
Zn-air	-	100-250	10-60	Developing
NaS	0.4	>1000	300-500	Commercialized
ZEBRA	-	150-300	100-200	Commercializing
Li-ion	0.004-10	1200-4000	600-2500	Commercialized
VRB	2	600-1500	150-1000	Commercializing
ZnBr	4	700-2500	150-1000	Demonstration
PSB	0.06	700-2500	150-1000	Developing
Reg-FC	0.312	500	15	Developing
Capacitor	-	200-400	500-1000	Commercialized
EDLC	0.0005	100-300	300-2000	Developing
SMES	0.015	200-300	1000-10000	Commercializing

The tabulated technologies refer to pumped-hydro energy storage (PHES), compressed-air energy storage (CAES), small-scale CAES (SS-CAES), liquid-air energy storage (LAES), different chemistries of secondary and flow batteries, regenerative fuel cells (Reg-FC), electrochemical double-layer capacitor (EDLC) and superconducting magnetic energy storage (SMES). Zn-air is the battery technology with the best volumetric and gravimetric energy density, which means that it constitutes the lightest option and occupy the least space. Flywheels, EDLC and SMES offer the highest energy capital cost while the highest power capital cost is provided by Li-ion secondary batteries.

The lifetime given in years promotes PHES and CAES. When measured in cycles, SMES and EDLC become more advantageous among others. Another important parameter refers to the daily self-discharge rate which reflect the stand-by, parasitic losses mostly affecting flywheels and EDLC. This critical parameter determines the suitable storage duration for each EES device. A further feature regards autonomy which defines the duration that a storage system can operate autonomously. For each technology, it is calculated by dividing the maximum energy capacity by the system power rating.

Table 10. Operational characteristics of EES [70]**.**

Technology	Daily self-discharge (%)	Lifetime (years)	Cycling times (cycles)	Round-trip efficiency (%)	DoD (%)
PHES	almost 0	30-50	10000-30000	70-85	95
CAES	almost 0	30	8000-12000	42-54	100
SS-CAES	almost 0	23+	30000	17-57	100
LAES	almost 0	25+	-	55-80	100
Flywheel	55-100	20	10^5-10^7	90-95	100
Lead-acid	0.1-0.2	5-15	200-2000	85-90	80
NiCd	0.1-0.2	10-20	1500-3000	60-90	100
NiMH	5-20	2-15	1200-1800	50-80	50
Zn-air	almost 0	0.17-30	100-300	50	100
NaS	almost 0	10-15	1500-5000	89-92	100
ZEBRA	20	10-14	1000	70-85	80
Li-ion	0.03	5-15	3000-10000	~100	80
VRB	almost 0	5-10	>16000	85	100
ZnBr	almost 0	5-10	2000-3500	75	100
PSB	almost 0	10-15	800-2000	75	100
Reg-FC	0.06-3	5-15	20000	20-50	90
Capacitor	40	~5	10^6	95	100
EDLC	20-40	10-12	10^6	85-98	100
SMES	10-15	20+	almost infinitely	95	100

Table 11. More operational characteristics of EES [70]**.**

Technology	Response time	Suitable storage duration	Autonomy at power rating	O&M cost ($/kW-year)
PHES	mins	hours-months	1-24h	3
CAES	mins	hours-months	1-24h	19-25
SS-CAES	sec-mins	3h	3h	very low
LAES	mins	hours	several hrs	-
Flywheel	msec	secs-mins	15sec-15min	20
Lead-acid	msec	mins-days	secs-hrs	50
NiCd	msec	mins-days	secs-hrs	20
NiMH	-	-	-	-
Zn-air	-	hours-months	secs-24h	-
NaS	msec	secs-hours	secs-hrs	80
ZEBRA	-	secs-hours	secs-hrs	-
Li-ion	msec	mins-days	mins-hrs	-
VRB	msec	hours-months	secs-10h	70
ZnBr	msec	hours-months	secs-10h	-
PSB	msec	hours-months	secs-10h	-
Reg-FC	secs	hours-months	secs-24h	0.002-0.02
Capacitor	msec	secs-hours	secs-hrs	13
EDLC	msec	secs-hours	secs-hrs	6
SMES	msec	≤30mins	mins-hrs	18.5

Broadly, EES systems are categorized into three types according to their power rating. PHES, CAES and LAES are suitable for large-scale applications (>100MW). Pb-acid, NiCd, PSB, SMES and regenerative FCs are suitable for medium-scale (10-100MW), while SS-CAES, flywheels, supercapacitors, NiMH, VRB, ZnBr, NaS, ZEBRA, Zn-air and Li-ion are falling into small-scale of lower than 1-3MW.

According to the time-scale of response, the various EES are distinguished to fast, relatively fast and not rapid. With response times within milliseconds to seconds, flywheels, supercapacitors, SMES, all kind of batteries and flow batteries, are falling into fast-response systems. Regenerative FCs together with SS-CAES provide relatively fast response in the range of seconds, whereas PHES, large-scale CAES and LAES offer slower response times of a few minutes.

The storage duration is a key element which helps distinguishing the EES technologies into short-term (seconds-minutes), medium-term (seconds-hours) and long-term (minutes-days). Storage duration is directly affected by self-discharge ratio and thus short-term storage is provided by flywheels due to their very high daily energy dissipation. Medium-term is offered by electromagnetic supercapacitors and SMES due to increased

parasitic losses, high-temperature/Na-based batteries because of the self-heating needs to maintain the operating temperature, SS-CAES and LAES. PHES, large-scale CAES, Pb-acid, NiCd, Li-ion, Zn-air, flow batteries and regenerative FCs are capable for providing long-term storage duration. However, Pb-acid, NiCd, and Li-ion batteries possess a moderate self-discharge rate and consequently they become inappropriate for storage durations longer than tens of days.

Related to storage capability, autonomy constitutes an important attribute in isolated systems and micro-grids relying on intermittent renewable sources. It refers to the duration that an EES system is able to continuously supply energy. Hence, EES technologies can be classified in terms of their energy capacity (amount of stored energy) against the power they can deliver (power rating). Typically, less autonomy is expected from electromagnetic devices of supercapacitors and SMES along with the flywheels. Higher autonomy involves SS-CAES, conventional and high-temperature batteries while PHES, large-scale CAES, LAES, flow batteries, Zn-air and regenerative FCs are considered capable of supplying autonomously for several hours.

Cycle or round-trip efficiency is a further key element in evaluating the EES options in power system applications. Very high efficiencies (>90%) appear in electromagnetic storage systems, flywheels and Li-ion batteries. The rest of batteries and flow batteries, SS-CAES and LAES provide high efficiencies of over 60%. Large-scale CAES, Zn-air and regenerative FC constitute more energy-intensive conversion processes and thus they provide low efficiencies which in the case of regenerative FCs may fall even by 20%. It must be noted that in some applications, efficiency becomes a crucial factor and even the cheapest technologies may be considered unsuitable. Such an example could be energy arbitrage where the electrical energy may be purchased and sold back excluding conversion losses. In these cases, the self-discharge rate should also be considered. In addition, the efficiency of transformers and power conversion systems should be included in the estimation since some technologies require high voltage AC to low voltage DC (and back to AC) conversions while others do not [71][72][73].

Additional factors affecting the overall investment cost are lifespan and cycle times. Electromagnetic EES devices provide extremely high cycling capability due to the absence of moving parts and chemical reactions realization. Mechanical components normally determine the lifetime of PHES, CAES and flywheel systems whereas all kind of chemical

EES systems are deteriorated by time due to the chemical elements and electrolytes degradation.

Apart from the significant improvements in efficiency and extended lifetimes, capital and O&M costs tend to be decreased by increasing R&D efforts. In this sense, mature and commercialized PHES and CAES offer the lowest energy capital cost becoming appropriate in high energy/long duration applications, followed by Zn-air and regenerative FCs which need further development to be proved as efficient. In terms of power capital cost, flywheel, supercapacitor and SMES technology are suitable for high power/short duration applications along with commercializing ZEBRA and developing Zn-air and regenerative FC. Flow batteries and Li-ion are still far too expensive while the rest of conventional and high-temperature batteries sit in the middle. Regarding O&M costs, electrochemical technologies that require chemical handling are disadvantageous against others followed by technologies that need additional equipment to maintain the energy stored.

6.2. EES technologies

EES technologies can be categorized by various criteria, such as, suitable storage duration (into short-term, mid-term or long-term), response time (into rapid or not), scale (into small-scale, medium-scale or large-scale) or based on the form of stored energy. A classification of the EES technologies according to the latest method is presented in Figure 21.

Depending on the form that the electrical energy can be stored, EES systems are divided into chemical, electrical, magnetic and mechanical. Batteries and hydrogen storage-fuel cells are falling in the chemical systems, whereas electromagnetic systems involve the supercapacitors and superconductors. Mechanical systems can be subdivided into kinetic energy storage including flywheels and potential energy storage where pumped hydro and compressed air systems are classified. Following, a detailed description along with the main technical characteristics regarding each storage technology is carried out.

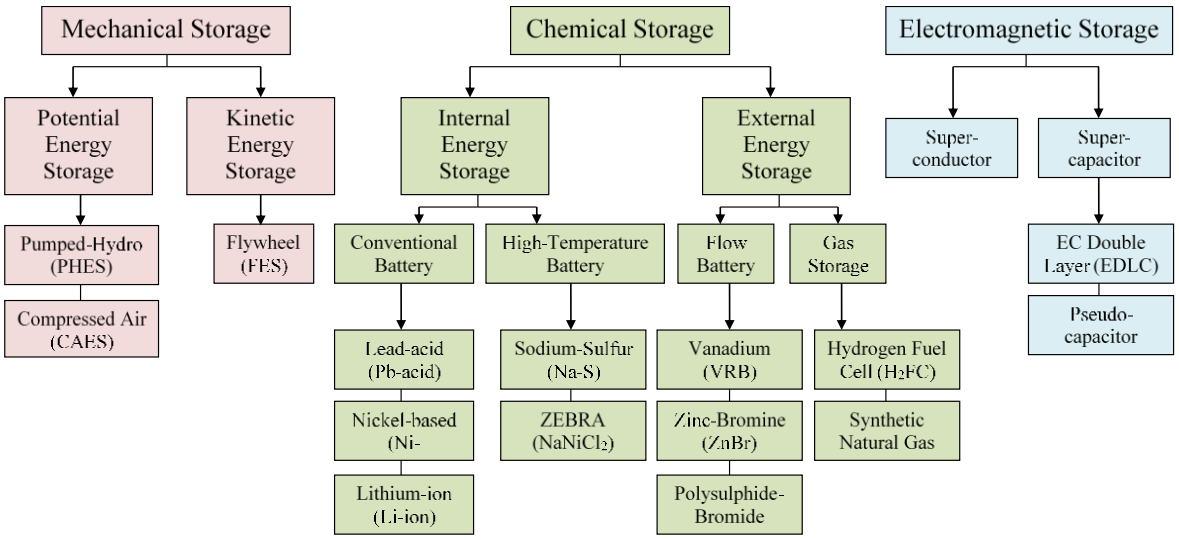

Figure 21: Classification of EES technologies by the form of stored energy [74]**.**

6.2.1 Pumped hydro

Pumped hydro energy storage (PHES) is currently the only proven and by far the most adopted technology for large scale (>100 MW) energy storage [75][76]. As shown in Figure 22, a PHES station typically consists of reversible pumps/generators through which, electricity is utilized by pumps to move water from a lower to an upper reservoir during off-peak hours and thus electric energy is stored in the form of hydraulic potential energy, whereas water is released from the upper reservoir during peak hours in order to produce electricity by generators [77]. Hence, the amount of stored energy is proportional to the height difference between the reservoirs h and the mass of water stored m according to Equation (6.1).

$$E = mgh \tag{6.1}$$

PHES technology is readily available offering long life in the range of 30-50 years, low operation and maintenance (O&M) cost and cycle efficiencies of average 75% due to elevation plus conversion losses [78]. It provides the highest capacity of all available technologies, since its size is limited only by the size of the upper reservoir. However, this technology requires specific site conditions the most essential of which are the availability of technically suitable locations with access to water [75]. Unfortunately, the high capital cost and environmental concerns are still the further limiting factors for PHES to be utilized as a storage technology option [79].

Since 1929 when the world's first large scale plant was constructed, there are now over 300 PHES plants with a total installed capacity of over 120 GW, representing almost 99% of worldwide installed electrical storage capacity and about 3% of global generation [80][81][82]. Due to their not-rapid response, PHES plants were initially built for energy management applications to maximize the base-load generation. Assuming that most of the suitable locations with a remarkable height difference have already been exploited, in short-term, innovative pumped hydro are foreseen to be upgraded by adding more turbines in order to become more flexible and offer higher ramp rates over a shorter time. This will also eliminate the main drawback of extremely long construction time needed.

A second innovation developed in recent years and being the focus of research for PHES technology, involves the variable-speed pump-turbines, enabling increased flexibility, efficiency and reliability in the expense of cost [83][84]. Aiming to address the constraints of suitable site availability and environmental impact, alternative reservoir types such as sub-surface instead of over-ground reservoirs, storing sea-water instead of fresh water and other innovative sea-based solutions have been studied. Apart from the increase in the suitable locations, by utilizing the open sea as the lower reservoir, the concerns over fresh water use are reduced.

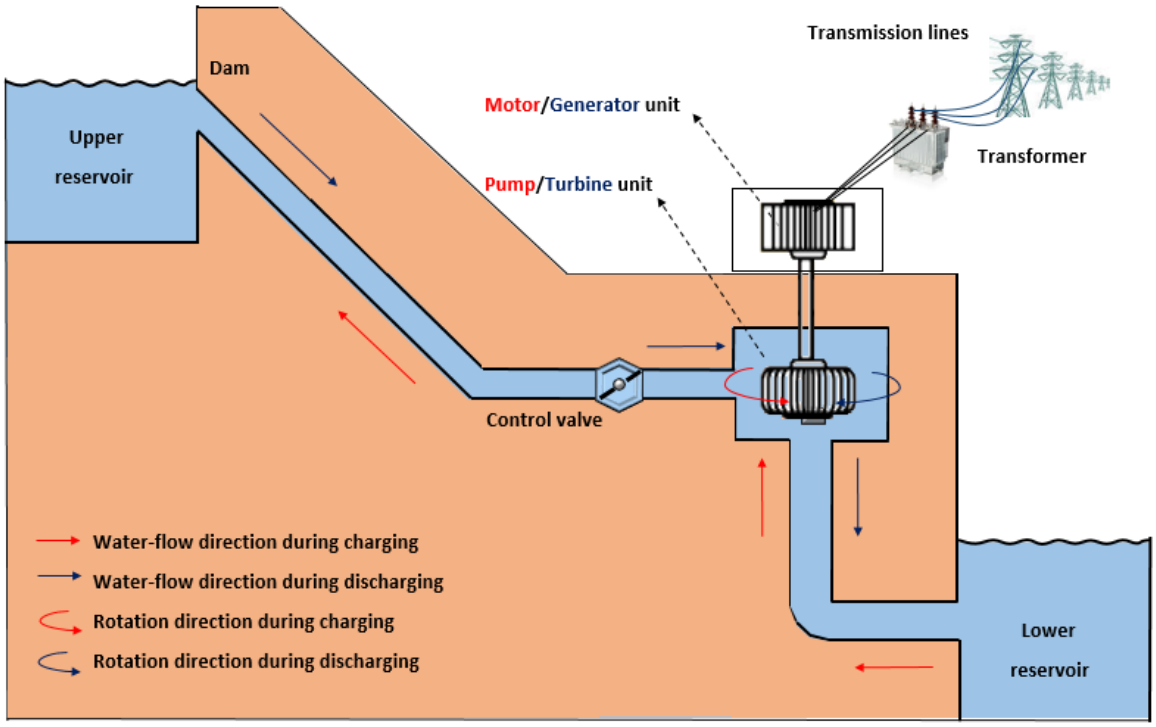

Figure 22: Schematic diagram of pumped hydro storage plant [70]**.**

However, additional costs relating to pumping may occur in both proposed technologies due to an event of a fracture or even a collapse in the sub-surface of a PHES, or the corrosive environment of operation in sea-water pumped hydro [84][85]. Finally, minimal environmental impact, larger energy capacities and reduced costs are also expected from other solutions proposed, such as the hydraulic lifting of masses during charging and discharge by releasing them to sink gravitationally forcing the water to pass through a turbine. Although these research proposals seem technically and economically feasible, a demonstration plant is needed for their commercialization and their contribution in a sustainable development [7].

6.2.2 Compressed air

Compressed air energy storage (CAES) systems are mainly equipped with a motor/generator, compressor and expander units, a turbine train and the storing cavity [78]. Typically, during off-peak hours, low-cost or excess electricity is used for storing high-pressured compressed air in a suitable underground cavern so electrical energy is converted into elastic potential energy which can be converted back into electricity during a peak of demand by the air being heated and expanded in a gas turbine [86]. In Figure 23, a schematic diagram of such a facility plant is presented. CAES is achieved at high pressures (typically 40-80 bar) at near ambient temperatures, resulting in less volume and consequently smaller storage reservoirs, the best option of which is given by deep caverns made of high quality rock, ancient salt mines or underground natural gas storage caves [87].

CAES is considered as one of the highest economic utility-scale storage technology which may contribute to future sustainable energy systems with a high share of fluctuating energy sources [86][88]. This technology offers high reliability in combination with low environmental impact and in addition, the storage volume is located underground which means that no further landscape is required [89]. Possessing high commercial maturity, CAES systems can provide huge capacities (>100 MW) but they require both special site preparations and underground storage caverns which may not exist [77]. However, in areas without water or suitable reservoir locations CAES is the only storage technology option which could be used on large scales [89]. There are only two operating first-generation systems, the first built in Germany (in 1978) and the second in Alabama (in 1991) [9][90].

Although CAES occupies a small land, it is associated with greenhouse gas emissions. In addition, first-generation, traditional CAES systems, exhibit low efficiencies in the range of 42-54% due to increased heat losses to the atmosphere during compression and thermal energy requirements when the decompressed air cools down the turbine [91]. To address the two critical issues constrained the overall efficiency, advanced adiabatic and isothermal CAES systems have been designed. Second-generation CAES systems exploit the heat released during compression process, which is transferred and stored in heat storage sites [92]. Advanced adiabatic CAES (AA-CAES) tends to consume little or no fuel or external energy to heat up the air during expansion, increasing the overall efficiency to a theoretical of 70% and eliminating the associated emissions [93][94][95][96][97].

Isothermal CAES includes the by-produced heat removal during compression to maintain a constant temperature and thus avoiding the expense needed to create a thermal storage. This can be achieved by compressing the air slowly, allowing the temperature to equalize with the surroundings [98]. These systems occur promising in terms of improved efficiencies in the range of 70-80% and relatively low costs [95].

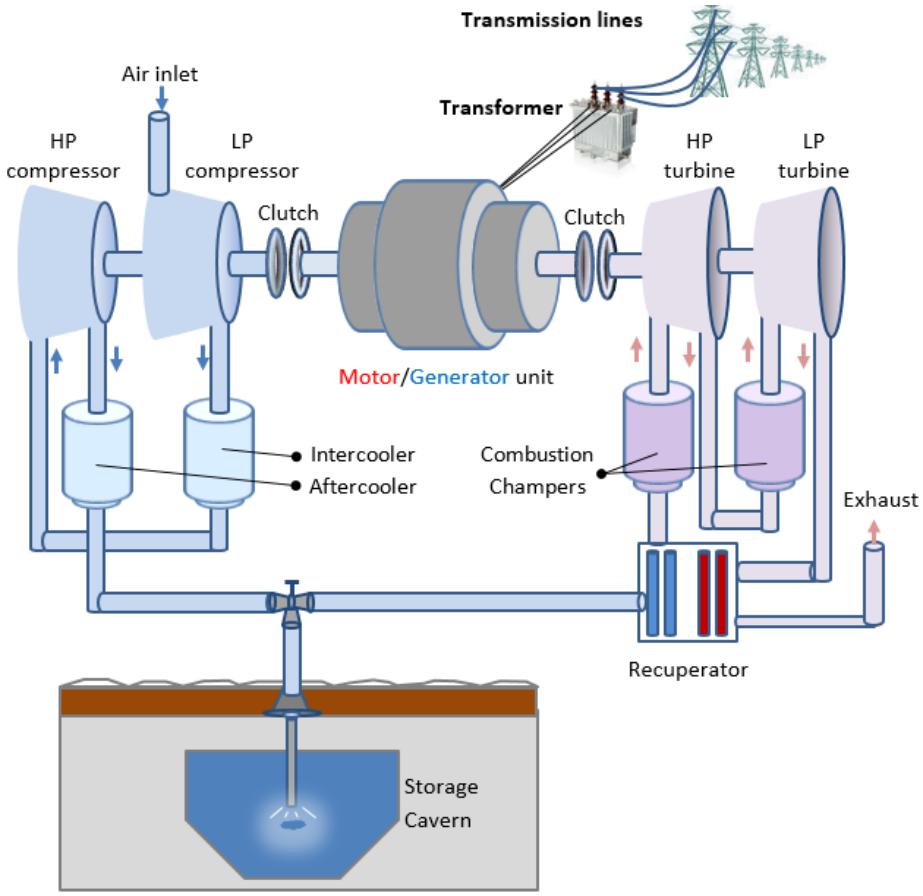

Figure 23: Schematic diagram of compressed air storage plant [70]**.**

Liquid air energy storage (LAES) is a new concept that is attracting attention. The whole equipment comprise a LAES plant is similar to that of CAES facility. It defers in that the heat lost to the atmosphere during air compression, in the instance of LAES is stored in a phase change material (PCM). Typically, employing cryogenic energy storage, the atmospheric air is converted into cryogen liquid and thus electrical and thermal storage are simultaneously achieved. When needed, the stored liquid is converted back to the gaseous state by being exposed to ambient temperature and expanded in turbine. LAES offer long storage duration and promising round-trip efficiency of up to 80% [78].

CAES options without the need of thermal or suitable underground storage caverns can be built in smaller scales. Small scale CAES (SS-CAES) has attracted the interest especially for industrial applications, to provide uninterruptible and buck-up power supply [99]. However, by using efficient and well-designed artificial storage vessels, it can significantly reduce the costs and associated emissions in distributed generation systems [95][100]. SS-CAES is considered less cost-effective than large-scale CAES, it therefore offers greater power and energy densities along with faster response [101]. Further advancements in the absence of underground cavern, refers to underwater-ocean storage in chambers to maintain the stored air pressure constant. Although they could be integrated with off-shore renewable generation technologies, they are at their infancy or exist on pilot scale only [85].

6.2.3 Flywheels

Flywheel energy storage (FES) device is comprised of a massive cylinder supported by bearings. In a high-speed (up to 100,000 rpm) structure magnetic bearings and composite disk are used, all contained in a vacuum to eliminate frictional losses and protect them from external disturbances, whereas low-speed (up to 10,000 rpm) FES includes mechanical bearings, steel flywheel and no vacuum enclose [102][103][104]. In Figure 24, a modern high-tech FES system is depicted in upright position to prevent gravity influence. In a FES system, electricity powers an electric motor which spins and increases the speed of the flywheel, thus converting electricity into kinetic energy the amount of which is proportional to the flywheel's rotor inertia (J) and to the square of its angular velocity (ω) [105]. When short-term back-up power is demanded, electricity is recovered by the same motor, acting then as a generator, which causes the flywheel to slow down thus the rotational energy is

converted back into electricity [59]. The energy stored in a flywheel can be calculated by equation (2). Since the moment of inertia depends on shape and mass of the flywheel ($J = 0.5mr^2 = 0.5\rho\alpha\pi r^4$), the stored energy increases by increasing the disk radius or using high density material [104].

$$E = \frac{1}{2}J\omega^2 \tag{6.2}$$

Flywheels have the ability to provide both high energy and power density for short duration discharges. High efficiency in the range of 90-95% can also be achieved through the use of a vacuum pump, permanent and magnetic bearings, which are necessary to overcome the friction forces during operation [77][78]. Furthermore, they offer extended cycle lives and as a buffer store could remove the need for downstream power electronics, to track the fluctuations derived from variable sources, which results in improved overall electrical efficiency [106][107]. Further advantages compared to other EES systems include their insensitivity to environmental conditions and no hazardous chemicals production [108]. Apart from the fact that flywheel technology is high costly, to store energy in an electrical power system high capacity flywheels are needed with the impact of increased friction losses and the consequent reduced efficiency [87]. According to those mentioned above, it is apparent that long-term storage of this type of devices is not feasible thus flywheels are employed in high power/short duration applications or as a supplement to batteries in uninterruptible power supply (UPS) systems [78][59]. In short-term, their contribution in the transport sector is expected to increase as an environmentally benign technology, capable of improving the overall efficiency and fuel economy in vehicles [109][110].

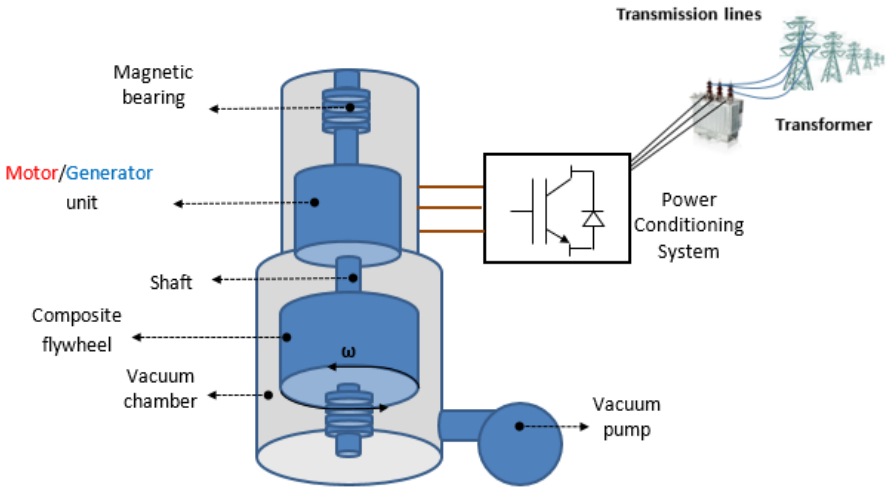

Figure 24: Schematic diagram of flywheel energy storage system [70]**.**

6.2.4 Batteries

Batteries are classified as primary which are not rechargeable and secondary which can be recharged. Rechargeable or secondary batteries consist of cells each comprising two electrodes immersed in an electrolyte and they can store and provide energy by electrochemical reversible reactions. Generally, during these reactions, the anode or negative electrode is oxidized providing electrons while the cathode or positive electrode is reduced accepting electrons through an external circuit connected to the cell terminals [77]. In order to adjust power generation to changing demand many technologies have been proposed and depending on the materials used as electrodes and electrolytes, secondary batteries can be divided into lead-acid, alkaline, metal-air, high temperature and lithium-ion [71].

As the oldest type of rechargeable batteries (invented in 1859), lead-acid (Pb-acid) is widely used in vehicles and boats for engine starting and a host of other facilities, but is therefore considered as one of the best suited for stationary applications as it can supply excellent pulsed power [42]. A schematic diagram of a Pb-acid battery operation is shown in Figure 25. In the charged state, the battery consists of lead (Pb) and lead oxide (PbO_2) both in 37% sulfuric acid (H_2SO_4), whereas in the discharged state, lead sulphate ($PbSO_4$) is produced both at the anode and the cathode while the electrolyte changes to water [85]. The chemical reactions at the anode and cathode are presented by equations (6.3) and (6.4), respectively [111]. The rated voltage of a Pb-acid cell is 2V and capable of operating in the range of -5 and 40^{o}C [77][112][113]. Although lead-acid technology has maturity of over a century and low manufacturing cost, the lead and sulfuric acid used to form the anode and the electrolyte respectively are toxic and its cycle life is relatively limited. In addition, flooded type devices require periodic water maintenance and large footprint due to their low specific energy (25Wh/kg) and discharging depth (70%), thus they become unfavorable for large-scale applications. From the invention of valve regulated lead-acid (VRLA) batteries, banks of up to 36MW are already being utilized for power generation from RES, as they achieve higher specific energy (30-50Wh/kg) and depths of discharge (80%) with negligible maintenance requirements [112][114].

$$Pb + SO_4^{2-} \rightleftharpoons PbSO_4 + 2e^- \quad (6.3)$$

$$PbO_2 + SO_4^{2-} + 4H^+ + 2e^- \rightleftharpoons PbSO_4 + 2H_2O \quad (6.4)$$

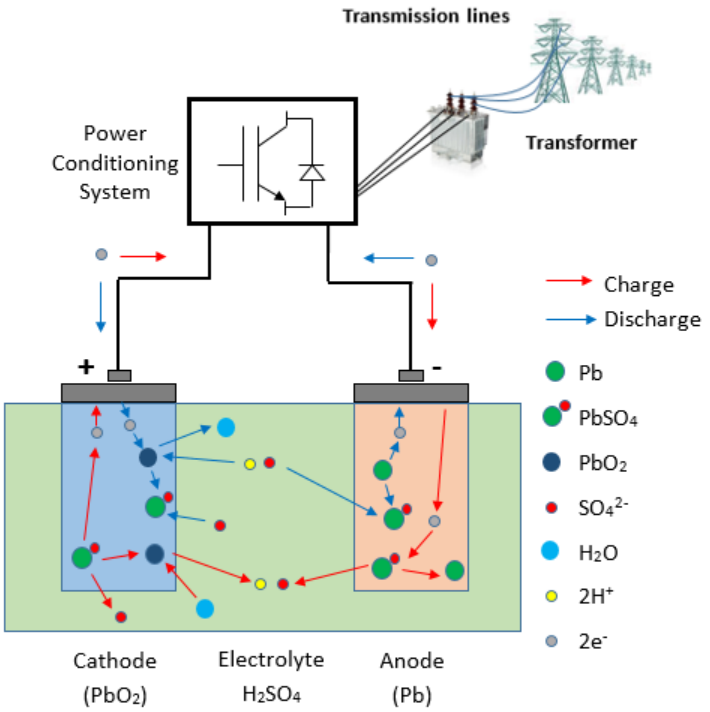

Figure 25: Schematic diagram of Pb-acid battery energy storage system [115]**.**

Nickel-iron (NiFe), nickel-cadmium (NiCd) and nickel-metal-hydride (NiMH) represent the alkaline batteries comprising nickel oxide for cathode and potassium hydroxide for electrolyte. The nickel-iron battery is considered unsuitable for electrical storage as it provides low electrical efficiency in combination with its self-discharge effect and as the corrosive iron anode requires high water maintenance [71]. Conversely, nickel-cadmium batteries are widely used in both portable and stationary applications providing chief advantages compared to lead-acid such as higher specific energy (60Wh/kg), longer cycle life (1500-3000 cycles) and lower water maintenance requirements, against the higher manufacturing cost [65].

At the charging state, they consist of a nickel oxyhydroxide NiOOH cathode, a metallic cadmium Cd anode, a separator and an alkaline electrolyte [78]. During the discharging process, the cathode NiO-OH reacts with water which exists in the aqueous potassium hydroxide ($KOH.H_2O$) to produce $Ni(OH)_2$ and hydroxide ion at the anode. The reversible reactions are given in equations (6.5) and (6.6) for the anode and cathode, respectively, while a better explanation can be obtained by Figure 26 through a flow diagram. However, both its maximum capacity and whole life are subject to memory effect and thus cannot be repeatedly recharged after being partially discharged [116].

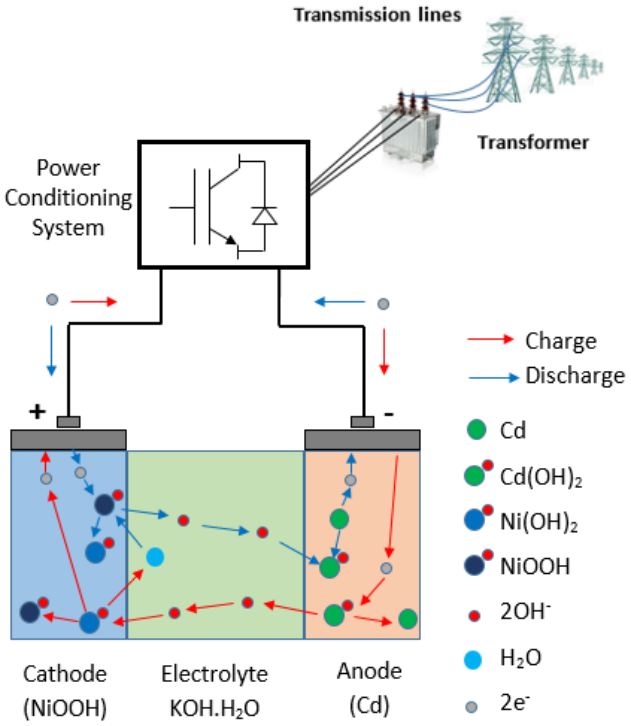

Figure 26: Schematic diagram of Ni-Cd battery energy storage system [115].

Similar to lead-acid, nickel-cadmium spent batteries create environmental concerns because of cadmium and nickel toxicity, and consequently are largely displaced [117].

As regards nickel-metal-hydride (NiMH), it defers in that a hydrogen-absorbing alloy is used to form the electrode instead of cadmium. The electrochemical reactions at the anode and cathode of such a device are represented by equations (6.7) and (6.8) respectively. Possessing the same with NiCd cell voltage of 1.2V, NiMH can achieve higher specific energy (up to 75Wh/kg) and reduced memory effect. In the contrary, it suffers from severe self-discharge issues (20% per day) and lower efficiency, thus it becomes an undesirable candidate for electrical storage from RES [102][118][119][120]. Nevertheless, the distinct advantage of the wide temperature-range of operation (from a minimum of -40 to 50^{o}C) of Ni-based batteries, make their use possible for some utility-scale EES applications [91].

$$Cd + 2OH^- \rightleftharpoons Cd(OH)_2 + 2e^- \quad (6.5)$$

$$2NiOOH + 2H_2O + 2e^- \rightleftharpoons 2Ni(OH)_2 + 2OH^- \quad (6.6)$$

$$MH_x + OH^- \rightleftharpoons M + \frac{x+1}{2}H_2O + e^- \quad (6.7)$$

$$NiO(OH) + H_2O + e^- \rightleftharpoons Ni(OH)_2 + OH^- \quad (6.8)$$

Metal-air batteries can be considered as special types of fuel cell which use metal instead of fuel and air as the oxidant. The anodes in these batteries are commonly available metals with high energy density such as lithium (Li), aluminum (Al) or zinc (Zn), while the cathodes are made of either porous carbon or metal mesh capable of absorbing oxygen (O_2) from air. The liquid or solid electrolytes are mainly good hydroxide ion (OH^-) conductors like potassium hydroxide (KOH) [112]. Although Li-air has a theoretical specific energy as high as 11140Wh/kg, there are concerns about a probable fire due to the high reactivity of Li with humid air [82][121][111]. Moreover, it possesses a much more expensive cell compared to Zn-air, which is environmentally benign and exhibits long storage life while un-activated [116].

Hence, Zn-air represents the only technically feasible example of metal-air batteries up to date, offering a high energy density (650Wh/kg). It provides a cell voltage of 1.6V, temperature range from -20 to 50°C and negligible self-discharge rate. On the contrary, it is difficult to be recharged and offers a limited cycling capability of a few hundred cycles along with a quite low efficiency of fairly 50% [78]. However, Zn-air constitutes a developing technology that occurs promising and able to contribute in future energy management applications. The chemical reactions, at the anode and cathode of a Zn-air cell shown in Figure 27, are provided in equations (6.9) and (6.10), respectively.

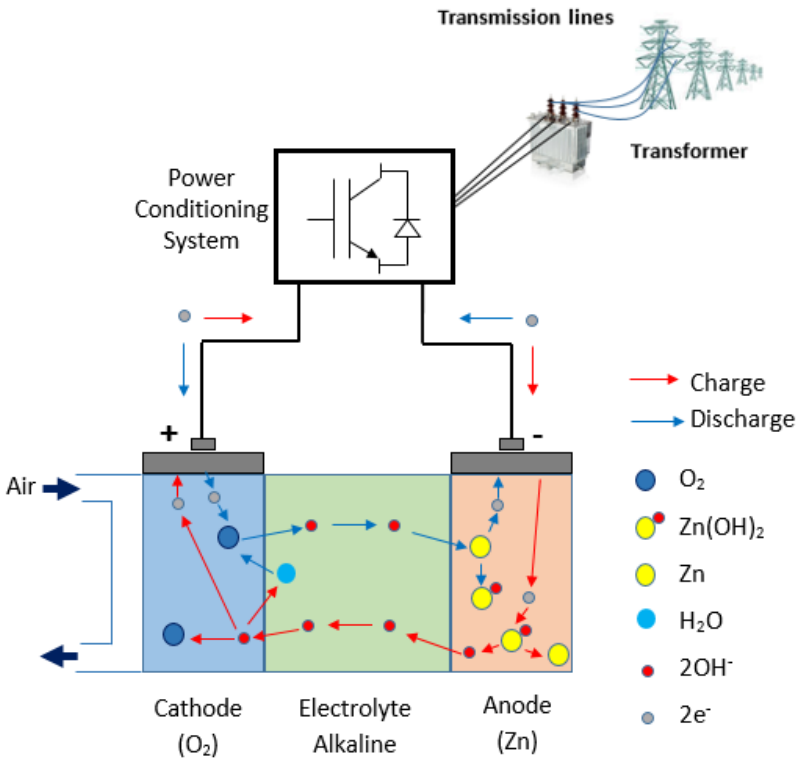

Figure 27: Schematic diagram of Zn-air battery energy storage system [115].

Other metals proposed to form the anode of a metal-air cell can be represented by a similar manner. Equations (6.11) and (6.12) are given as an example of an under-research metal-air battery of aluminium (Al) anode.

$$Zn + 2OH^- \rightleftharpoons Zn(OH)_2 + 2e^- \quad (6.9)$$

$$H_2O + \frac{1}{2}O_2 + 2e^- \rightleftharpoons 2OH^- \quad (6.10)$$

$$Al + 4OH^- \rightleftharpoons \{Al(OH)_4\}^- + 3e^- \quad (6.11)$$

$$\frac{3}{4}O_2 + \frac{3}{2}H_2O + 3e^- \rightleftharpoons 3OH^- \quad (6.12)$$

High temperature batteries consist of molten sodium anode material, a solid electrolyte of beta-alumina and according to the cathode solid reactant they are subdivided into sodium-sulfur (NaS) and sodium-metal-chloride (NaNiCl or ZEBRA) [122]. NaS batteries are constructed from inexpensive materials and are considered as an attractive option for large-scale stationary electrical storage applications since they offer high energy density (150-345kWh/m^3) and cycle efficiency (89-92%), long cycle life (1500-5000 cycles) and they are much smaller and lighter than NiCd, NiMH and Pb-acid [102][114][123].

The main disadvantages of NaS technology are the corrosive nature of manufacturing materials and the requirement for constant heat input in order to maintain the electrolyte's molten state which is ensured at 300-350^{o}C increasing the hazard of probable reaction between electrode materials and associated fire [71]. A demonstration of a charge/discharge cycle concerning a NaS cell is illustrated in Figure 28 while the reactions realized at the negative and positive electrodes are shown in equations (6.13) and (6.14) respectively.

On the other hand, ZEBRA technology has some advantages relative to NaS systems including lower mean temperature of 250 to 350^{o}C and a much safer cell, no corrosion problems, high cell voltage (2.58V) and the ability to withstand limited overcharge and discharge [65][60]. The overall chemical reaction occur in a ZEBRA battery is represented by the equation (6.15).

$$2Na \rightleftharpoons 2Na^{+} + 2e^{-} \quad (6.13)$$

$$S + 2e^{-} \rightleftharpoons S^{2-} \quad (6.14)$$

$$2NaCl + Ni \rightleftharpoons NiCl_2 + 2Na \quad (6.15)$$

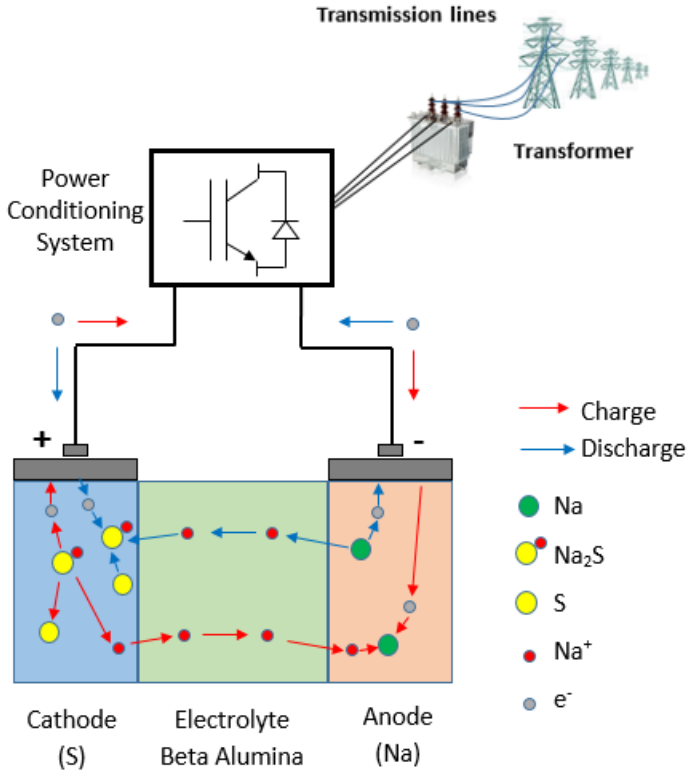

Figure 28: Schematic diagram of Na-S battery energy storage system [115].

The last major type of battery storage technology is lithium-ion (Li-ion) system containing a graphite anode, a cathode formed by a lithium metal oxide ($LiCoO_2$, $LiMO_2$, $LiNiO_2$ etc.) and an electrolyte consisting of a lithium salt dissolved in an organic liquid (such as $LiPF_6$), thus electrodes can reversibly accommodate ions and electrons [124]. Finally, a separator is deployed in order to prevent a short-circuit between the electrodes and associated hazard of flame burst. A typical structure of a Li-ion battery with a cathode made of $LiCoO_2$ is demonstrated in Figure 29.

During discharging, lithium atoms (Li) are oxidized to lithium ions (Li^{+}) releasing electrons. While the electrons are flowing through the external circuit to reach the cathode, Li^{+} are moving through the electrolyte to the cathode where they react with the cobalt oxide

(CoO_2) and electrons to form lithium cobalt oxide ($LiMO_2$) [125]. Equations (6.16) and (6.17) show the chemical reactions realized at the anode and cathode of the demonstrated example. However, the reactions can be generalized into equations (6.18) and (6.19) to explain the similar operation occur if different lithium metal oxides ($LiMO_2$) are used to form the cathode [78][91].

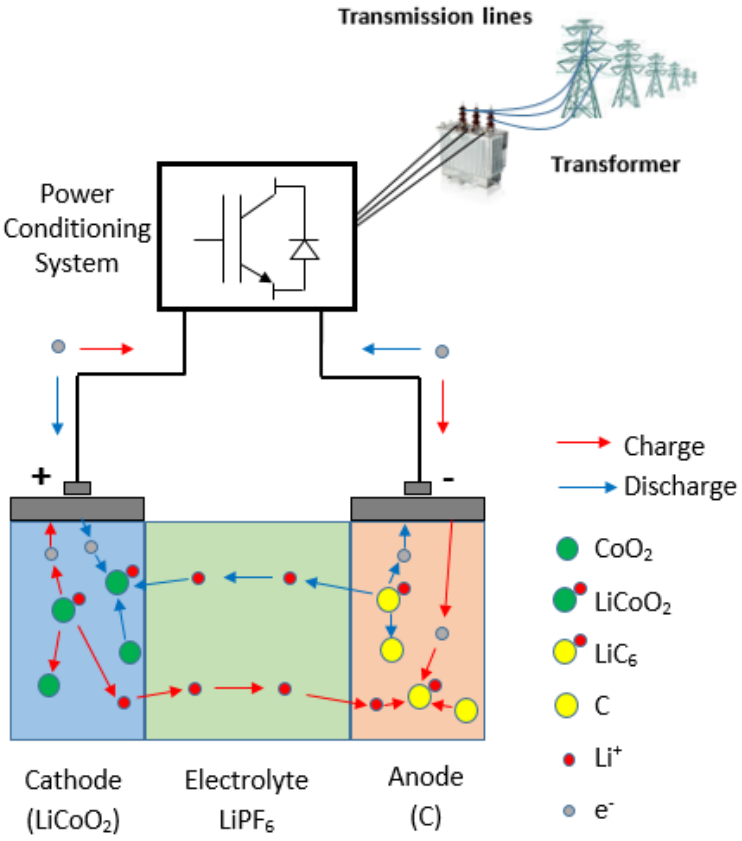

Figure 29: Schematic diagram of Li-ion battery energy storage system [115].

Lithium-ion batteries offer chief advantages over the nickel-cadmium and lead-acid, as they provide the highest specific energy (200Wh/kg), specific power (500-2000W/kg) and nominal voltage (3.7V), energy storage efficiency of close to 100%, lower self-discharge rate (0.03% per), no memory effect and extremely low maintenance requirements [77][85]. Moreover, their small size and low weight make them suitable to portable applications (such as in smartphones and laptops) where are almost exclusively being used and electric vehicles where are proved to become the most promising option [114]. Despite the above advantages, the high cost as well as the prohibitive for their lifetime deep discharging, are the main drawbacks of lithium-ion batteries that restrict their use in large-scale applications [102].

Although considerable efforts are paid to lower the cost, concerns still exist relating to an increasing consumption in the future, since the depleting worldwide lithium reserves may lead to increasing raw material costs [110][126]. A further disadvantage is the sensitivity they provide to high temperatures and thus are equipped with a battery management system to at least provide overvoltage, over-temperature and overcurrent protection [110][127]. Their suitable temperature range of operation is rated between -30 and 60^{o}C [112].

$$LiC_6 \rightleftharpoons Li^+ + e^- + 6C \quad (6.16)$$

$$CoO_2 + Li^+ + e^- \rightleftharpoons LiCoO_2 \quad (6.17)$$

$$Li_xC \rightleftharpoons xLi^+ + xe^- + C \quad (6.18)$$

$$LiMO_2 + xLi^+ + xe^- \rightleftharpoons Li_{1+x}MO_2 \quad (6.19)$$

6.2.5 Flow Batteries

In contrast to conventional batteries which store energy in solid state electrodes, flow batteries convert electrical energy into chemical potential which is stored in two liquid electrolyte solutions located in external tanks, the size of which determines the capacity of the battery [65]. The principal three existing types of flow batteries are vanadium-redox (reduction-oxidation), zinc-bromine and polysulfide bromide. Flow batteries may require additional equipment, such as pump sensors and control units. They may also provide variable and generally low energy density, however they present major advantages in comparison with standard batteries as they have long cycle life, quick response times, can be fully discharged and they can offer unlimited capacity by increasing their storage tank size [114].

The vanadium redox flow battery (VRB) is one of the most mature flow battery system [78][112]. In such a system, vanadium in sulfuric acid is employed in both the electrolyte loops but in different valence states [71]. Thus, it stores energy by using

vanadium redox couples (V^{2+}/V^{3+} and V^{4+}/V^{5+}) in the anolyte and catholyte tanks, respectively, as can be seen in Figure 30. By using a hydrogen-ion permeable polymer membrane, H^+ are allowed to reversibly be exchanged through it, balancing the charge in the cell and allowing the chemical reactions of equations (6.20) and (6.21) to occur at the negative and positive half-cells. Consequently, in the charging state the anolyte contains V^{3+} and the catholyte V^{4+}, whereas their containments in the absolute discharged state are V^{2+} and V^{5+}, respectively.

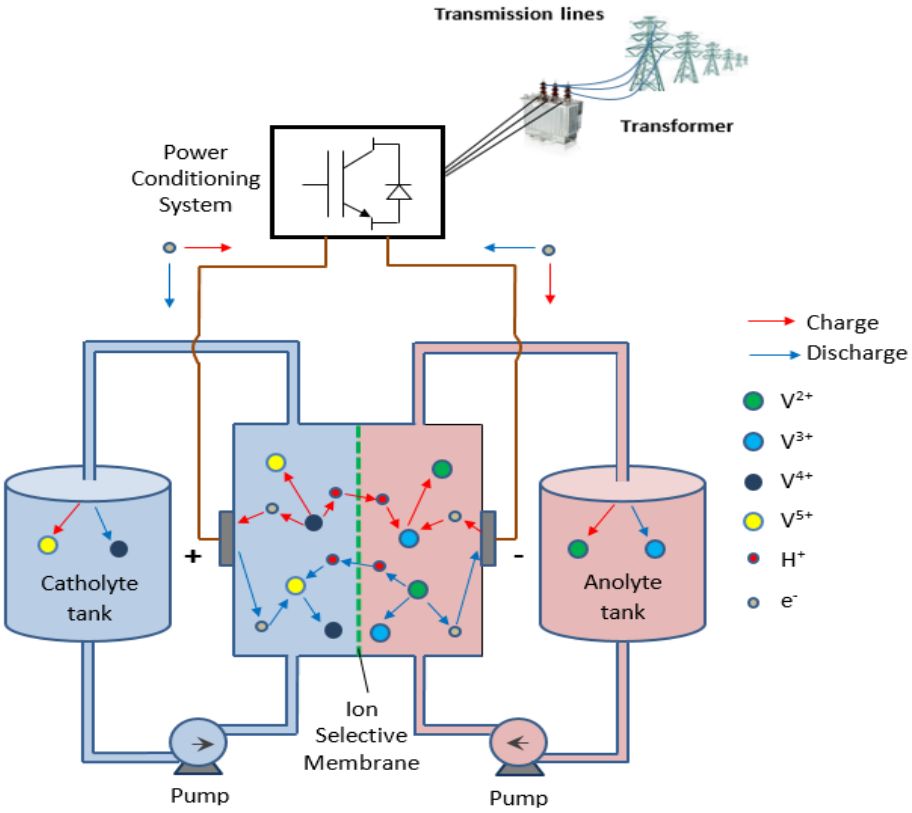

Figure 30: Schematic diagram of vanadium redox flow battery energy storage system [70].

The technical and operational features of a VRB system include 30-50Wh/kg specific energy and 80-150W/kg specific power, fast responses in the order of milliseconds, high cycling capability (>16000 cycles) and relatively high efficiencies of up to 85%. The cell voltage is 1.2-1.6V and the operating temperature in the range of 0-40ºC [112][110]. Also, they offer no self-discharge rate, can withstand deep discharging and require low maintenance [60]. Being able to provide an energy capacity of near 2MWh and considering the aforementioned benefits, VRB is considered as an attractive option for large scale EES

applications and therefore the high capital cost (1500$/kW) needs to be further reduced [128][129].

$$V^{3+} + e^{-} \rightleftharpoons V^{2+} \tag{6.20}$$

$$V^{4+} \rightleftharpoons V^{5+} + e^{-} \tag{6.21}$$

Zinc bromine (ZnBr) falls into the hybrid flow batteries category. Hybrid flow batteries are distinguished from conventional redox flow batteries by the fact that at least one redox couple species is not fully soluble and may be either a metal or a gas [128]. In ZnBr both the electrolyte loops employ an electrolyte of zinc-bromine [65]. In the charge state, metallic zinc (Zn) is plated as a thin film on one side of the carbon-plastic composite electrode while bromine oil (Br_2) sinks to the bottom of the electrolytic tank at the other side (Figure 31).

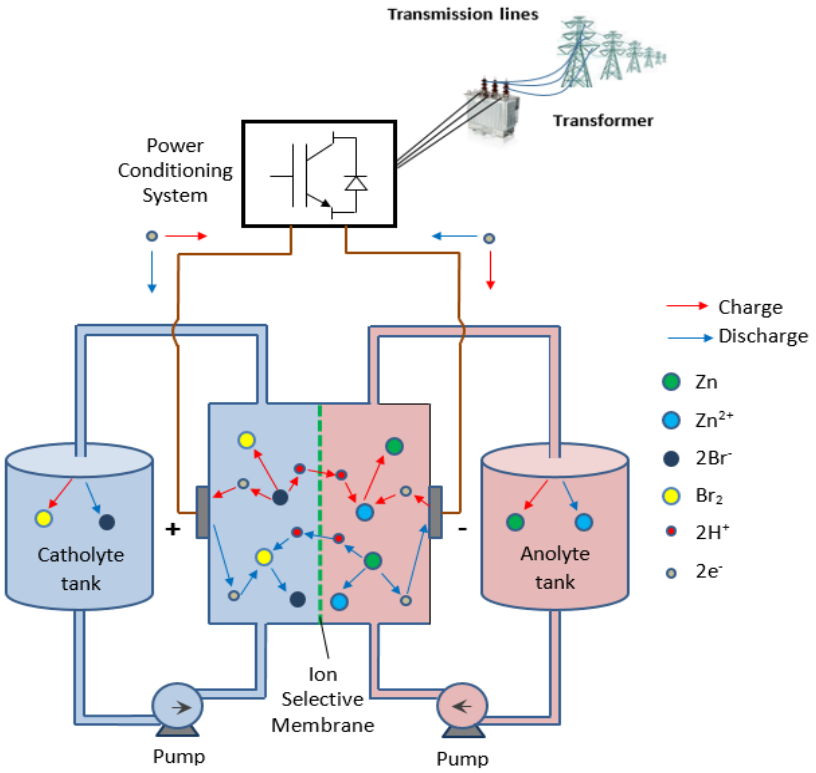

Figure 31: Schematic diagram of zinc bromine flow battery energy storage system [70]**.**

The two compartments are separated by a microporous polyolefin membrane [78]. Equations (6.22) and (6.23) represent the chemical reactions at negative and positive compartment of the ZnBr cell during the reversible process of a charge/discharge cycle.

Similar to VRB, ZnBr offers no self-discharge rate, no degradation due to deep discharge and as narrow temperature operation as VRB [112]. Compared to VRB, ZnBr offers higher specific energy (75-85Wh/kg) and cell voltage (1.8V) [110][60]. The disadvantages of this system are the lower efficiency (75%), cycling capability (2000-3500 cycles) and the metal corrosion [91]. Although many ZnBr devices have been built and tested, their use in utility-scale EES applications is in the early stage of demonstration.

$$Zn^{2+} + 2e^{-} \rightleftharpoons Zn \tag{6.22}$$

$$2Br^{-} \rightleftharpoons Br_2 + 2e^{-} \tag{6.23}$$

Polysulfide bromide (PSB) or Regenesys is a regenerative fuel cell involving a reversible electrochemical reaction between two salt solution electrolytes namely, sodium bromide ($NaBr_3$) and sodium polysulfide (Na_2S_2) and it constitutes another type of redox flow battery [112]. The electrodes are electrically connected through the external circuit while the electrolytes are separated by a polymer membrane that only allows positive sodium ions (Na^{+}) to go through, producing a cell voltage of 1.5V [78][110]. The electrochemical reactions occur at the anode and cathode of the half-cells are respectively represented by equations (6.24) and (6.25).

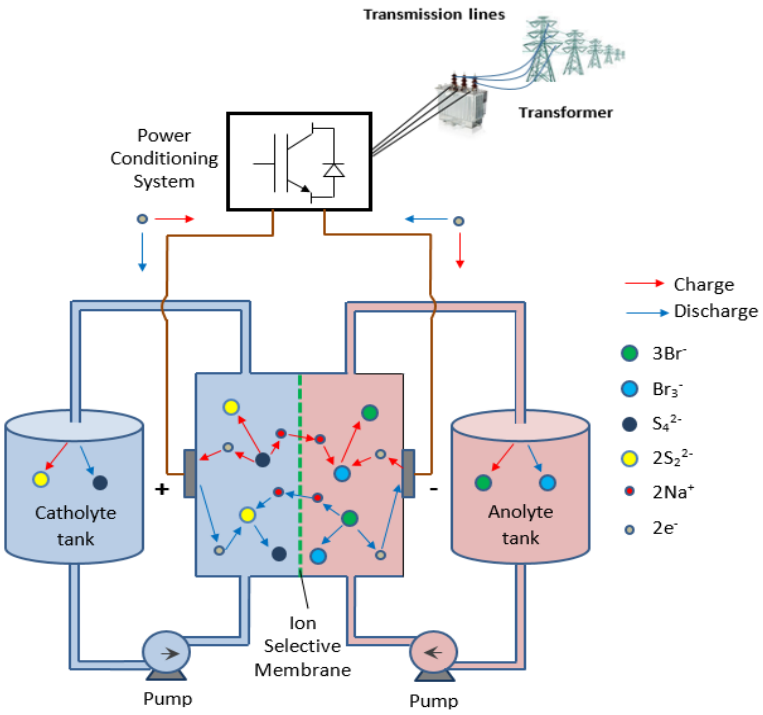

Figure 32: Schematic diagram of polysulfide bromine flow battery energy storage system [70]**.**

According to Figure 32, during the charging process the sodium bromide (NaBr) becomes to sodium tribromide ($NaBr_3$) at the anode while sodium polysulfide (Na_2S_4) is converted into sodium disulfide (Na_2S_2) at the cathode. Operating within the same temperature range (0-40^oC), PSB systems offer longer lifetime (10-15 years) and a net efficiency of 75%. However, chemical handling becomes a serious aspect, especially in large scale EES applications, due to existing environmental concerns regarding the bromine and sodium sulfate crystals formation during operation [91].

$$3Br^- \rightleftharpoons Br_3^- + 2e^- \tag{6.24}$$

$$2S_2^{2-} + 2e^- \rightleftharpoons 3S_4^{2-} \tag{6.25}$$

6.2.6 Regenerative fuel cell

Hydrogen is the only carbon-free and possesses the highest energy content compared to any known fuel producing only water when is utilized for energy production [130][131][132]. Although it is colorless and odorless (and therefore difficult to detect), and in order for 1 kg of H_2 to be stored at ambient temperature and pressure a volume of $11m^3$ is required, at the user end is considered as the most versatile fuel [4][133]. Hence, it constitutes an electricity storage pathway through electrolysis of water, a process in which electricity splits water into its simplest components of H_2 and O_2. Electrolyzers are typically used for such a method, whereas the inverse procedure of producing electricity via H_2 is realized through fuel cells, where hydrogen gas reacts with the oxygen of air, providing electricity and water which can be recycled and reused to produce more hydrogen [134][135][136].

A typical electrolysis unit consists of a cathode and an anode immersed in an electrolyte and depending on the technology, water is introduced at the anode or cathode where it is split into hydrogen ion H^+ and oxygen O_2 or hydrogen H_2 and hydroxide ion OH^- respectively, thus molecular hydrogen is always produced or remain at the cathode. A similar concept but in reverse order is observed in fuel cells [133][137]. To date, the developed and commonly used electrolysis technologies are alkaline (A), proton exchange membrane (PEM) and solid oxide (SO) electrolysis cells, while the five major groups of fuel cells are alkaline (AFC), proton exchange membrane (PEMFC), solid oxide (SOFC), phosphoric acid

(PAFC) and molten carbonate (MCFC) [91]. The chemical reactions that take place in the main fuel cells mentioned here, are included in [133]. The major advantage of fuel cells is their ability to convert chemical energy directly to electricity, without involving any intermediate energy-intensive steps and noisy moving parts [138]. The voltage of a FC stands below 1.5V as it uses an aqueous technology [139].

Regenerative fuel cells are devices that combine the function of the fuel cell (FC) and the electrolyzer into one device. Although all FC can operate as regenerative FC, they are typically optimized to perform only one function [110]. In Figure 33, a PEMFC is demonstrated as a typical example of a regenerative FC which provides the most efficient cycle of hydrogen and electricity production. The hydrogen produced can be stored as compressed gas, cryogenic liquid or solid hydride [140][141][142][143]. In over-ground tanks or underground geological formations is effectively stored as pressurized gas providing a daily loss of near 3% [77], while if transmitted by tracks or pipelines where is to be used it is preferred to be stored as cryogenic liquid mainly due to the reduced daily boil-off losses in the range of 0.06-0.4% [4][141][133].

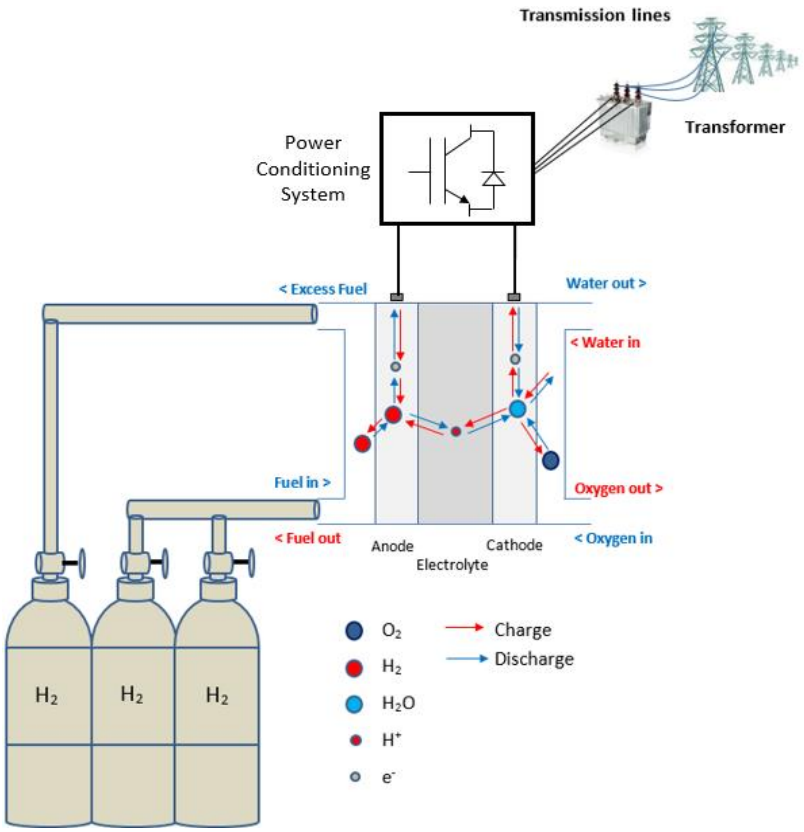

Figure 33: Schematic diagram of regenerative PEMFC energy storage system [70]**.**

Regenerative FC can be characterized as long-term EES devices. They offer the highest specific energy accounted at a maximum of 1200Wh/kg and excellent cycle capability of 20,000 cycles [91]. Their daily self-discharge is rated at 3%, the depth of discharge at 90% and the overall efficiency somewhere between 20-50% (with electrolysis being the weakest link in the chain) [78][144]. Except from their application in the transport sector where they potentially replace fossil fuels for vehicles, such EES devices occur promising in providing both stationary and distributed power [145][146][147]. However, they are still in the development stage and applications are limited to a few relating to stand-alone renewable energy systems [148][149].

6.2.7 Capacitor and Supercapacitor

A capacitor consists of two conducting metal-foil electrodes separated by an insulating dielectric material normally made of ceramic, glass or plastic film. The stored energy is a result of the electric field produced by opposite charges, which occur on the electrodes' surface when a voltage is applied [91]. Already commercialized, capacitors can be charged faster and offer higher than that of conventional batteries specific power but they experience high self-discharge rate and lower energy density [78].

Supercapacitors (also named ultra-capacitors, electrochemical capacitors or electric double-layer capacitors), are energy storage devices with special features somewhere between conventional capacitor and battery. As illustrated in Figure 34, their structure includes two metal electrodes of carbon surface, separated by a porous membrane soaked in an electrolyte, which simultaneously has the role of electronic insulator and ionic conductor [150]. Their capacitance, which is determined by the effective area of the plates (A), the distance between the electrodes (d) and the dielectric constant of the separating medium (ε), is 100-1000 times greater than that of conventional capacitors ($C \propto \varepsilon A/d$). As the stored energy given by equation (6.26) is directly proportional to both the capacitance and the square of voltage, ultra-capacitors also offer greater than that of capacitors energy density [85]. The maximum voltage is dependent on the electrolyte type and is rated at 1V or 3V for aqueous or organic electrolytes respectively [102].

$$E = \frac{1}{2} C V^2 \tag{6.26}$$

Supercapacitors ideally store the electric energy in the electrostatic field of the electrochemical double layer, rather than perform any chemistry, thus can be cycled millions of times and have much longer lifetime compared to batteries [151]. They achieve higher than that of batteries power density due to the short time constant of charging, but they provide lower energy density because of the limited surface area of the electrode [152]. Moreover, ultra-capacitors exhibit very high efficiencies up to 95% due to low resistance which results in reduced loss of energy and can be charged/discharged faster as compared to batteries since the transport of ions in the solution to the electrode surface is rapid [150].

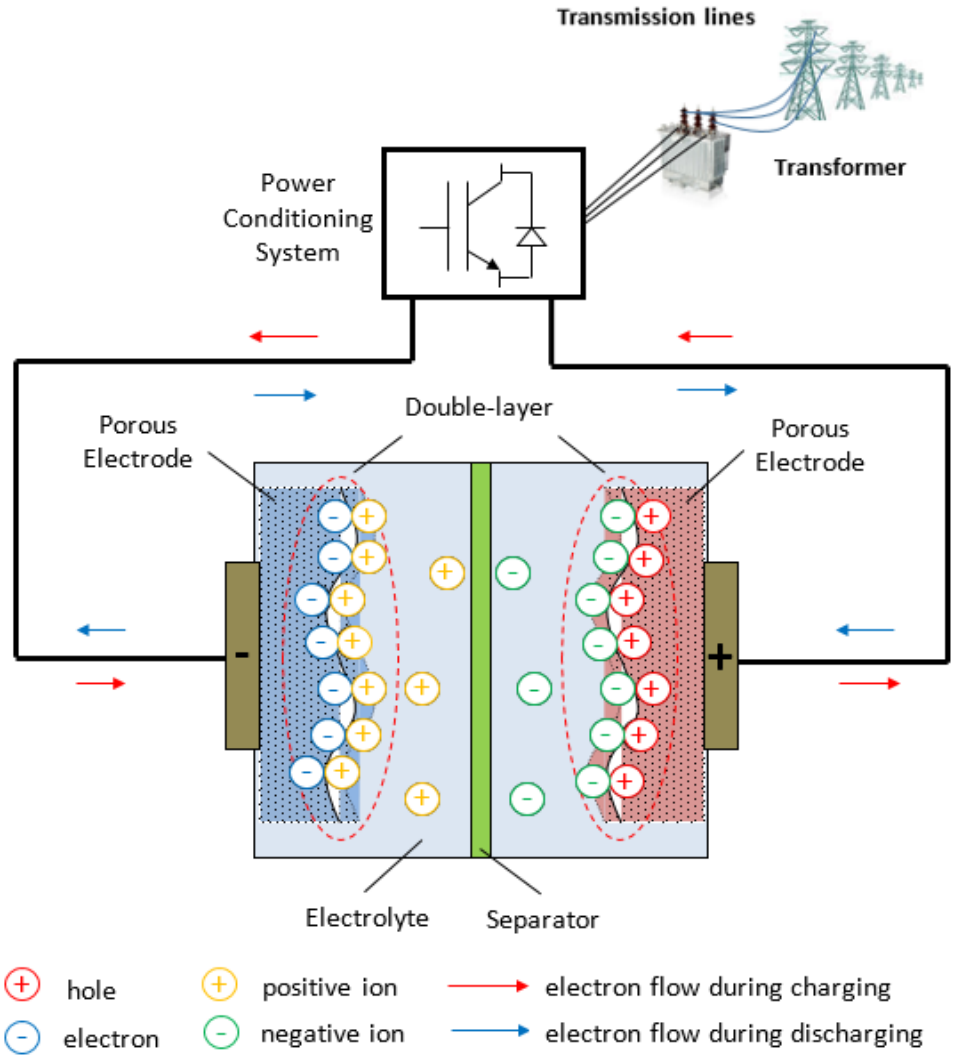

Figure 34: Schematic diagram of electrochemical double-layer capacitor [70]**.**

Although this technology is susceptible to self-discharging and is currently applied in portable electronics and automotive industries [102], ultra-capacitors can also be used in electric or hybrid vehicles in order to supply the peak power needed during acceleration

[153]. In recent years, ultra-capacitor banks have been used in power applications to provide voltage sag compensate, intermittent renewable storage and smoothing [150][154]. Finally, through efficient use of diverse EES technologies, supercapacitors may hide their drawback of low energy density, forming a hybrid system with extended cycle life and high enough specific power to respond in pretentious applications.

A new energy storage technology that has gained interest for grid-scale applications, involves the electrochemical flow capacitors (EFC). Aiming to decouple the power and energy capacity, after the double layers being charged, the slurry particles together with their charged surfaces are transferred to external tanks. When it is required, the stored energy can be recovered by pumping these particles back through the cell. A four-tank design for such a technology is needed in order to occasionally (charging/discharging) accommodate the slurry particles of the two layers [155]. Although a guidance for future EFC designs has been provided, more R&D is needed in order for such systems to become viable options for large-scale EES applications.

6.2.8 Superconductors

Superconducting magnetic energy storage (SMES) system is briefly composed of superconducting coil, power conversion system and cryogenically cooled refrigerator (Figure 35). Typically, electric energy is stored in the magnetic field created by the flow of rectified current in a coil made of niobium-titanium cables of extremely low resistance [156]. In order for the superconducting state to be maintained, the device must be cooled to -264ºC (9.2K), allowing current to flow permanently through the inductor [102]. The stored energy calculated by equation (6.27), is proportional to the wire inductance (L) and the square of direct current (I). It can be returned back by discharging the coil when the network demands the excess power [78].

$$E = \frac{1}{2} L I^2 \tag{6.27}$$

Superconductors offer high efficiency of storage, up to 98%, due to the nearly zero resistance resulting in negligible energy losses and rapid response in comparison with other energy storage systems as the current can be injected and extracted very quickly [156]. Moreover, these devices can be cycled almost infinitely and are capable of discharging the near totality of the stored energy [87]. The major drawbacks of the low-temperature

superconducting (LTS) coils are the high cost of superconducting wire and the increased energy requirements of cooling, and as a result, they are currently used for short duration energy storage applications to improve power quality [59]. In addition, they are susceptible to daily self-discharge (10-15%) and have a negative environmental impact due to the strong electromagnetic field [78]. New, high temperature superconducting (HTS) coils are in development, reaching the superconducting state at -163ºC (110K) and significantly improving the economics and overall efficiency [157][158][159].

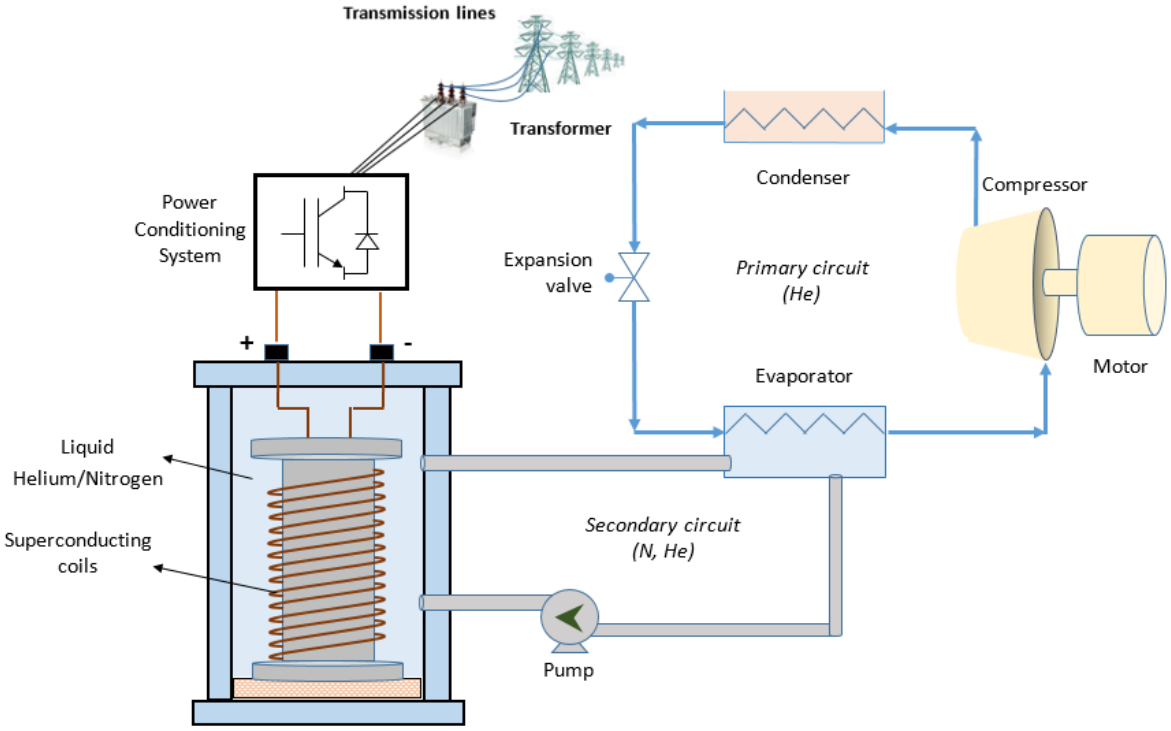

Figure 35: Schematic diagram of superconducting magnetic energy storage [70]**.**

6.3. Applications of EES

Apart from the potential support that EES technologies offer in mobile devices, automotive vehicles, space applications and the rest of autonomous or isolated systems, for several years now, EES is attracting increasing interest for power quality regulation, bridging power and energy management applications in power system operations.

Power quality refers to the extent to which provision of power is reliable and maintains nominal voltage levels, unity power factor, nominal frequency levels (50Hz or 60Hz depending on the country's standard), and a purely sinusoidal waveform with zero harmonics and no transients [9]. Power quality regulation services are the fastest acting,

enabling operation within seconds to a few minutes. Following are bridging power services, which are capable of working within minutes to an hour, constituting a bridge between the limited generation capability of energy sources and highly variable electricity demand, and assuring continuity when switching from one source to another [7][59]. The rest of the applications facilitate energy management and concerns all applications that provide time-shifting in the range between hours to days or even months to decouple the timing of generation and consumption of electrical energy [160].

Several applications providing grid support and management already exist while others will emerge in the future. Table 12 presents by chain the most essentials, based on storage duration, whereas a more detailed description of each application is included below. Also, a broad overview of these applications across the power chain from generation to end-users can be obtained from Figure 36.

Table 12. Applications of EES technologies per value chain.

Power Quality Regulation	**Bridging Power**	**Energy Management**		
≤ 1min	**1min – 1h**	**1 – 12h**	**hours – days**	**≥ 4 months**
Fluctuation Suppression	Forecast Hedge Mitigation		Unit Commitment	
Oscillation Damping	Load Following			
Frequency Regulation	Contingency Reserve	Peak Shaving	Load Levelling	Seasonal Storage
	Black-start	Energy Arbitrage		
Reactive Support		Transmission Curtailment		
		Transmission Deferral		
Low Voltage Ride-Through		Distribution Curtailment		
Voltage Regulation		Distribution Deferral		
UPS	Emergency Back-up	Demand Shifting		
<RES Integration>	**<Generation>**	**<Transmission>**	**<Distribution>**	**<End-User>**

6.3.1 Fluctuation suppression

Fast output fluctuations from renewable sources can occur due to variations in weather conditions, in the time range of up to a minute [111][61]. Such variations can become fatal for some power electronic, information and communication systems in the grid. In order to mitigate this recurring effect, fast-response EES capable of providing high ramp rates and

cycling times can be applied [91]. The facility could be charged/discharged within seconds to minutes, to smooth generation from intermittent renewable sources [78][101][161][62].

6.3.2 Oscillation damping

Up to a certain penetration rate, the integration of renewables into the power mix can be managed by existing flexibility sources. As the penetration increases, it may compromise the system stability against disturbances, especially in weak or isolated grids [162]. Therefore, an EES is needed, providing fast response and high ramp rates within one-minute time, to avoid system instability and consequent brownout or blackout, by absorbing and discharging energy during sudden decreases in power output over short duration variations [61].

6.3.3 Frequency regulation

Frequency regulation is needed to maintain a balanced system. Although daily, weekly and seasonal patterns exist, it is impossible for the power consumption to predict in accuracy, leading to generation-demand imbalances (or nominal-frequency deviations), which can cause brownouts or blackouts [163][164]. Systems that can be used in such applications, require high cycle life and fast response rates in combination with good ramp rates (i.e., 10-20MW/s) [60][165]. Stored energy, in these applications is requested to increase or decrease the output for seconds or less, to continuously maintain the frequency within electricity network standards [59][166].

6.3.4 Reactive support

Power converters used to facilitate RES integration, introduce several undesired harmonics to the system. On the other hand, some kind of wind generators consume large amounts of reactive power, also influencing voltage degradation and synchronisation with current. Devices capable of correcting the phase difference, are those which provide reactive support and includes generators, loads or energy storage equipment. EES used in such applications, offers both the distinct advantage of being available even when the power generation does not take place and high enough ramp rates in short time scale support [9][60]. The regulation can be realized either mechanically or via automated generation control. It is worth noting

that in both cases, the power conversion system applied possesses essential role since both active and reactive power must be compensated from the storage device [167].

6.3.5 Low voltage ride-through

The low voltage ride-through, also known as fault ride-through, defines the ability of a power generator to remain connected to the grid throughout a short voltage drop or a total failure of the system. It is crucial for a power system to sustain the supply on-line, in order to avoid a possible chain event where the voltage may be caused to drop further and down enough, forcing another generator to trip and so on. The integration of an EES system, with high power ability and instant response, at the point of connection with the external grid, enables the continuous connection of the power plant and reduces the risk of a network collapse [168][169].

6.3.6 Voltage regulation

Apart from the frequency, stable voltage must be maintained within technical limits among the whole value chain of a power system, an issue not always guaranteed by the grid. Voltage is generally controlled by taps of transformers but in order for modern systems to withstand the dynamic changes in active and reactive power, EES technologies could be deployed [82][170][171]. Fast-response EES located at the end of a heavily loaded line may improve voltage drops and rises by withdraw or inject electricity, respectively [91][172][63].

6.3.7 Uninterruptible power supply

Uninterruptible power supply (UPS) acts as a time-delay off switch during interruptions, voltage peaks or flickers, and becomes crucial for some residential and commercial consumers who possess fire protection and security systems, computer, server databases, and other automation systems that need to be protected or continuously keep data recorded in memory. Since such appliances require continuity of supply, EES systems with instantaneous reaction can be deployed to improve power quality and provide back-up power during power disruptions [10][78][82][64]. This application adds considerable value in cases where power quality is a concern and power outages occur frequently.

6.3.8 Forecast hedge mitigation

Power output from renewable sources varies according to daily or seasonal patterns and weather conditions, both of which are imperfectly predictable and uncontrollable [173][174]. Moreover, while RES have the priority in the generation mix, the net load variations (demand minus intermittent output) may fluctuate far more widely than the demand curve, giving high uncertainty to the generation units that are to be dispatched. Consequently, forecast hedging mitigation constitutes a major application, especially in systems that are highly dependent on variable renewables, so that the risk of exposure of consumers to high market prices along with financial impacts related to forecast error to be reduced [78].

6.3.9 Load following

Generation support and optimization involves the accurate adaptation of power output to changing demand. Depending on the flexibility needed, generators are currently dispatched upon the request of power system operators [175][176]. However, as the penetration of renewables increases, alternative sources with good ramping capability are needed to meet the mismatches between production and consumption, and shape the energy profile [10]. This is commonly referred to as load following and includes storage devices capable of providing energy in the time frame of minutes to an hour. A suitable for this purpose EES system could offer ramp rates of 0.3-1 MW/s and sufficient stored energy and power capacity [60].

6.3.10 Contingency reserve

Contingency reserves are distinguished by the time needed to achieve their maximum power output into spinning, non-spinning and supplemental reserve ancillary services. Because of the rapid response needed to replace production deficit, a large fraction of primary reserve is provided by plants that are operating and synchronized (spinning) to the system and thus is referred to as spinning reserve [177]. Spinning reserves must be available within ten minutes. Then, secondary and tertiary reserves, also known as non-spinning and supplemental, respectively, that need not be operating and synchronized when called upon, can be activated by the system operator’s decision.

Non-spinning reserves must be available within ten minutes and operable until they will be replaced by supplemental reserves [178]. The need for fast-responding, partially loaded power plants capable of providing the necessary contingency reserves, results in uneconomic dispatch and increases in the capital and O&M costs, reinforcing the requirement for EES applications especially in isolated systems [179][180][181][182].

6.3.11 Black-start

Many power plants require electrical energy from the grid to perform start-up operations such as to build up a reference frequency for synchronization and help other units to restart [177]. This service forms an integral part in a power system and has been performed by using diesel generators or hydroelectric units to provide the initial supply needed for the power grid to restart after a full black-out. Without taking power from the grid, EES units must sit fully charged and discharge when black-start capability is demanded to assist other facilities to start-up and synchronize to the grid [78][183][184].

6.3.12 Emergency Back-up

Energy storage can provide a source of back-up power that allows customers to ride-through a utility outage and continue normal operation [78]. It is operated as a substitute to an emergency diesel generator which is typically installed and changed-over to support important users, including healthcare facilities, telecommunication services, commercial and industrial customers. For increased reliability, emergency back-up storage requires instant-to-medium response time and relatively long duration of discharge [101][185][186]. The rated power output and energy capacity of such applications depends on whether they are deployed to ride-through an outage until conventional back-up generator can start-up or they completely mitigate the event by themselves [178].

6.3.13 Peak shaving

If cheap energy is stored at off-peak demand periods at night, and injected into the network during periods of maximum electricity demand during the day, economics of a power generation plant improves greatly [61][187]. This service, also known as peak-shaving, must

be operable in the time frame of 1 – 10h, in order to meet daily peak demand and hence, to be able to de-activate expensive peak generation plants [188][189][190][191].

6.3.14 Energy arbitrage

Electricity prices are highly unstable, but tend to a daily pattern of low prices during night-time off-peak hours and high prices during day-time on-peak hours [178]. Energy arbitrage involves operating storage in a manner that it consumes energy (self-produced and/or bought from others) during low market prices and releases the energy when market prices are higher [9][85][192]. Consequently, bulk energy storage becomes advantageous in that it can provide both generation and load, allowing to arbitrage the production price of the two periods and improving the load factor of the generation [78][193].

6.3.15 Transmission and distribution congestion relief

In most power networks, the generation is located far from the populated areas and electricity is delivered with some losses to the consumers. Congestion may occur either on high voltage transmission lines or more locally on the distribution system due to several reasons, such as when transmission lines cannot be enhanced in time to meet the increasing demand, in the event of an overload at the distribution equipment or due to extremely high penetration of distributed generation [9]. In both cases, where power generation or load demand exceeds the maximum delivery capacity, either excess energy must be curtailed, or a system upgrade must take place to provide sufficient capacity to accommodate or meet the changes, respectively. These two constraints are usually distinguished into two individual applications in the literature and are referred to as Transmission Curtailment and Transmission & Distribution Deferral.

An EES device capable of providing energy in the time frame of 5 – 12 h would mitigate such power delivery constraints imposed by insufficient delivery capacity [181][194][195][196]. Instead of being curtailed, excess generation could be stored and injected back when the delivery capability is available again, whereas the increased demand would be treated without the additional losses burdened the transmission lines by simply shift the delivery of generation from on-peak to off-peak periods. According to the appropriate node side at the substations where EES systems are intended for use, they could

be large scale or smaller, stationary or transportable to provide supplemental energy to the end-users during overload situations [10]. This way, both transmission curtailment is reduced, and investment upgrades are deferred for years, whilst improving the utilization factor of the existing network.

6.3.16 Demand shifting

Apart from the firm power that energy storage provides to off-grid users, grid-tied consumers may profit from a time-varying electricity price often set by power utilities. This can be therefore achieved by shifting electrical energy purchases from on-peak (with high time-of-use charges) to off-peak periods (when time-of-use charges are lower) [197]. In a similar manner, large commercial and industrial customers (whose demand charge is based on a peak load measured over a defined period) can reduce their demand charges in future bills by constantly reduce their peak load measured by the utility meter [178]. For the current requirements of a power system, EES devices with capacities of 1-10 kW and capable of providing energy in the time frame of 2-4 h would be sufficient [61]. Associated with local generation and/or in conjunction with a micro-grid formation able to be operated in island mode, power capacities may need to be increased for a time frame of 5-12 h. The feasibility of such storage systems is highly site-specific and depends on the existing incentives given by utilities [82][112][198][199].

6.3.17 Unit commitment

Unit commitment applications contribute to a proper scheduling of generators for certain time periods. The maximum share of RES fed to the grid is constrained by the minimum generation capacity of the conventional units being committed. As the penetration of variable renewable energy sources increases, it is more than usual for utilities to over-schedule and keep the plants partially loaded, to avoid curtailment. This implies uneconomic dispatch due to increased start-up costs and operation at inefficient output.

Storage technologies are needed to provide energy in the time-frame of hours to days, in order to compensate forecast errors in a case of an under-predicted renewable source and enhance a joint operation through efficient unit commitment [177][200][201].

6.3.18 Load levelling

Whatever the season, minimum power consumption during the day approximates nearly half of the maximum peak. However, as a function of peaks, production is over-dimensioned in the expense of its economics which are improved if it had been designed to fulfil average demand [87]. Load levelling is another example of time-decoupling of generation and consumption. By charging of storage during periods of low demand and discharging as needed, the gap between peak and off-peak is reduced, reducing the requirements of peaking generators to a minimum [85].

Electricity storage technologies able to provide energy for many hours to days, allow the load to become flatter, thereby improving the generation efficiency, and reducing capital and O&M costs related to fuel avoidance and lighter design, respectively [82].

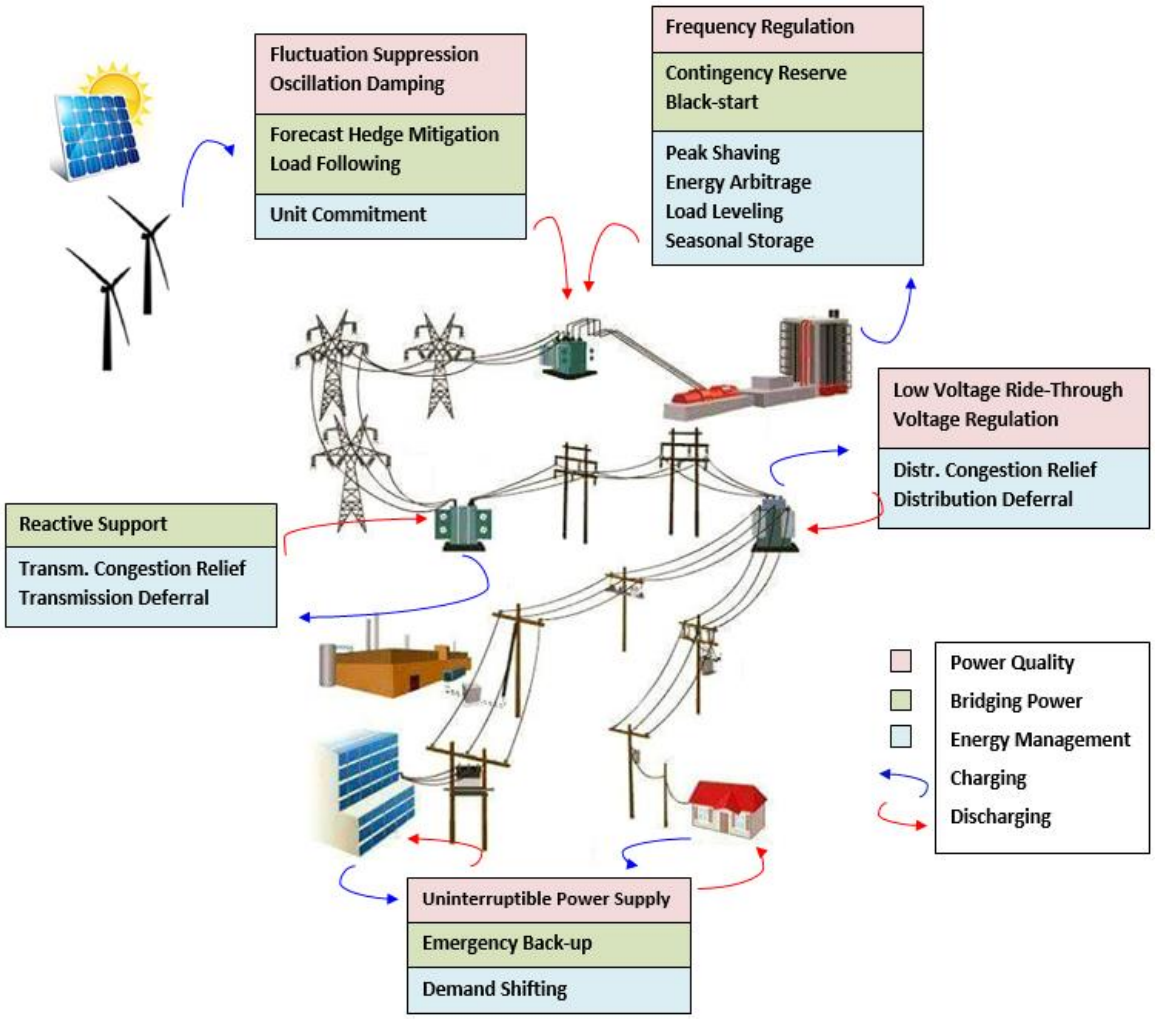

Figure 36: Power grid applications of EES [74].

6.3.19 Seasonal storage

Systems exposed to large seasonal variations in the level of either power generation or demand, may use storing energy in the time frame of months. Such a long-term electricity storage is currently limited by storing primary energy sources including coal, gas, oil, biomass or water, which can be converted to power at a later time [202]. However, EES technologies with a very large energy capacity and no self-discharge rate would be eligible, while if other quantifiable benefits (such as emissions avoidance) could be taken into account, they will become technically viable options [203][204][205].

7. Qualitative and Quantitative assessment of EES

For our research to be complete, a methodology is needed for evaluating and comparing EES technologies with different cost structures in potential grid applications, distinguishing their power-related and capacity-related costs. Aiming to apply the same evaluation method to all cases, we seek for an algorithm which incorporates the initial project cost, storage replacement cost, fixed and variable O&M costs over the life of an EES facility. To gain a deep understanding of how electrical storage affects power system operations, both qualitative and quantitative analyses are needed.

7.1. Life-cycle cost analysis of EES

Since electricity is considered as the most versatile form of energy, electrical energy storage (EES) can assist in the improvement of the modern power systems' stability, energy security and quality of supply with a wide variety of technologies and plenty of applications. Optimal planning of such systems, allows separating the power production from its consumption, both in space and time [206]. Generally, EES system planning involves four basic steps, namely the type selection, sizing, siting and operation and control. The specific EES technology is chosen according to the requirements and preferences of the application that it is intended for use. Once the EES type is determined, its optimal sizing can be found by balancing the benefits and cost, while its optimal placement can be addressed considering the geographical and topographical conditions in combination with the expected equipment-upgrade deferral or network losses reduction. Finally, the operation and control strategies are designed in relation to the stakeholders and services across the different locations in the power chain, the desired purpose and the function performed [207][208].

Based on the development status and cost metrics extensively published in the literature, EES technologies are continuously being studied, analyzed and compared. However, considering the performance and capital costs, most comparisons between

different EES systems participating in distinguished applications are qualitatively assessed. Some recent research has been conducted on the performance of EES in power system operations, investigating a specific technology in a specific application or using profitability analysis and calculation of cost per stored unit of electricity [209][210][211][212][213]. Even when the composition of cost is studied in great detail, the cost per kWh is not the optimal expression of a storage application service. Besides selling stored energy, other services such as emergency back-up or black start capability cannot be valued in terms of cost per kWh, while in the case of seasonal storage, a difficulty exists in evaluating the purchased energy since it may have been absorbed at different time intervals and in differing amounts.

In this chapter, we present a methodology to evaluate and compare EES technologies with different cost structures in potential grid applications, distinguishing their power-related and capacity-related costs. Aiming to apply the same method to all cases, the viability of EES systems in different stationary applications is examined by the development of an algorithm which incorporates the initial project cost, storage replacement cost, fixed and variable O&M costs over the life of an EES facility. Once the costs of the subsystems comprising the whole facility are defined, the calculation of life-cycle cost is ascribed to the present value in terms of the power rating ($/kW). The levelized cost of storage (LCOS) provided, constitutes a quick and useful metric for EES facility owners to compare between technologies that may possess different characteristics, such as response time, power rating, suitable storage duration, round-trip efficiency, depth of discharge, self-discharge rate, cycling capability, lifespan times, capital and O&M costs, etc.

Implementation of electricity storage can be possible in all five major subsystems of the electric power system: RES generation, thermal power plants, transmission, distribution and final consumers [214]. The EES applications are distinguished by the roles they play for different stakeholders and services across the power chain. These applications aim to satisfy their operational objectives as efficiently as possible, minimizing environmental impacts and maximizing system reliability and dynamic stability, at a reasonable cost. Governments, regulators, balancing authorities, dispatchers, marketers, RES plant owners, utility companies, transmission and distribution system operators, transmission and distribution network owners, all sorts of suppliers and end-users can benefit from the integration of EES systems via different power grid operations.

Either in international networks with centralized or distributed generation, or microgrids in islanded or interconnected mode, the presented approach functions similarly and minor differences are only found in sizes and scales [15]. Power quality involves fast acting services with the requirement of a few-milliseconds response and multiple annual charge-discharge cycles. Considering their storage duration and discharge time preferences, short-term/short-duration EES technologies are considered adequate systems for such applications. Fluctuation suppression and oscillation damping is needed to mitigate fast output variations and smooth generation from intermittent RES, while frequency regulation and spinning reserve are capable of managing generation-demand imbalances and retaining system stability. In medium scales, energy can be absorbed/injected through voltage regulation and low voltage ride-through, in order for the supply to be sustained on-line, reducing the risk of a network collapse. At the demand-side of the meter, the most common power quality application, known as uninterruptible power supply (UPS), ensures the continuity of supply during sudden power disruptions [74].

The second category represents a bridge between the limited generation capability of energy sources and highly variable electricity demand. Bridging power applications require medium-response times and operation within minutes to hours. Their main objective is to store and provide energy in order to reduce forecast errors (Forecast hedging mitigation), shape the energy profile (Load following), avoid start-up and O&M costs of partially loaded power plants (Non-spinning reserve), assist other generating systems to start-up and synchronise (Black-start) or support customers in the event of a utility outage (Emergency back-up) [70].

The last category accommodates the energy management applications which call for long-term storage in the range between hours to days or even months. Based on the market prices, energy arbitrage is equivalent to peak shaving and the only difference relies on the participation in electricity wholesale market [215]. In a similar manner, but in quite smaller scales, customers are allowed profit from time-varying demand charges through absorbing/returning energy during low/high time-of-use charges respectively. The applications of transmission and distribution congestion relief may occur in between them. By deploying EES downstream from regions of congested transmission or distribution, the need for energy curtailment is reduced and investment upgrades can be deferred for years [74]. Footprint limits mostly exist in urban areas where the facilities are roofed and strictly enclosed, while in rural areas the restrictions can be less noticeable or entirely neglected.

Load levelling and unit commitment are two further applications aiming to support power generation and RES integration for a proper scheduling of generators and improved economics in terms of capital, O&M and fuel costs. The former is needed to reduce the gap between peak and off-peak, whereas the latter is used to ensure the flexibility adequacy [216]. Finally, the longest storage duration is required by seasonal storage, an application by which the fulfilment of the yearly averaged demand is guaranteed with lighter designs and consequent improved economics. The requirements and conditions concerning all applications discussed so far are listed in Table 13 along with the addition of discharge time, annual operating cycles and examined life-cycle. In our analysis, the load profile is considered similar for all days of the year, requiring steady, full charging-discharging cycles. Also, the function performed along with the benefits achieved are provided in Table 14 for the various applications extensively published in the literature.

The EES technologies considered in this study include pumped hydro (PHES), compressed air (CAES), small-scale compressed air (SS-CAES), flywheel (FES), valve-regulated lead-acid (VRLA), advanced lead-acid, nickel-cadmium (NiCd), zinc-air (Zn-air), sodium-sulphur (NaS), ZEBRA, lithium-ion (Li-ion), vanadium redox (VRB), zinc-bromine (ZnBr), polysulphide-bromide (PSB), hydrogen fuel cell (H_2FC), electrochemical double layer capacitor (EDLC) and superconducting magnetic energy storage (SMES). All technologies are modelled using the most realistic technical, operational and cost data obtained from industry reports, white papers, government databases, project summaries, journal articles and IEEE conferences.

The most essential performance characteristics which make a storage device favourable or unfavourable to the application that is intended for use are: response time, power rating, suitable storage duration, autonomy, self-discharge rate, depth of discharge, cycle and chronological life, round-trip efficiency and spatial requirement. All this information regarding each EES technology is included in Table 15.

The most suitable EES technologies are selected to compete in a certain application according to its specific parameters and conditions. In this regard, all types of batteries, flywheels, EDLC and SMES can respond in time for all applications, while PHES and CAES, for those with a requirement of minutes and greater. The rest of the technologies can compete in applications with response time between seconds to minutes. Power rating sets the minimum scale at which the selection of an EES device is considered feasible. Consequently, SS-CAES cannot take place in smaller than 0.003MW application scales,

followed by VRB (0.03MW), ZnBr and NaS (0.05MW), SMES (0.1MW) and PSB for which a requirement of at least 1MW must be satisfied. In larger scales, CAES and PHES require a minimum scale of 5 and 100 MW respectively.

Finally, the discharging time must be satisfied, and storage duration be within the required limits. Although the majority of technologies can retain and release energy for hours, flywheels and SMES cannot take place in applications that require longer than 30 minutes of storage. In general, battery energy storage (BES) devices can compete in most system operations due to their rapid response and no power-rate limitations. PHES and CAES are selected for large-scale/long-duration storage while FES, EDLC and SMES for short-duration [74]. On this basis, and according to the requirements and preferences of the individual applications across the power chain, the selected EES candidates are presented in Table 16.

Table 13. Requirements and conditions of EES Applications [217]**.**

No	Application	Response time	Power rating (MW)	Storage duration	Discharge time	Cycles (y^{-1})	Life-time (y)
1	Distributed Fluctuation Suppression and Oscillation Damping	msecs	1-10	30min-1hour	30min-1hour	5000	20
2	Centralized Fluctuation Suppression and Oscillation Damping	msecs	100-400	15-30min	15-30min	10000	20
3	Forecast Hedging Mitigation	secs	0.2-400	1min-1hour	1min-1hour	4500	15
4	PV Load Following	secs	1-2	15min-4hours	15min-4hours	5000	15
5	Wind Load Following	secs	100-400	5-10hours	5-10hours	500	20
6	Unit Commitment	mins	10-1000	hours-days	8-12hours	400	20
7	Frequency Regulation	msecs	1-1000	15min	1-15min	8000	15
8	Spinning Reserve	msecs	10-1000	1-5hours	15min-1hour	500	20
9	Non-Spinning Reserve	secs	10-1000	1-5hours	1-5hours	500	20
10	Black Start	secs	100-1000	days-months	2-4hours	3	20
11	Peak Shaving	mins	10-1000	2-6hours	2-6hours	400	15
12	Energy Arbitrage	mins	10-1000	5-12hours	2-6hours	400	20
13	Load Levelling	mins	10-1000	hours-days	5-12hours	150	20
14	Seasonal Storage	day	10-1000	3-6months	2-6days	4	25
15	Voltage Regulation	msecs	10-100	15min	1-15min	5000	20
16	small footprint Transmission Congestion Relief	mins	0.25-10	2-8hours	2-8hours	400	15
17	no-footprint limits Transmission Congestion Relief	mins	10-100	2-8hours	2-8hours	400	20
18	Low Voltage Ride-Through	msecs	0.002-1	2-4hours	2-4hours	150	10
19	Reactive Support	msecs	1-10	2-4hours	2-4hours	150	15
20	small footprint Distribution Congestion Relief	mins	0.25-1	2-8hours	2-8hours	400	10
21	no-footprint limits Distribution Congestion Relief	mins	1-10	2-8hours	2-8hours	400	15
22	Uninterruptible Power Supply	msecs	0.002-10	15-30min	15-30min	50	10
23	Emergency Back-up	secs	0.002-10	4-10hour	2-6hour	50	15
24	Demand Shifting	mins	0.001-0.01	2-6hours	2-4hours	350	15

Table 14. Applications of EES technologies per value chain [74]**.**

System Operations	Application	Function	Benefit
Power Quality and Regulation	Fluctuation Suppression (FS)	Absorb/inject energy to smooth generation from intermittent RES.	Mitigate fast output variations improving reliability.
	Oscillation Damping (OD)	Absorb/discharge energy during sudden decreases in power output.	Avoid system instability and consequent brownout or blackout.
	Frequency Regulation (FR)	Increase/decrease the output to continuously maintain nominal frequency	Manage generation-demand imbalances retaining system security.
	Reactive Support (RS)	Sourcing/sinking reactive power handling undesired system harmonics.	Avoid voltage degradation and synchronization with current.
	Low Voltage Ride-Through (LVRT)	Absorb/inject energy to remain connected throughout a short voltage drop.	Sustain the supply on-line reducing the risk of a network collapse.
	Voltage Regulation (VR)	Withdraw/inject electricity to maintain the voltage within technical limits.	Withstand the dynamic changes in active and reactive power improving voltage drops and rises.
	Uninterruptible Power Supply (UPS)	Absorb/discharge energy during sudden power disruptions.	Ensure continuity of supply improving power quality.
Bridging Power	Forecast Hedging Mitigation (FHM)	Absorb/discharge energy to mitigate uncertainty concerning RES.	Reduce forecast error and the risk of exposure to high market prices.
	Load Following (LF)	Withdraw/inject energy to accurately adapt power output to changing demand.	Meet the mismatches between production and consumption shaping the energy profile.
	Contingency Reserve (CR)	Store/provide energy to replace production deficit of spinning, non-spinning and supplemental reserves.	Avoid start-up, capital and O&M costs of partially loaded power plants and uneconomic dispatch.
	Black-start (BS)	Sit fully charged and discharge to build up a reference frequency for synchronization when call upon.	Assist other facilities to start-up and synchronize to the grid improving reliability.
	Emergency Back-up (EB)	Operate as a complement or substitute to an emergency diesel generator.	Support customers to continue normal operation in the event of utility outage.

Energy Management	Peak Shaving (PS)	Store/inject energy at off-peak/on-peak demand periods.	Improve economics by allowing expensive peak generation units to be de-activated.
	Energy Arbitrage (EA)	Consume energy during low market prices and release when market prices are higher.	Improve the load factor of generation whilst enabling production price arbitrage.
	Transmission & Distribution Congestion Relief (T&D CR)	Store excess generation and inject back when the delivery capability is available again.	Improved utilization factor, reduced energy curtailment and investment upgrades are deferred for years.
	Demand Shifting (DS)	Absorb energy during low time-of-use charges and return at high time-of-use charges.	Allow customers profit from time-varying demand charges.
	Unit Commitment (UC)	Absorb/discharge energy to enhance a joint operation through efficient unit commitment.	Compensate forecast errors, increase the penetration of VRES, contribute to a proper scheduling of generators.
	Load Levelling (LL)	Charge during low demand periods and discharge as needed to reduce the gap between peak and off-peak.	Reduce the requirements of peaking and over-dimensioning generators, improving generation efficiency and economics in terms of capital, O&M and fuel costs.
	Seasonal Storage (SS)	Long-term electricity storage to recover large seasonal variations at a later stage.	Lighter designs to fulfil yearly averaged demand, improving economics.

Table 15. Technical and operational characteristics of EES [217]**.**

Technology	Daily self-discharge (%)	Lifetime (years)	Cycling times (cycles)	Round-trip efficiency (%)	DoD (%)	Time of response	Suitable storage duration	Autonomy at power rating	Power Rating (MW)
PHES	almost 0	30-50	10000-30000	70-85	95	mins	hours-months	1-24h	100-5000
CAES	almost 0	30	8000-12000	42-54	100	mins	hours-months	1-24h	5-300
SS-CAES	almost 0	23+	30000	17-57	100	sec-mins	3h	3h	0.003-3
Flywheel	55-100	20	10^5-10^7	90-95	100	msec	secs-mins	15sec-15min	0-0.25
Lead-acid	0.1-0.2	5-15	200-2000	85-90	80	msec	mins-days	secs-hrs	0-20
Advanced LA	0.1-0.2	5-15	4000-17000	85-90	80	msec	mins-days	secs-hrs	0-20
NiCd	0.1-0.2	10-20	1500-3000	60-90	100	msec	mins-days	secs-hrs	0-40
Zn-air	almost 0	0.17-30	100-300	50	100	mins	hours-months	secs-24h	0-0.01
NaS	almost 0	10-15	1500-5000	89-92	100	msec	secs-hours	secs-hrs	0.05-8
ZEBRA	20	10-14	1000	70-85	80	-	secs-hours	secs-hrs	0-0.3
Li-ion	0.03	5-15	3000-10000	~100	80	msec	mins-days	mins-hrs	0-0.1
VRB	almost 0	5-10	>16000	85	100	msec	hours-months	secs-10h	0.03-3
ZnBr	almost 0	5-10	2000-3500	75	100	msec	hours-months	secs-10h	0.05-2
PSB	almost 0	10-15	800-2000	75	100	msec	hours-months	secs-10h	1-15
H_2-FC	0.06-3	5-15	20000	20-50	90	secs	hours-months	secs-24h	0-50
EDLC	20-40	10-12	10^6	85-98	100	msec	secs-hours	secs-hrs	0-0.3
SMES	10-15	20+	almost ∞	95	100	msec	≤30mins	mins-hrs	0.1-10

Table 16. EES technology-application pairs.

	Apps	PHES	CAES	SS-CAES	Flywheel	VRLA BES	Advanced LA	Ni-Cd BES	Zn-air BES	Na-S BES	ZEBRA BES	Li-ion BES	VRB FBES	Zn-Br FBES	PSB FBES	H_2FC	EDLC	SMES
1	Distributed Fluctuation Suppression and Oscillation Damping					✓	✓	✓		✓	✓	✓					✓	
2	Centralized Fluctuation Suppression and Oscillation Damping				✓	✓	✓	✓		✓	✓	✓					✓	✓
3	Forecast Hedging Mitigation			✓	✓	✓	✓	✓		✓	✓	✓					✓	✓
4	PV Load Following			✓		✓	✓	✓		✓	✓	✓					✓	
5	Wind Load Following					✓	✓	✓		✓	✓	✓	✓	✓	✓	✓		
6	Unit Commitment	✓	✓			✓	✓	✓	✓			✓	✓	✓	✓	✓		
7	Frequency Regulation					✓	✓	✓		✓	✓	✓					✓	✓
8	Spinning Reserve				✓	✓	✓	✓		✓	✓	✓	✓	✓	✓		✓	
9	Non-Spinning Reserve					✓	✓	✓		✓	✓	✓	✓	✓	✓	✓		
10	Black Start								✓				✓	✓	✓	✓		
11	Peak Shaving	✓	✓			✓	✓	✓	✓	✓	✓	✓	✓	✓	✓	✓		
12	Energy Arbitrage	✓	✓			✓	✓	✓	✓	✓	✓	✓	✓	✓	✓	✓		
13	Load Levelling	✓	✓			✓	✓	✓	✓			✓	✓	✓	✓	✓		
14	Seasonal Storage	✓	✓						✓							✓		
15	Voltage Regulation				✓	✓	✓	✓		✓	✓	✓					✓	✓
16	small footprint Transmission Congestion Relief			✓		✓	✓	✓	✓	✓	✓	✓	✓	✓	✓	✓		
17	no-footprint limits Transmission Congestion Relief	✓	✓			✓	✓	✓	✓	✓	✓	✓	✓	✓	✓	✓		
18	Low Voltage Ride-Through					✓	✓	✓				✓	✓	✓			✓	
19	Reactive Support					✓	✓	✓		✓	✓	✓	✓	✓	✓			
20	small footprint Distribution Congestion Relief			✓		✓	✓	✓	✓	✓	✓	✓	✓	✓				
21	no-footprint limits Distribution Congestion Relief		✓			✓	✓	✓	✓	✓	✓	✓	✓	✓	✓	✓		
22	Uninterruptible Power Supply					✓	✓	✓				✓					✓	
23	Emergency Back-up			✓		✓	✓	✓	✓			✓					✓	
24	Demand Shifting			✓		✓	✓	✓	✓			✓				✓		

Overall expenditures of an EES facility consider both the investment (initial project and replacement costs) and operation (purchased energy, fixed and variable O&M costs). The initial project cost (IPC) is composed of the three primary components of energy storage medium (ESM), power conversion system (PCS) and balance of plant (BOP). While specific power and energy can be quite different, the power and energy capital costs are largely decoupled from each other. The ESM components include the energy-related costs (battery banks, air/gas/electrolyte tanks, cavern excavation, water reservoir construction, etc.) whereas power-related costs (inverter/rectifier, pump, compressor, turbine, motor, generator, electrolyzer, fuel cell, etc.) are represented by PCS component. BOP encloses all costs associated with project engineering, construction management, grid integration, system isolation/protection, land and access, site buildings and foundation, monitoring, control and HVAC systems, procurement, shipment and installation, permitting and so on [218][219]. *IPC* can be calculated based on the following equation:

$$IPC = C_{ESM}.h_d + C_{PCS} + C_{BOP} \tag{7.5}$$

where h_d is the discharging-time hours. To meet the requirements of each individual application in terms of output (useful) energy, C_{ESM} must be divided by the round-trip efficiency. Since the quantification of the generated profit is beyond the scope of this work, round-trip efficiency (η) concerns only the charge/discharge efficiency without considering further transmission, transformation or conversion losses. In addition, ESM must be oversized for those devices that cannot be fully discharged (constrained by their allowed depth of discharge-*DoD*) and are distinguished from the rated to the net capacity [220]. In this regard, no memory effect (associated mainly with BES) is observed and the performance characteristics of EES systems are retained over their specified lifetime [221]. Finally, self-discharge rate (SDR) is a crucial parameter that directly affects the discharged energy according to the application's storage duration needs (h_s). While steady, full charge-discharge cycles were assumed, *SDR* can accurately be incorporated to reform the *IPC* as follows:

$$IPC = \frac{C_{ESM}}{\eta.DoD}.\left(1 + \frac{SDR}{24}.h_s\right).h_d + C_{PCS} + C_{BOP} \tag{7.6}$$

According to the quality of the manufacturer and the guarantee, the lifespan of the electronic equipment (inverter, rectifier and control system) is usually higher than 15 years and thus, replacement costs (C_R) stem from the number of replacements of the ESM compartment [222]. The year and the number of replacements are found according to the application's lifespan and cycling times over each technology, via Equations (7.7) and (7.8), respectively.

$$L_{ESM} = \min\left\{ \frac{L_{ESM_C}}{N_k} \, , \, L_{ESM_Y} \right\} \tag{7.7}$$

$$N_R = \text{Integer}\left(\frac{L_k}{L_{ESM}}\right) \tag{7.8}$$

, where L_{ESM} is the ESM durability life or equivalent replacement year, L_{ESMC} and L_{ESMY} is the ESM lifetime in cycles and years respectively, N_K and L_k are the application's requirements in cycles per year and examined lifespan in years, and N_R represents the number of replacements.

During the span of each EES facility's useful lifetime, O&M is a further key element affecting the total cost. Operational costs that do not change as a function of plant output are expressed via fixed O&M costs ($C_{fO\&M}$), while variable O&M costs ($C_{vO\&M}$) represent the operational costs that change as a function of energy output [26]. Fixed costs regard the routine maintenance required to keep the system operational and consist of the plant staff employment, planned inspections, tests and analyses, annual taxes and fees, insurance, carrying charges, energy availability, etc [26]. Variable O&M cost comprises the small-scale fault restorations, unplanned replacements of mechanical or electronic parts, auxiliary equipment overhauls, rented maintenance equipment, fluid leakage treatment, substances and materials consumed during maintenance and other operational energy needs [223]. In data models where variable O&M values are not incorporated into fixed cost metrics, operating hours per cycle ($h_o = h_c + h_d = 2.h_d$) are used to calculate the impact of $C_{vO\&M}$ on annual O&M cost ($C_{O\&M}$) using the Equation (7.9).

$$C_{O\&M} = C_{fO\&M} + C_{vO\&M}.N_k.(2h_d) \tag{7.9}$$

In order for the annual operating hours to be counted, N_k (annual number of cycles) is applied to Equation (7.9). On the contrary, for the $C_{fO\&M}$ already expressed in \$/kW-year, a triple variation is utilised to gain a broader overview from independent applications in the power chain. As a result, $C_{fO\&M}$ differs when an EES technology is used for bulk energy storage, distributed generation or power quality purposes. The cost metrics regarding each EES technology are included in Table 17. Finally, for each application *k* and for each individual technology *j* selected for it, the levelized cost of storage can be computed as the present value of the system in terms of power rating through the use of Equation (7.10).

$$LCOS = \sum_{t=1}^{L_k} \frac{C_R(t) + C_{O\&M}(t)}{(1+i)^t} \tag{7.10}$$

At this point, it should be noted that all cost data involved for the EES systems and derived from different sources, range over no greater than 5 years, so that inflation rates *i* have remained relatively stable and no further adjustments have to take place. In addition, each cost component is assumed to scale linearly, so LCOS does not vary with system size.

Table 17. Cost metrics of EES.

Technology	BOP ($/kW)	PCS ($/kW)	ESM ($/kWh)	Fixed O&M ($/kW-year)			Variable O&M ($/MWh)
				Bulk energy	Distributed generation	Power quality	
PHES	270-580	0-4.8	5-100	2.50	-	-	0.25
CAES	270-580	46-190	2-50	2.50	10	-	2.95
SS-CAES	*	1072-1195	134-158	-	2.95	-	2.55
Flywheel	110-600	120-1200	200-500	-	1000	5.76	0.27
Lead-acid	120-600	58-180	200-500	4.29	15	10	0.20
Advanced LA	120-600	58-180	200-500	4.29	15	10	0.20
NiCd	120-600	50-180	800-1500	5.36	25	-	**
Zn-air	120-600	0-120	10-60	-	-	-	-
NaS	120-600	0-120	300-500	20	-	2.68	0.40
ZEBRA	120-600	0-120	100-200	4.42	-	4.42	0.51
Li-ion	120-600	0-120	600-2500	2.68	25	10	0.54
VRB	120-600	0-120	150-1000	4.56	20	-	0.27
ZnBr	120-600	60-120	150-1000	4.29	20	-	0.40
PSB	120-600	36-120	150-1000	-	-	-	-
H_2-FC	*	1383-4453	15	21.44	3.80	-	**
EDLC	180-580	50-12000	300-2000	-	-	5	**
SMES	140-650	50-12000	1000-10000	-	-	10	**

* BOP is included in PCS cost.

** Variable O&M cost is included in fixed O&M costs.

Following, an analysis is performed on the LCOS for each EES participant, to determine which properties add most uncertainty according to the intended use in individual applications, based on their performance characteristics extensively published in the literature. The uncertainties resulting from the large technological variations between system types, along with their extremely challenging behaviour prediction, require flexibility on each input parameter that affects both the investment and operation costs.

The selected parameters of capital cost, efficiency, lifetime and self-discharge rate, were subjected into variations between their minimum and maximum value while keeping the rest parameters constant. As a result, their range deviated around the median value (mean value for all input parameters) whereas their impact was differed from the worst and best case. To reach an apparent inference of the representative LCOS of EES technologies in a specific application, the storage duration and discharge times were set to their maximum demand. It is worth noting that recycling and disposal costs regarding each individual component of a whole EES facility, provide additional uncertainty to LCOS and should be included. However, these costs are strongly dependent on each country's policy and legislation and are, therefore, difficult to collect and process.

7.2.1 Effect of capital cost

The variation in cost of different technologies participating in wind load following, unit commitment, transmission congestion relief with small and no-footprint limits, and distribution congestion relief with small and no-footprint limits can be observed in Figure 37. Considering the middle range of costs, VRB is dominated by its capital cost range as the lower and upper bounds coincide with minimum and maximum values. VRB is followed by ZEBRA, PSB, ZnBr, H_2 fuel cells and Li-ion, for which their capital cost accounts for the 78.8, 73.5, 64.8, 56.6 and 52.2% of the total cost disparity respectively.

From the ownership perspective, minimum LCOS and overall range constitute the most important elements in terms of affordability and reliability. Where footprint is not an inhibiting factor, PHES is the least-cost technology option, whereas CAES is preferred only when the power-rate limits restrict PHES technology to participate. As a result, PHES is the

least-cost technology for transmission congestion relief with no footprint limits and unit commitment, while CAES is favourable in distribution congestion relief with no-footprint limits. H_2-FC provides the lowest LCOS in wind load following and small footprint transmission congestion relief, followed by Zn-air systems which are considered the next cheapest and consequently the best type for small footprint distribution congestion relief. In terms of reliability, PHES and CAES present the smallest range (followed by H_2-FC), reducing the investment risks and empowering EES facility owners to proceed to implementations.

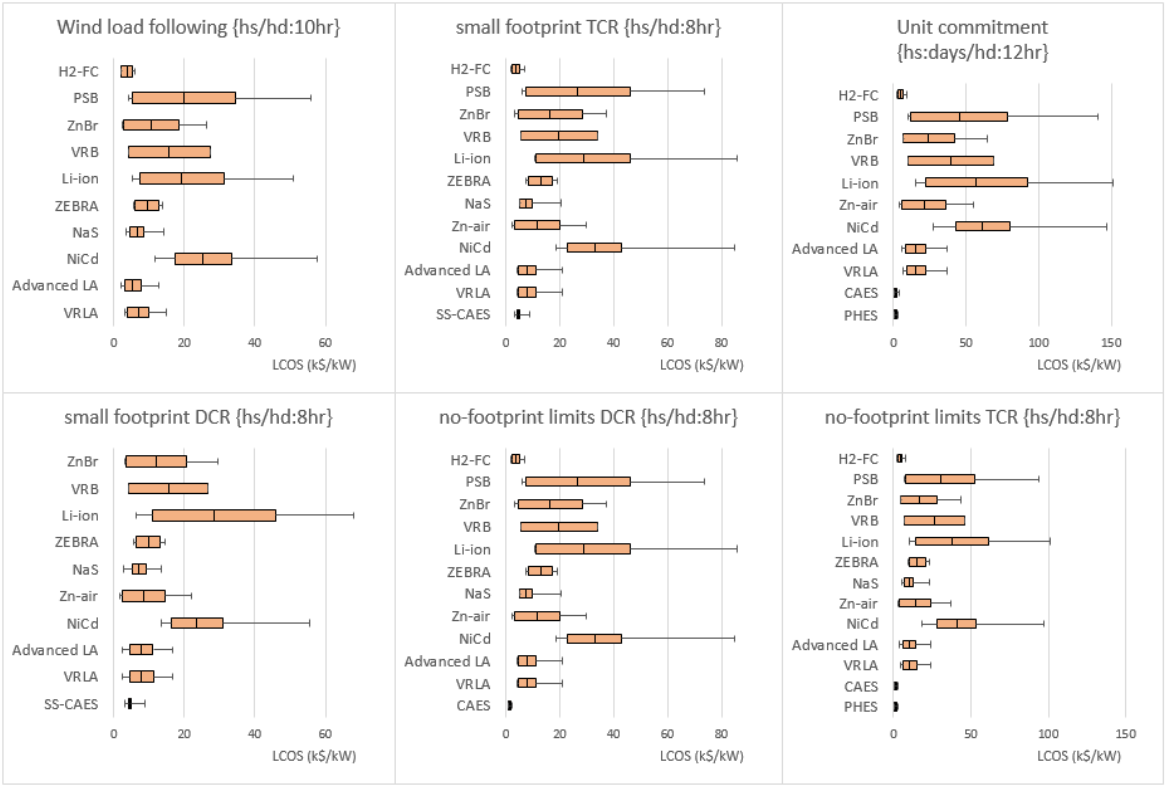

Figure 37. LCOS with varying capital cost for EES participating in Applications 5, 6, 16, 17, 20 and 21 shown in Table 16.

7.2.2 Effect of efficiency

Figure 38 depicts the LCOS of different EES facilities applied in low voltage ride-through, reactive support, uninterruptible power supply and demand shifting. The efficiency range is responsible for the 81.6% of uncertainty that governs SS-CAES, 29.1% for NiCd and to a lesser extent for ZEBRA, VRLA and EDLC. Similar results are obtained from Figure 39

where non-spinning reserve, peak shaving, energy arbitrage and emergency back-up are listed.

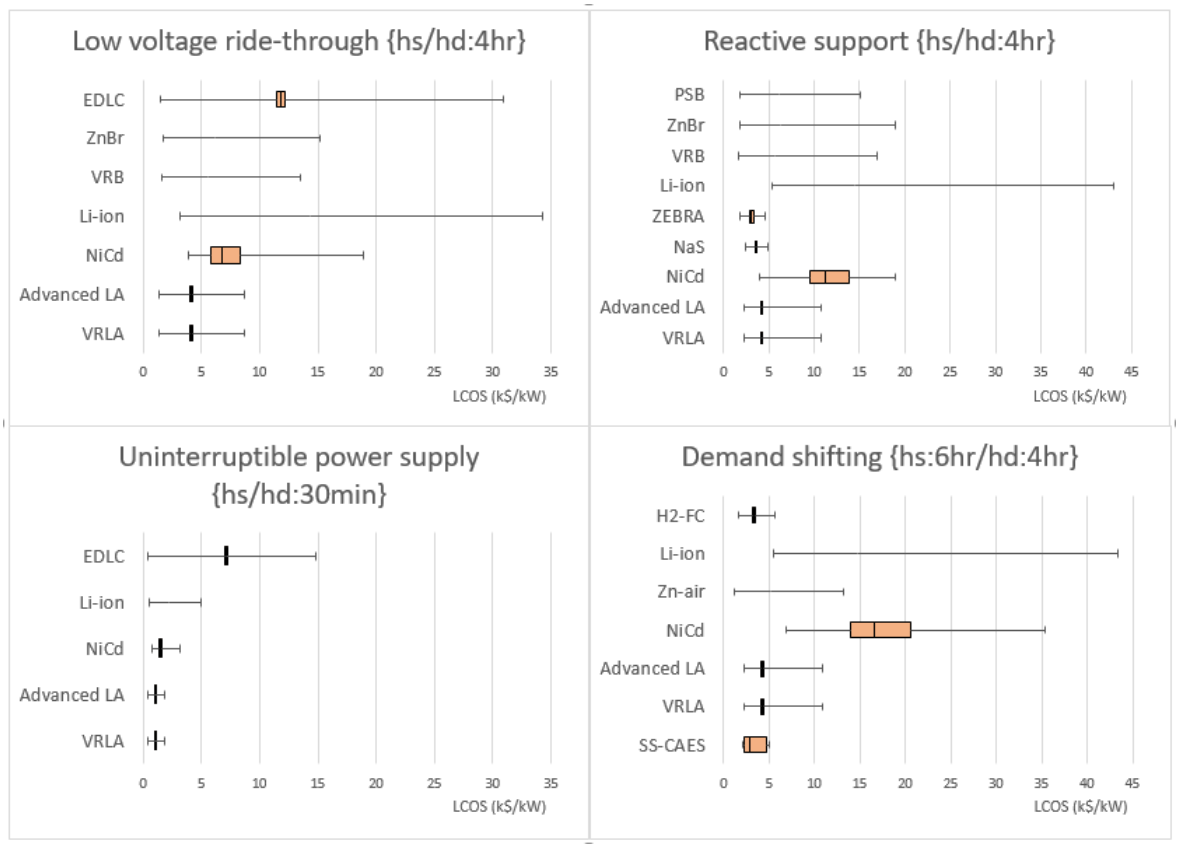

Figure 38. LCOS with varying efficiency for EES participating in Applications 18, 19, 22 and 24 shown in Table 16.

According to the results, minimum LCOS and min/max range favours PHES and CAES for large scale applications such as peak shaving and energy arbitrage. VRLA becomes the cheapest option for low voltage ride-through and uninterruptible power supply, whereas Zn-air BES can be applied for emergency back-up and demand shifting at the demand-side of the meter. In non-spinning reserve applications, H_2 fuel cells can appropriately be integrated, providing the least-cost technology and acceptable range. Finally, reactive support costs less with the application of VRB FBES but the wide range of cost variation adds risk in such an investment. This range is significantly reduced by 83.6 or 81.1% using NaS or ZEBRA BES, respectively.

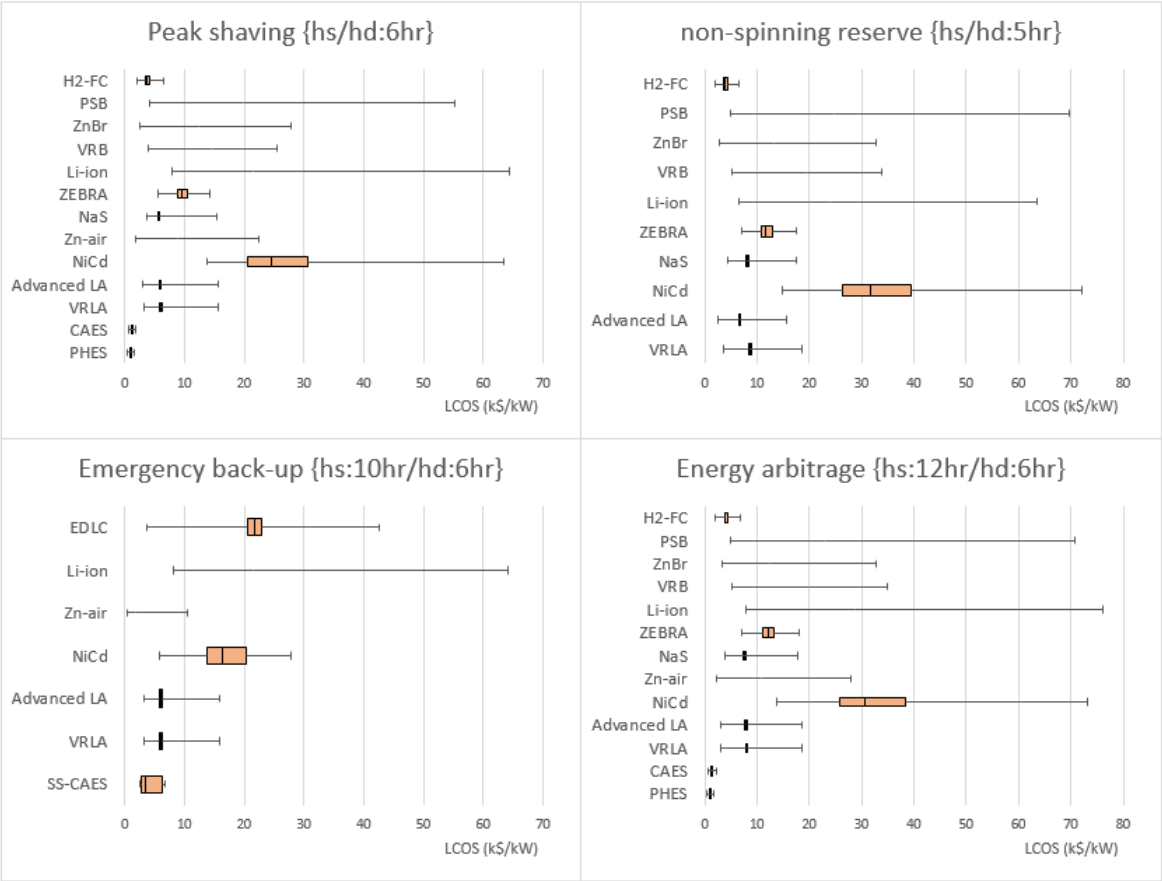

Figure 39. LCOS with varying efficiency for EES participating in Applications 9, 11, 12 and 23 shown in Table 16.

7.2.3 Effect of lifetime

The effect of the variation of lifetime on the LCOS is shown in Figure 40. In order to evaluate its impact, the most frequently cycled applications were selected, namely distributed and centralized fluctuation suppression, forecast hedging mitigation, PV load following, frequency and voltage regulation [107]. Lifetime mainly affects BES facilities due to the degradation of chemical elements and electrolytes. The greatest uncertainty (overall range between best and worst case) is given by Li-ion, the middle range of which accounts for the 40.3% of LCOS range. This share is exceeded by NaS and advanced lead-acid BES which occupy near 52% but with reduced overall range. When the median value of costs is taken into account, advanced lead-acid constitutes the first choice followed by NaS and VRLA. However, considering the minimum costs, EDLC possesses the lowest LCOS compared to the rest of technologies in each of the six applications presented in Figure 40.

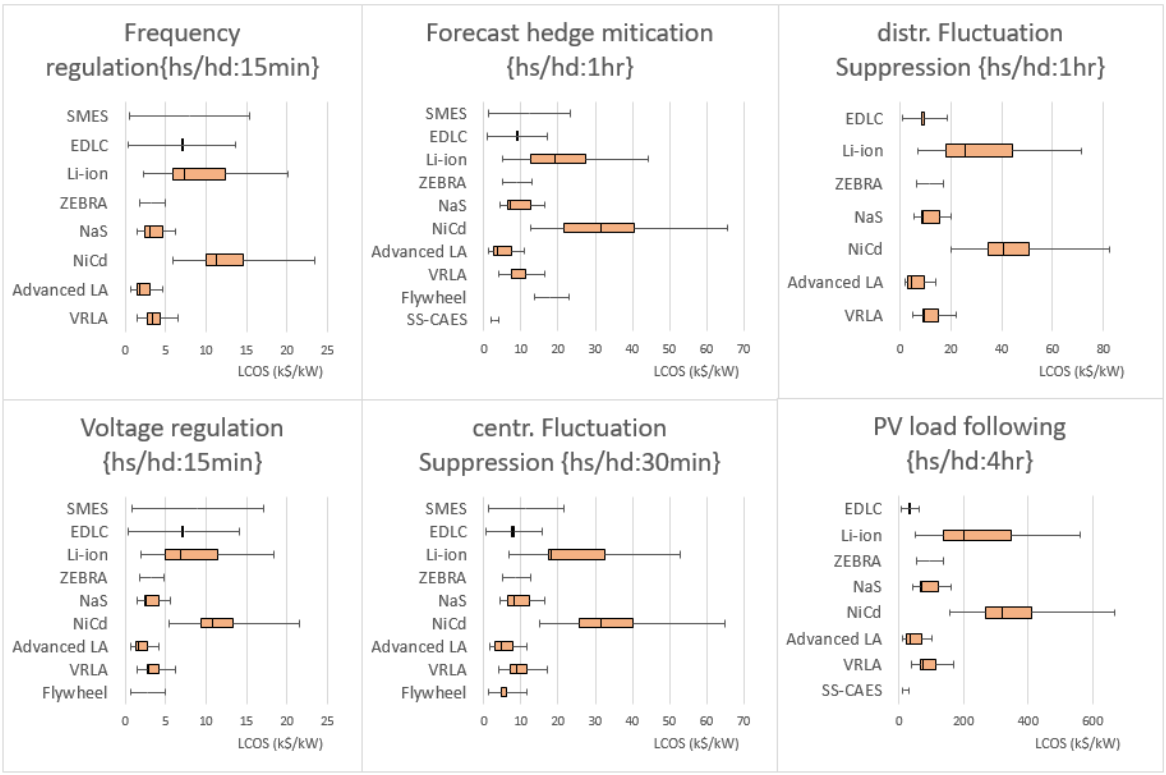

Figure 40. LCOS with varying lifetime for EES participating in Applications 1, 2, 3, 4, 7 and 15 shown in Table 16.

7.2.4 Effect of self-discharge rate

While self-discharge rate constitutes a critical parameter that directly enhances the storage losses, the consistent selection of the appropriate technologies to compete in the proposed applications has prevented its precise impact from being revealed. The selected applications characterized by extended storage periods include load levelling, black-start and seasonal storage. As can be observed, H_2-FC is heavily affected by SDR adding 25.5% of uncertainty to LCOS. Since PHES and CAES systems require large storage reservoirs for acquiring a certain amount of power and energy, H_2-FC would be applicable only in smaller scales. Aiming to reach a clear view of SDR effect on flywheels, spinning reserve was selected and depicted in Figure 41 along with the other three applications mentioned here. As can be seen, SDR variation is superior in a Flywheel system even when the storage period does not exceed a few hours. Based on the middle range, this variation is responsible for the 31.1% of the added uncertainty.

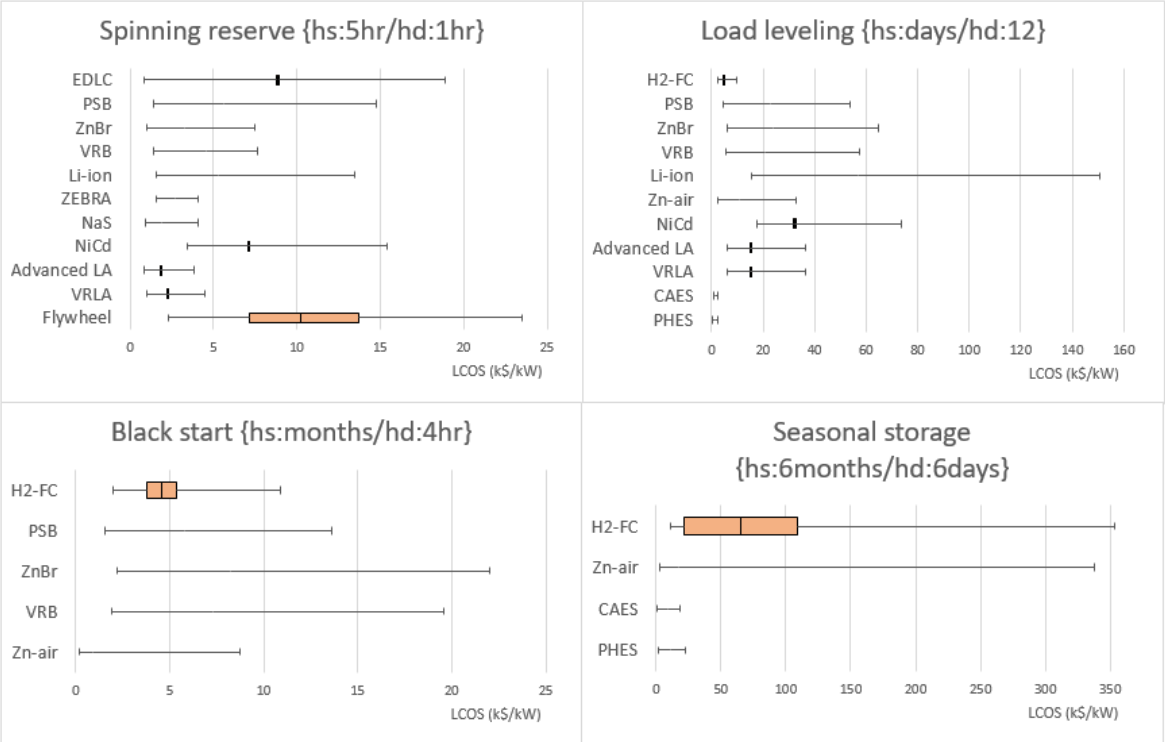

Figure 41. LCOS with varying self-discharge rate for EES participating in Applications 8, 10, 13 and 14 shown in Table 16.

Regarding the minimum LCOS achieved in the best case, PHES plants are preferred in load levelling and seasonal storage while Zn-air is promoted for black start services. Spinning reserve favours advanced lead-acid BES which offers both the lowest minimum cost value and overall uncertainty.

The derived results showed that the LCOS uncertainty favors PHES in unit commitment, peak shaving, energy arbitrage, load leveling, seasonal storage and TCR with no footprint limits. CAES is preferred only when power-rate limitations restrict PHES technology from taking place, while H_2-FC facilities are applicable in smaller scales as non-spinning reserves or for small footprint TCR and wind load following. In short-term and frequently cycled applications (fluctuation suppression, forecast hedge mitigation, PV load following, frequency and voltage regulation), EDLC holds primacy considering minimum cost value.

In terms of uncertainty, advanced lead-acid adds the lowest risk in such investments, while VRLA becomes favourable in low voltage ride-through and uninterruptible power supply. Although, Zn-air constitutes the least-cost technology for emergency back-up and demand shifting operations, SS-CAES would fit better as technology-application pairs based

on the min/max LCOS range. However, it offers the greatest potential in black start provision. Finally, a similar conclusion was drawn from the application of VRB in reactive support where it was displaced by NaS or ZEBRA if overall LCOS range was taken into account. The resulting minimum LCOS values by application are provided in Figure 42.

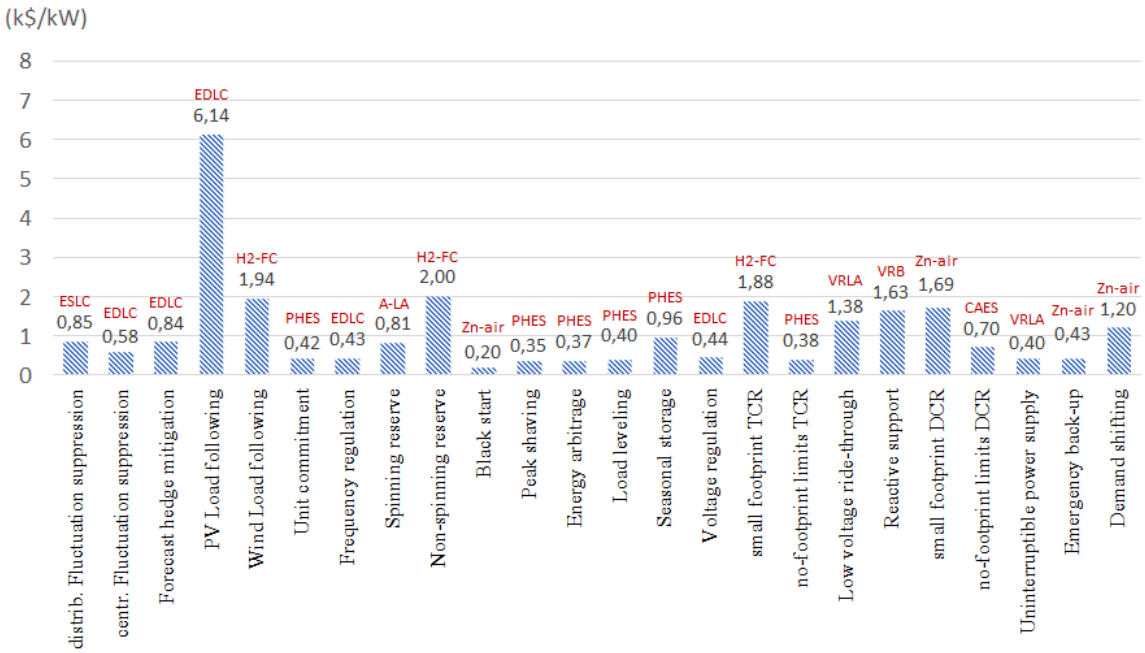

Figure 42. Least-cost EES technology per application.

7.2. A Multi-criteria decision method

In this chapter, an attempt is undertaken to qualitatively compare a total of 19 EES technologies based on their technical and operational characteristics. This constitutes a multi-criteria decision method to validate the findings of the previous quantitative analysis. In order to effectively assess the feasibility of those systems in existing and emerging power grid applications across the power chain, the performance characteristics of interest are normalized. The ranking is selected from 0 to 10, where the range between the worst and ideal is defined accordingly. The normalization is based on 5 different functions according to the expression and which value represents the ideal. Two functions are selected to evaluate the characteristics expressed in real units, while two further are needed for those in percentage values. The last function is typically used to quantify a special technical feature.

In this sense, lower costs (C_i) and self-discharge rates (SDR_i) show higher rankings and thus "0" represents the highest cost and "10" indicates the ideal case. To be consistent with such an assumption, equation (7.11) is used to give the normalized values for the real units of power capital, energy capital and O&M costs, whereas to estimate the rank of self-discharge rates equation (7.12) is applied.

$$Rank(C_i) = 10\frac{maximum - C_i}{maximum} \tag{7.11}$$

$$Rank(SDR_i) = 10(1 - SDR_i) \tag{7.12}$$

Conversely, higher potential features (F_i) including ratings, densities, and specific power and energy, cycling and lifetime, show high rankings and thus are estimated by equation (7.13), while efficiencies (η_i) are normalized based on equation (7.14) which determines a poor performance with "0" and an ideal of 100% with "10".

$$Rank(F_i) = 10\left(1 - \frac{maximum - F_i}{maximum}\right) \tag{7.13}$$

$$Rank(\eta_i) = 10\eta_i \tag{7.14}$$

Finally, the special feature of technical maturity of each technology is normalized as follows: "2" corresponds to "developing" technologies, "4" to demonstration, "6" to commercializing, "8" to commercialized, and "10" to mature. The normalized values for the selected technical and operational features are provided in tables. Assumptions made here, include only the costs derived from different sources but in the range of no greater than 10 years so that the exchange rates have remained relatively stable and no present value adjustments have to take place.

Mechanical EES technologies are summarized and compared Figure 43. As can be seen, the most mature is PHES technology followed by CAES and FES which are commercialized and commercializing, respectively.

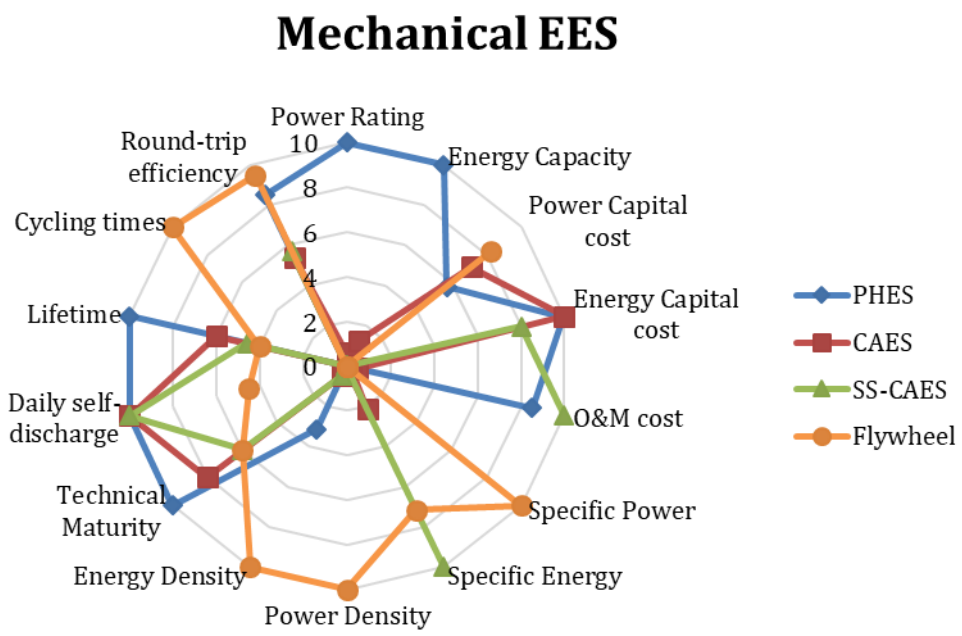

Figure 43: Potential characteristics of mechanical energy storage technologies.

The highest power rating and energy capacity correspond to PHES which exhibits the advantage over the others, with the FES being the last in the row. On the other hand, PHES and CAES offer quite low performance per unit mass and volume, requiring large storage reservoirs for acquiring a certain amount of power and energy.

Consequently, they become disadvantageous in relation to FES technology in applications where space and weight are limiting factors. The capital costs follow a reverse order per units of energy and power. The highest power capital cost concerns PHES technology favouring FES, whereas the highest energy capital cost corresponds to FES and promotes the rest of two, with CAES occurring slightly less expensive. PHES offers the longest lifetime and the less O&M cost, while FES enjoys the highest efficiency and cycling capability. Finally, the parasitic losses are superior in a FES system resulting in even a full daily self-discharge, while PHES and CAES plants possess negligible losses and almost zero daily self-discharge rate.

Compared to the rest of technologies and according to those mentioned in Chapter 4, in large-scale applications (of greater than 100MW) PHES and CAES achieve the lowest energy capital cost for extended storage durations of days to months. FES devices are presented less cost-effective compared to electromagnetic storage mainly due to their high capital cost. It is worth noting that the capital cost of auxiliary equipment needed for power

conditioning in electromagnetic systems is not included. Also, the overall efficiency (due to AC/DC and back to AC conversions) may favour flywheels which do not require voltage rectification before interconnect with network.

Historically, chemical EES systems have by far spurred the greatest interest of research, demonstrating many different chemistries and topologies to meet the ever-increasing demand from the old 1859s up to date. The first conventional secondary battery, Pb-acid, was invented in 1859. Since the beginning of the next century (and specifically in 1915), NiCd batteries have been used commercially, followed by the introduction of NaS in the 1960s. Although Li-ion battery was first proposed in the same year, the first was produced 31 years later. In 1980, VRB flow battery was pioneered in Australia and the basic patents were bought in 1998, whereas the ZnBr was developed in 1970 and demonstrated in 1991. ZEBRA technology was acquired by MES (Swiss) in the early 1999 [78]. Although many other chemical technologies, including secondary batteries, flow batteries and fuel cells, have been investigated and found technically possible, they are still under development.

The most popular chemical EES technologies, both conventional, molten salt and metal-air batteries, and regenerative fuel cells, are examined and compared in Figures 44 and 45. Pb-acid batteries accounts for the largest secondary battery market share in the world. The low cost and maintenance combined with relatively high-power output and efficiency, make them attractive in automotive, telecommunications and UPS industries.

Despite the high environmental impact, this kind of battery has been also used in MW-scale stationary applications in conjunction with renewables. NiCd batteries also provide high environmental impact. With similar features such as high efficiency, specific power and moderate self-discharge, NiCd offers more cycling times and longer lifetime, higher energy density and power ratings, whereas it becomes disadvantaged in capital costs and power density. Improved performance is achieved by NiHMe which provides higher power and energy densities, lower capital costs, no self-discharge in the expense of lower efficiency, cycle capability and lifetime. For a given amount of energy, Li-ion batteries require the smallest volume and weight. Along with their higher efficiency of near 100% and extended cycle times, Li-ion batteries offer widespread uses in portable devices and promising potential in transportation and small-scale stationary applications.

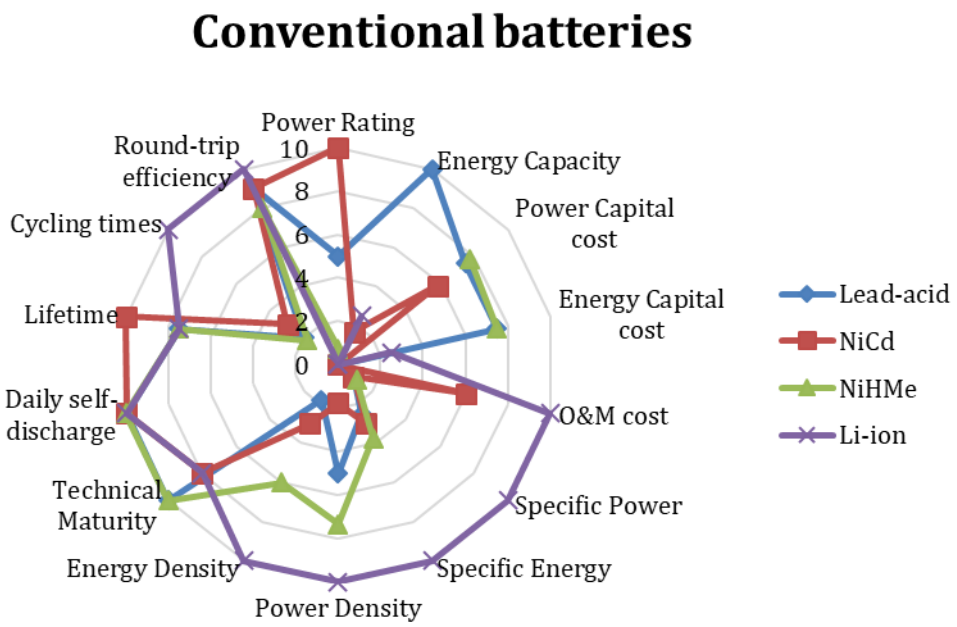

Figure 44: Potential characteristics of conventional battery technologies.

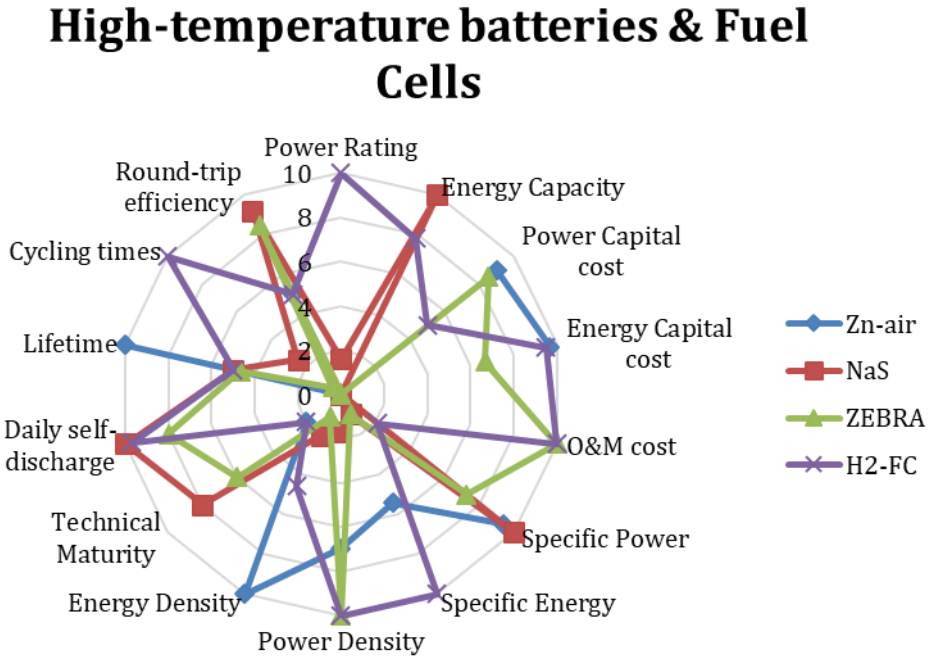

Figure 45: Potential characteristics of high-temperature battery and fuel cell technologies.

High energy batteries including NaS, ZEBRA and Zn-air, together with PEM regenerative FC are summarized in Figure 45. One can be seen is that NaS technology

possesses the highest efficiency followed by ZEBRA, while Zn-air and regenerative FC provide the lowest one of fairly 50%. Regarding the energy density, Zn-air occurs promising while the regenerative FC becomes advantageous in specific energy. The key limitations of Zn-air are found in cycling capability and power rating whereas the major advantages include long lifetime and low capital investment. Regenerative FC are able to provide power density as high as ZEBRA but with lower energy capital cost, limited maintenance cost and better cycling capability. In addition, ZEBRA exhibits severe self-discharge rate in contrast to almost zero of NaS within a day. NaS constitutes the most expensive EES investment in the category and in order for the rest of the technologies to become competitive, more research is needed to improve the round-trip efficiency and lower the cost.

Constituting a developing technology, regenerative FCs provide excellent energy-cost performance able to compete even the mature PHES and CAES for storage durations of up to 12 hours, while they are exclusively preferred when footprint becomes a crucial factor. Transmission congestion relief could be a reference scenario to demonstrate such a requirement. Although they provide the best energy performance of all battery chemistries, NaS systems possess the most expensive O&M costs followed by flow batteries since they both require additional equipment to maintain the energy stored.

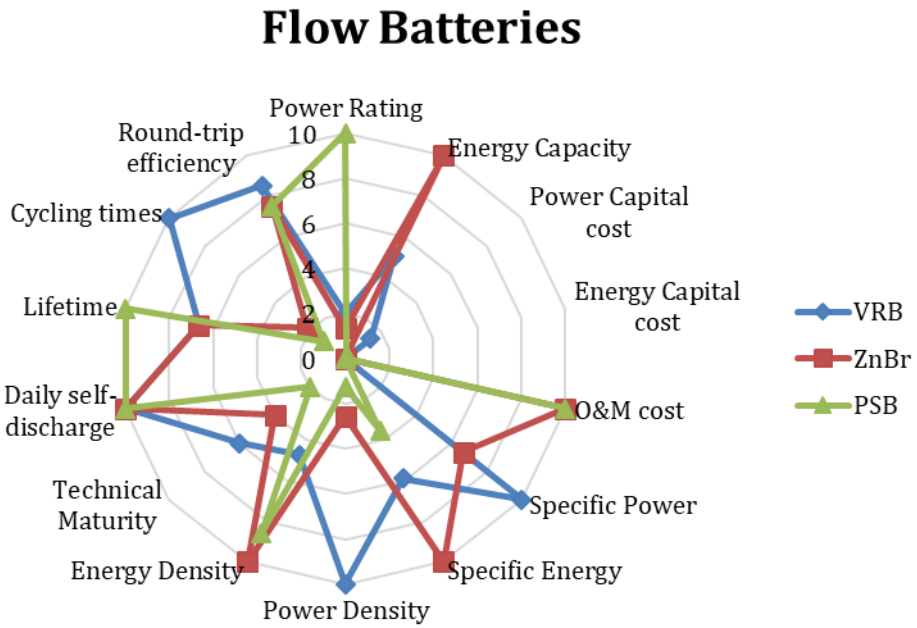

Figure 46: Potential characteristics of flow battery technologies.

VRB flow batteries outweigh the ZnBr and PSB in technical maturity, efficiency, cycling capability, specific power and power density. However, they provide moderate specific energy and the lowest energy density, constraining their use in applications where bulk energy storage needs to take place. All this information is presented in Figure 46 and as shown, with a similar capital investment such potential features can be greatly improved by a factor of two, utilizing the different topologies of ZnBr or PSB flow batteries. Hence, improvements in both cycle efficiency and lifetime are needed in order to become competitive and contribute in future power system applications.

Capacitors and inductors are appropriate to store small quantities of energy. Recent advances have extended the use of capacitive and inductive technologies to larger scale applications. Figure 47 demonstrates the selected potential features of capacitors, supercapacitors and superconductors, allowing a direct comparison between them. Supercapacitors experience the highest efficiency and lowest investment and whole life costs. SMES can be cycled almost infinitely and provides the longest lifetime, whereas it occurs disadvantageous in terms of power and energy performance along with capital and O&M costs. Due to increased parasitic losses, electromagnetic EES technologies suffer from severe self-discharge and thus they become favourable only in high power/short duration applications. The daily self-discharge rate slightly favours SMES.

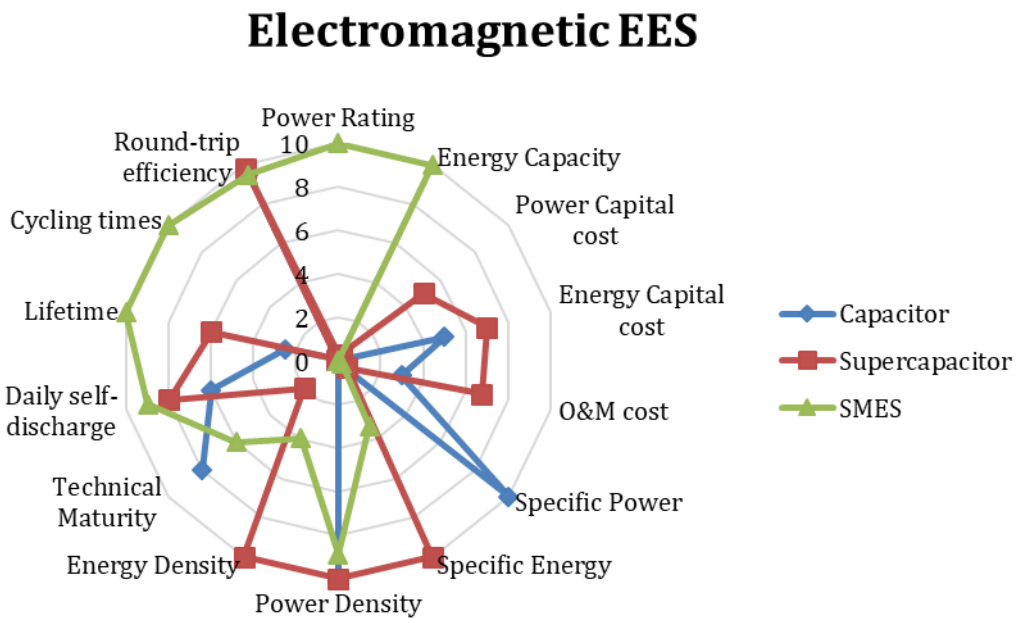

Figure 47: Potential characteristics of electromagnetic energy storage.

Apart from the significant improvements in efficiency and extended lifetimes, capital and O&M costs tend to be decreased by increasing R&D efforts. Mature technologies offer the lowest energy capital cost reducing the investment risk in large-scale/long duration applications. Regarding O&M costs, chemical technologies that require chemical handling are disadvantageous against others, followed by technologies that need additional equipment to maintain the energy stored (e.g. NaS battery and VRB flow battery). In terms of power capital cost, devices that can deliver high power are required when the discharge period is short, whereas for extended discharge periods of several hours or more, there is a requirement for devices that can store large amounts of energy with low O&M costs.

8. Isolated power grids: A demonstration of our integrated solution

We conclude this thesis by providing a comprehensive and consolidated demonstration of our integrated approach. The solution consists in finding both the optimal size of the intended EES facility and UC schedules based on actual annual data. The evolved formulation takes into account the variable renewable energy contribution, embedding a large number of real-world constraints regarding an isolated power network.

In contrast to the large interconnected power systems, the integration of intermittent RG in autonomous island grids is subject to security and reliability limitations. As a result, operating reserves (both spinning and non-spinning) are required to cover the uncertainty caused by forecast errors, whereas sufficient ramping capability is necessary to address the variability issues which often occur at high time resolutions (e.g. minute-to-minute) [224]. Spinning reserves represent the on-line capacity synchronized to the grid and ready to meet electric demand within 10 minutes while non-spinning is the off-line generation capacity that can be ramped to capacity and synchronized to the grid within 10 minutes and can maintain that output for at least two hours.

Due to the isolation, small area and remoteness, electricity supply for people inhabited in more than 50 thousand islands on the earth, mainly rely on imported fossil fuels the price of which is 3-4 times higher than that in the mainland. On the other hand, for most islands the sunlight is sufficient for generating abundant electricity from PV in summer while in winter wind power can be the main contributor to electricity supply [225]. Consequently, it is crucial for a solution to be examined, in order to facilitate a shift towards decarbonization without degrading the continuity and quality of power supply in islands but reducing the exposure of such weak economies to varying fuel prices or shortages [226].

Electrical energy storage (EES) constitutes a potential candidate capable of regulating the power generation to match the loads via time-shifting. EES may favor some technologies from being applied in contingency reserves, based on two main requirements namely, the time of response and storage duration. First, the rapid response needed to provide a large fraction of both primary and secondary reserves favors the flywheels, electrochemical and electromagnetic storage technologies. The second requirement invites the storage system to retain the energy stored for several days and operate as a complement or substitute when needed instead of increasing/decreasing its output to continuously maintain the generation-

demand balance. This excludes flywheels and electromagnetic storage (both capacitive and conductive) from participating because of their increased daily parasitic losses expressed by their self-discharge rate [70]. Within the wide variety of electrochemical storage systems, Nickel-based technologies are also excluded because of memory effect aspects [74].

Based on the previously described concept, the performance of battery-based energy storage facilities applied in an island's power system is investigated. The considered technologies include lead-acid (Pb-acid), zinc-air (Zn-air), sodium-sulfur (Na-S), lithium-ion (Li-ion) batteries and vanadium-redox (VRB), zinc-bromine (Zn-Br) and polysulfide-bromide (PSB) flow batteries. The spinning reserve requirements (power rating and energy capacity) derives after strongly restricted unit commitment (UC) optimization solved via a novel Lagrange Relaxation method, based on real data of both generation and demand. Each EES system is subjected to life-cycle cost analysis distinguishing their power-related and capacity-related costs. Once optimally planned, the systems are analysed and compared through an ablation analysis concerning the most recent technological variations in development status and cost metrics in research.

Aiming at minimizing the spinning reserve requirements, our investigation is focused on a methodology performed in four steps; 1) the robust formulation for the UC problem considering both operational and technical constraints; 2) the extraction of the optimal solution based on maximum RES integration subject to the complex constraints; 3) the determination of EES optimal size; and 4) the life-cycle cost analysis of the examined EES models.

8.1. Problem Formulation

The total production cost (TPC) of a power system consisting of traditional thermal units is mainly the cost of fuel (C_F), start-up (C_{SU}) and shut-down (C_{SD}) costs, maintenance cost (C_M), emission cost (C_E), and cost of energy not served (C_{ENS}). By denoting the number of generating units with N and the number of periods with T, a formulation for the UC problem is as follows:

$$\min \sum_{t=1}^{T} \{ \sum_{i=1}^{N} \{ \left[F_i\left(P_i^t\right) + E_i\left(P_i^t\right) + C_{M_i}^t + \left(1 - U_i^{t-1}\right) C_{SU_i}^t \right] U_i^t + \left(1 - U_i^t\right) C_{SD_i}^t U_i^{t-1} \} + C_{ENS}^t \} \quad (8.1)$$

$$s.t.$$

$$\sum_{i=1}^{N} P_i^t = P_{netD}^t + P_{loss}^t \tag{8.2}$$

$$\sum_{i=1}^{N} P_{i,\max\_cap}^t \geq P_{netD}^t + SR^t \tag{8.3}$$

$$P_{i,\min}^t . U_i^t \leq P_i^t \leq P_{i,\max}^t . U_i^t \tag{8.4}$$

$$U_i^t = 0 \rightarrow 1 \quad if \quad \sum_{t=td}^{t-1} (1 - U_i^t) \geq MD_i \tag{8.5}$$

$$U_i^t = 1 \rightarrow 0 \quad if \quad \sum_{t=tu}^{t-1} U_i^t \geq MU_i \tag{8.6}$$

$$P_i^t - P_i^{t-1} \leq RU_i, \quad if\ generation\ increases \tag{8.7}$$

$$P_i^{t-1} - P_i^t \leq RD_i, \quad if\ generation\ decreases \tag{8.8}$$

While the objective (8.1) is the sum of total production cost in all periods, U_i^t and P_i^t are used to model various operational constraints. Constraint (8.2) ensures that the sum of the power produced from all committed units meets the net load demand (P^t_{netD}) along with transmission loss (P^t_{loss}) at each time-interval, considering the contribution of renewable generation (P^t_{RG}) normally treated as negative load so that $P_{netD}^t = P_D^t - P_{RG}^t$. Constraint (8.3) guarantees that the power margins cover the spinning reserve requirements SR^t based on the maximum ramping capacity ($P^t_{i,max\text{-}cap}$) of each unit. The maximum and minimum rated power forcing the generating units to operate within their boundaries are represented by constraint (8.4). Considering the time a unit has started-up (t_u) or shut-down (t_d), the satisfaction of predefined minimum up (MU_i) and down (MD_i) times before a change in state occurs is constraint by (8.5) and (8.6), respectively. The last constraints (8.7) and (8.8), represent the ramp-up (RU_i) and ramp-down (RD_i) rate restrictions between consecutive periods.

Further constraints may include the unit status restrictions and plant crew constraints. Unit status may restrict a unit in three possible states namely, the must-run, must-out and run at a fixed-MW output. The number of units that can simultaneously start-up is restricted

by the plant crew constraints depending on the number of operators available or the maximum water availability for feeding multiple boilers.

8.2. Optimal EES sizing

The role of the proposed EES facility is to store and provide energy, in order to replace the deficit of spinning reserves. Aiming to evaluate the improvement achieved by the application of EES, two case-studies are investigated with weekly simulations carried out for the entire duration of a year. In the first case, the optimal UC schedules along with the total production costs are evaluated based on non-zero spinning reserve requirements ($SR \neq 0$) and model (8.1) - (8.8). The procedure is repeated in the second case where the application of EES adequately replaces the spinning reserve margins. Sitting fully charged and ready to be brought online when called upon, the EES facility makes the system capable of handling net-load dynamic changes ensuring the operation reliability. Thus, the second case considers zero spinning reserve requirements ($SR=0$) from thermal power plants.

The optimal scheduling of generating units to meet the net load demand is solved over a short-term horizon of 336 half-hours. To initialise the process, some initial states of generating units took place: minimum up and down times are considered qualified, all units are assumed to operate between minimum and maximum power limits and start-up costs add no value for the first-time slot. Aiming to evaluate both the impact of intermittent RES and the improvement achieved by the application of EES systems, we investigated the two case-studies with weekly simulations carried out for the entire duration of the year.

The first case accounts for the RES contribution, considering biomass as a firm import but solar and wind as variable renewable energy sources (VRES). In this regard, spinning reserve requirement is differentiated according to Equations (8.9) and (8.10):

$$SR^t = 6\%.\, P^t_{netD} + 100\%.\, P^t_{VRES} \tag{8.9}$$

$$P^t_{VRES} = P^t_{wind} + P^t_{solar} \tag{8.10}$$

, where P^t_{wind} and P^t_{solar} are the instantaneous, summed power output from wind and solar generators, respectively. Finally, we completely neglect and exclude the spinning reserve

requirement from the objective function in the second case. The integration of sufficient in terms of power rating and energy capacity EES devices, guarantees the adequacy of spinning reserve margins and makes the system capable of handling net-load dynamic changes and ensures the operation reliability. We model the cost of energy not served C_{ENS}^{t} based on Equation (8.11) which assigns the constant maximum cost of all units being online and operating at their maximum power output. The start-up costs can be calculated based on formulation (3.6).

$$C_{ENS}^{t} = \sum_{i=1}^{N} F\left(P_{i,max}^{t}\right) \tag{8.11}$$

To adequately replace SR requirements the optimal size (both rated power and energy capacity) considers the worst-case scenario. Therefore, the rated power (P_{rated}^{*}) can be defined according to the maximum difference between spinning reserve margin without storage and power margin from committed units when storage was applied to eliminate it, as follows:

$$P_{rated}^{*} = \max_{t} P_{rated}\,(t) \quad , \forall t \in \mathcal{T} \tag{8.12}$$

$$P_{rated}(t) = \sum_{i=1}^{N} \{P_{i,max-cap}^{t}\,(SR \neq 0) - P_{i,max-cap}^{t}(SR = 0)\} \tag{8.13}$$

On the other hand, energy capacity (E_{cap}^{*}) is determined by the highest requirement to provide power for h_s hours, as defined by Equations (8.14) and (8.15).

$$E_{cap}^{*} = \max_{t} E_{cap}\,(t) \quad , \forall t \in \mathcal{T} \tag{8.14}$$

$$E_{cap}(t) = \int_{t}^{t+hs} \sum_{i=1}^{N} \{P_{i,max-cap}^{t}(SR \neq 0) - P_{i,max-cap}^{t}(SR = 0)\}dt \tag{8.15}$$

Performing weekly simulations for a whole year, the annual profitable return (*APR*) can be computed according to Equation (8.16).

$$APR = \sum_{t=1}^{T} [TPC_{SR\neq 0}(t) - TPC_{SR=0}(t)] \quad (8.16)$$

8.3. Life-cycle cost analysis

The selected EES facilities are modeled considering both the investment and operation costs. Power-related costs concern the power conversion system (PCS) and balance of plant (BOP) while energy storage medium (ESM) involves the energy-related costs. As a result, the initial project cost (IPC) can be expressed as a function of rated power (P^*_{rated}) and energy capacity (E^*_{cap}) based on the following equation:

$$IPC = E^*_{cap}.C_{ESM} + P^*_{rated}.(C_{PCS} + C_{BOP}) \quad (8.17)$$

To meet the requirements of the intended application in terms of output (useful) energy, C_{ESM} must be oversized to take into consideration the ac-to-ac conversion losses, the maximum permitted capacity and parasitic losses. Hence, IPC is rewritten as a function of the round-trip efficiency (η), depth of discharge (*DoD*), self-discharge rate (*SDR*) and storage duration (h_s):

$$IPC = E^*_{cap}.\frac{C_{ESM}}{\eta.DoD}.(1 + SDR.h_s) + P^*_{rated}.(C_{PCS} + C_{BOP}) \quad (8.18)$$

Operation and maintenance (O&M) cost accounts for both fixed O&M values ($C_{fO\&M}$) expressed per kW-year and variable O&M values ($C_{vO\&M}$) which represent the operational costs that change as a function of annual discharged energy (E_{dis}) [26]. The total O&M cost ($C_{O\&M}$) is calculated through the use of Equation (8.19).

$$C_{O\&M} = C_{fO\&M}.P^*_{rated} + C_{vO\&M}.E_{dis} \quad (8.19)$$

For each individual technology *k* selected to participate, the life-cycle cost (*LCC*) (during the span of the EES facility's useful lifetime) can be computed as the present value of the system by Equation (8.20). The net present value (*NPV*) for each EES facility *k* is finally achieved by Equation (8.21).

$$LCC_k = IPC_k + \sum_{t=1}^{N} \frac{C_{O\&M}^k(t)}{(1+i_R)^t} \tag{8.20}$$

$$NPV_k = -IPC_k + \sum_{t=1}^{N} \frac{APR(t) - C_{O\&M}^k(t)}{(1+i_R)^t} \tag{8.21}$$

, where N is the examined lifespan in years and i_R the discount rate.

8.4. Case study system

A medium-sized energy system is selected with a peak demand of 1108MW and a load factor of 53% which constitutes a representative example of an island's autonomous, non-interconnected power system. This is the system of Cyprus powered by three thermal power plants consisting of a total of twenty generating units whose main technical and economic characteristics are listed in Table 18, as well as by domestic renewable resources including biomass, solar PV and wind. According to the Cyprus Energy Regulatory Authority (CERA), during the year from 01 January 2017 to 31 December 2017 the installed capacity for thermal, wind, PV and biomass generating units was 1278MW, 157.5MW, 112.2MW and 9.81MW, respectively. Their contribution in electricity production can be observed from a Sankey diagram depicted in Figure 48 [227].

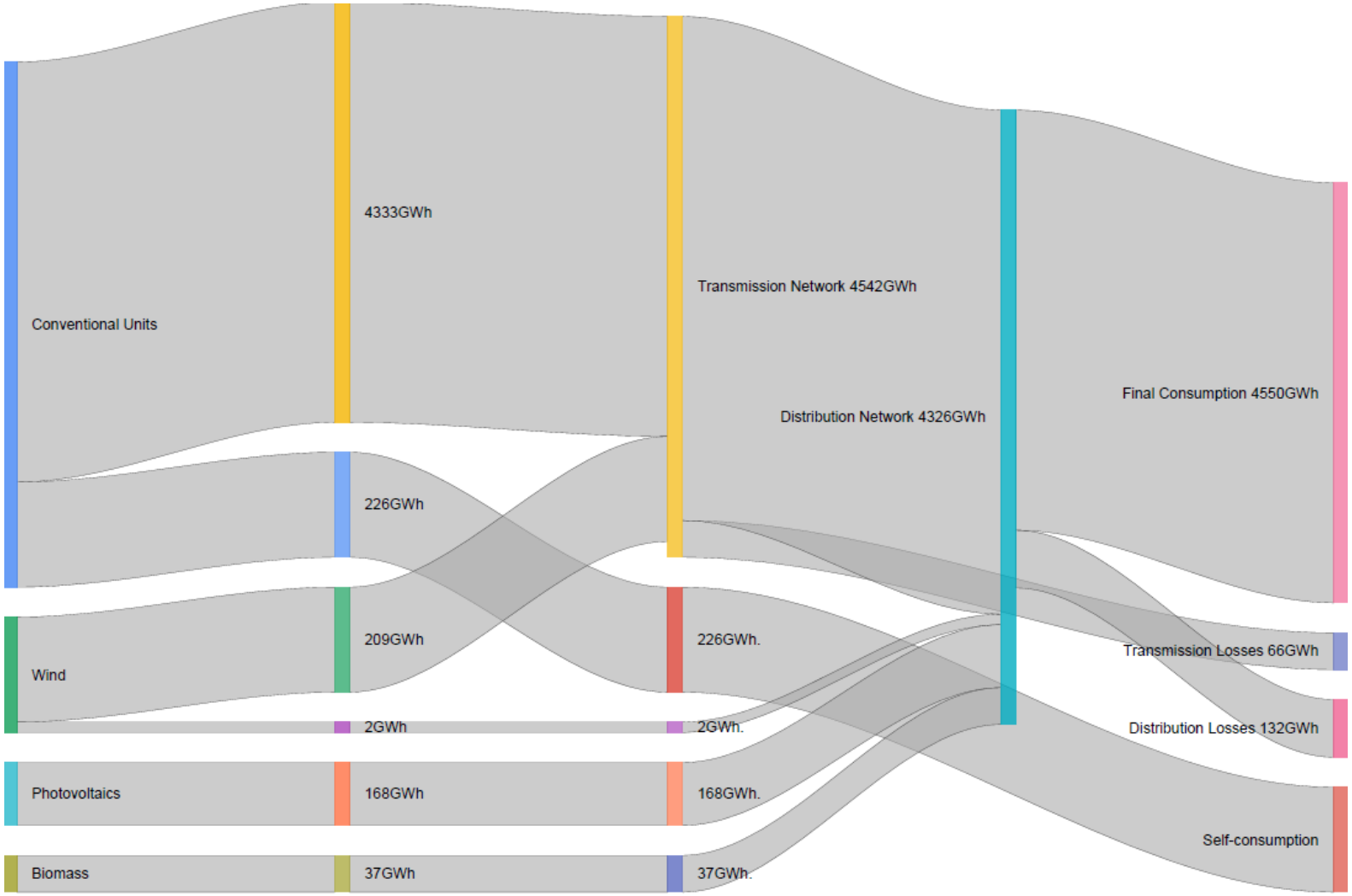

Figure 48: Sankey diagram for the total electricity generation during 2017.

Table 18. Parameters of the thermal generating units.

Group	Num. of units	Pmin (MW)	Pmax (MW)	a (€/h)	b (€/MWh)	c (€/MW^{2}h)	RU (MW/min)	RD (MW/min)	MU (hr)	MD (hr)	HSU (€)	CSU (€)	t_{cold} (hr)
1-Gas turbine	4	4	37	949.05	67.84	0.213	5	5	3	0.5	15	104	0
2-Steam turbine_1	6[1]	30	58	1002.75	62.133	0.2827	1	2	8	2	1586	5786	4
3-Internal combustion engine_1	3	8.75	17	154.745	62.247	0.0215	1	1	2	1	33	66	1
4-Internal combustion engine_2	3	14.5	17	189.698	51.666	0.4377	1	1	2	1	33	66	1
5-Steam turbine_2	3[1,2]	66	124	1236.079	56.694	0.0662	4.2	4.2	8	12	2520	9200	6
6-Combined cycle	2[3]	66	216	2476.761	43.193	0.0395	12	12	6	12	30	208	2

[1] One of the units is constantly in must-run mode.

[2] One of the units was out of service for 2017.

[3] Operating in 2+1 mode.

Table 19. Technical characteristics and cost metrics of EES technologies.

Technology	Daily self-discharge (%)	round-trip efficiency (%)	DoD (%)	BOP ($/kW)	PCS ($/kW)	ESM ($/kWh)	Fixed O&M ($/kW-year)	Variable O&M ($/MWh)
Pb-acid	0.1-0.2	85-90	80	120-600	58-180	200-500	4.29	0.20
Zn-air	almost 0	45-55.8	100	120-600	0-120	10-60	-	-
Na-S	almost 0	89-92	100	120-600	0-120	300-500	20	0.40
Li-ion	0.03	~100	80	120-600	0-120	600-2500	2.68	0.54
VRB	almost 0	85	100	120-600	0-120	150-1000	4.56	0.27
Zn-Br	almost 0	67.5	100	120-600	60-120	150-1000	4.29	0.40
PSB	almost 0	67.5	100	120-600	36-120	150-1000	-	-

To assess the impact of EES on system operation, both weekly and yearly simulation results are required. The necessary data obtained from CERA regard the half-hourly power demand during the year of 2017 along with the real-time generation from renewable energy sources (RES). Two case studies are carried out to evaluate the profitable return derived by the application of EES. The first case assumes a spinning reserve requirement accounting for 6% of the total power demand and 100% of the variable renewable energy sources (VRES). Offering a monthly-constant power output, biomass is considered as a firm import, whereas VRES refers to wind and PV generation for each time interval of the year. By the application of EES in the second case, the spinning reserve requirements become zero and the optimization procedure is repeated recording the total production cost.

The variation in load demand for the whole year of 2017 and weekly representative profiles for summer, winter and spring is provided in Figure 49 and Figure 50, respectively [45]. Based on a single bus model we assume that the demand is satisfied as soon as the total production is approximately equal to the total consumption and spinning reserve requirements are qualified.

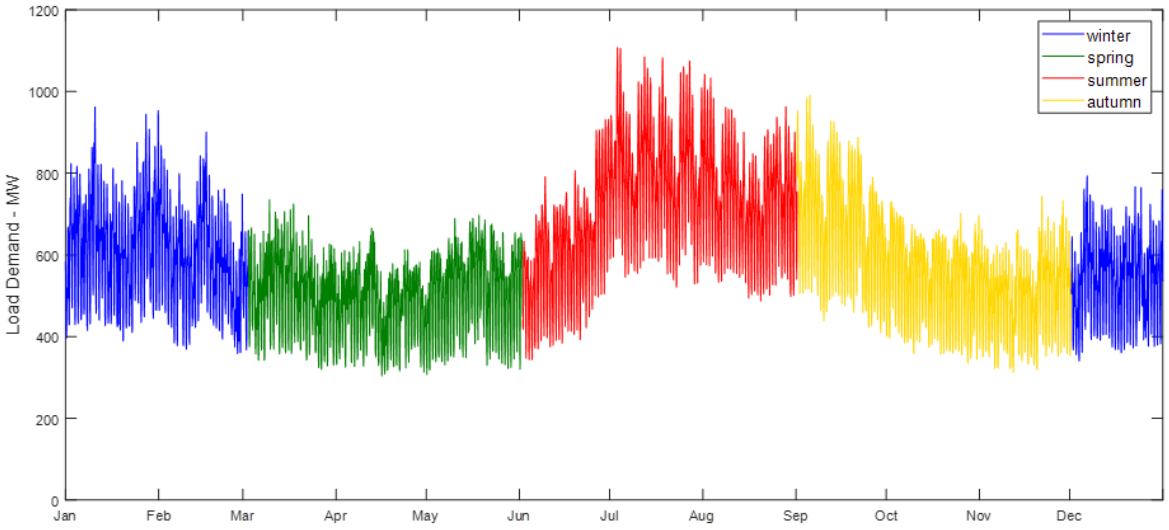

Figure 49. Annual electricity demand variation during the entire year of 2017.

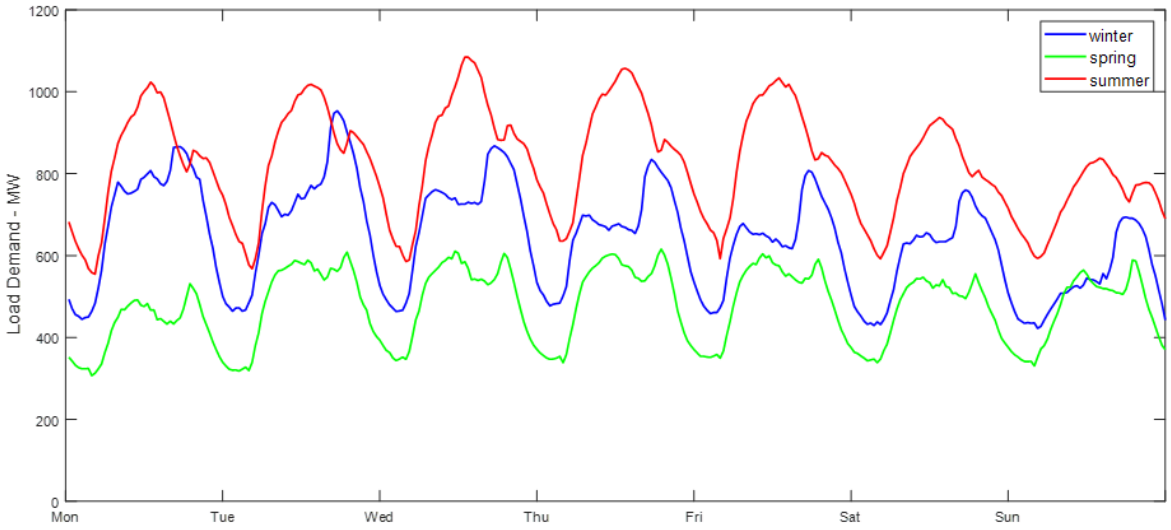

Figure 50. Weekly profile of seasonal electricity demand of the year 2017.

8.5. Results

For comparison purposes and based on actual, real-time data, the deterministic formulation of UC is advisable and useful. The optimal scheduling of generating units to meet the net load demand is solved over a short-term horizon of 336 half-hours to let ramp-rate limitations be involved. Completing the second's case 52-week optimization process, the *APR* achieved was rated at €55,839,700 according to Equation (8.16). Undoubtedly, SR provides a high influence on the TPC. Forcing the utilities to over-schedule and individual units to operate partially-loaded, leads to increased start-up costs, inefficient and uneconomic dispatch.

The contribution of RES during the week which comprises the worst-case scenario is presented in Figure 51. The high variability of the net load cannot be satisfactorily absorbed by the weak power system (due to ramp-up and -down limitations), requiring faster-response and expensive gas turbine generation to take place. The resulted UC programs for the worst-case scenario derived from the two case-studies are depicted in Figure 52. By making use of Equations (8.12-8.13) and (8.14-8.15) the optimal size of EES system was determined. In terms of power rating and energy capacity to 143.94MW and 498.94MWh, respectively.

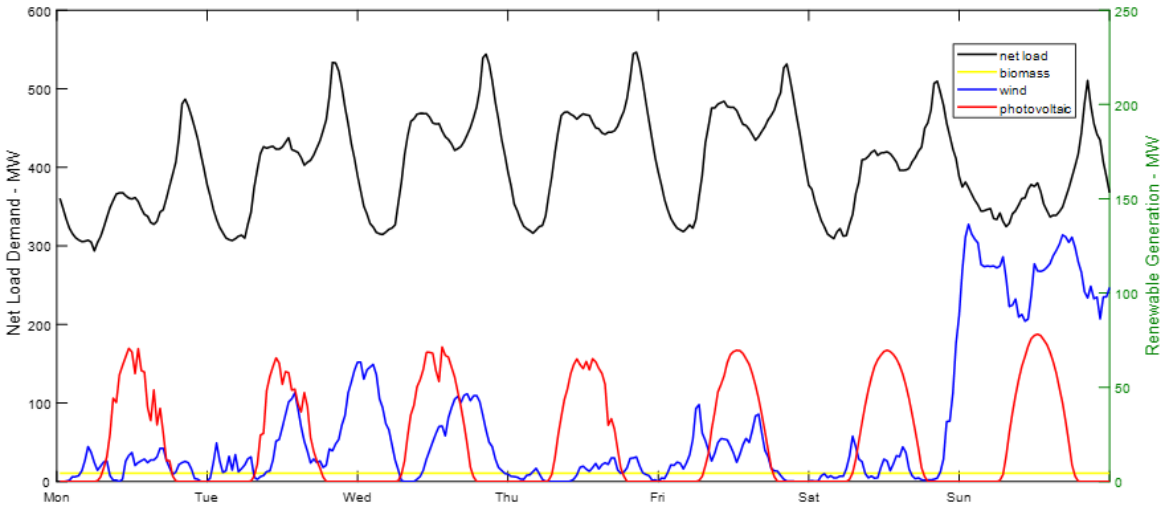

Figure 51. Net load demand vs. RES contribution for the week comprising the worst-case scenario (23 April 2017).

All necessary information regarding the different EES technologies selected is listed in Table 19. The ac-to-ac conversion efficiency assumed to be 90% including both transformers and converters, while we considered zero transmission losses (placement of devices near thermal generation units) [228]. The examined lifetime (*N*) was set at 10 years in order to avoid any replacements based on the lifetime of the main components comprise each EES facility [229]. Since the costs relating to fixed O&M and variable O&M were unavailable for Zn-air battery and PSB flow battery, the maximum values based on the rest of technologies were assumed. The main characteristics affecting the life-cycle cost analysis performed are enclosed in Table 20.

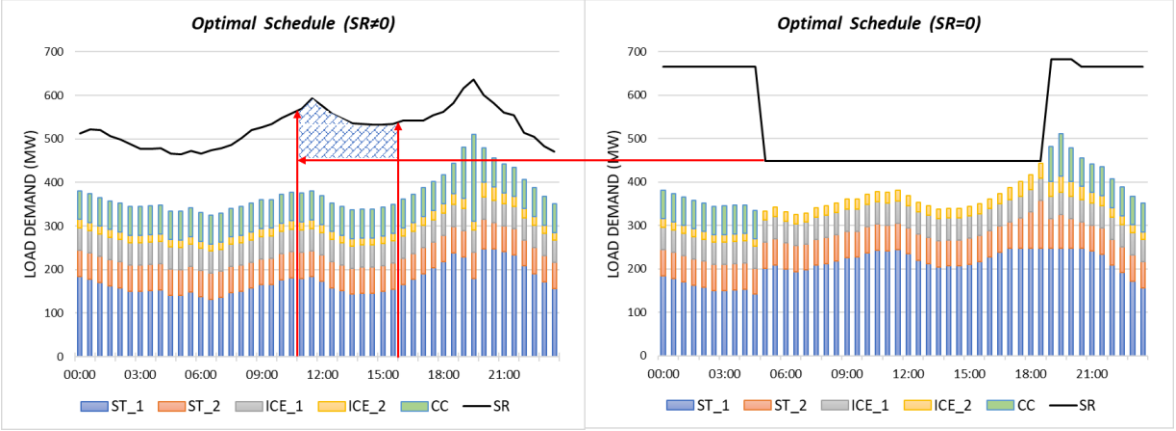

Figure 52. Optimal power scheduling for the worst day of the year before EES (SR≠0) and in the presence of EES (SR=0).

Table 20. Main characteristics considered in overall analysis of EES.

Characteristics	Value
Life-cycle cost analysis	
APR	€ 55,839,700
Discount rate (i_R)	2.5 %
Conversion losses	10 %
Examined life-time (N)	10 years
Replacement cost	-
Storage duration (h_s)	5 h
vO&M discharged energy (E_{dis})	Annual self-discharge losses (MWh)
Unit Commitment	
Number of weekly time intervals	336
Balance tolerance	0.1 MW
Crew constraint per power plant	≤ 3

Finally, in order to include the uncertainties due to the large technological variations between system types, we performed uncertainty analyses considering the variation range between all input parameters. Table 21 lists the calculated results while their graphic representation is shown in Figure 53. The median value indicates the *NPV* for averaged values for all inputs to decide whether investing in a technology is feasible. Min/max range refer to the extremities between low performance/high costs and high performance/low costs. The middle range results from the individual variation from highest to lowest values for both performance characteristics and cost metrics, deviating around the median. Min/max range shows the risk and increases by increasing *IPC* while the middle range indicates the degree of dependence of each technology on their initial investment.

Table 21. Net present value (M€) for the participating EES facilities.

EES	median	middle range	min/max range
Pb-acid	134.26	-16.65÷292.35	-42.30÷302.61
Zn-air	364.55	300.255÷435.23	293.87÷436.29
Na-S	158.03	58.59÷259.37	48.43÷265.46
Li-ion	-651.49	-1354.37÷51.40	-1354.37÷51.40
VRB	47.49	-272.88÷367.86	-272.88÷367.86
Zn-Br	-53.72	-441.63÷334.19	-441.63÷334.19
PSB	-71.79	-461.43÷317.85	461.43÷317.85

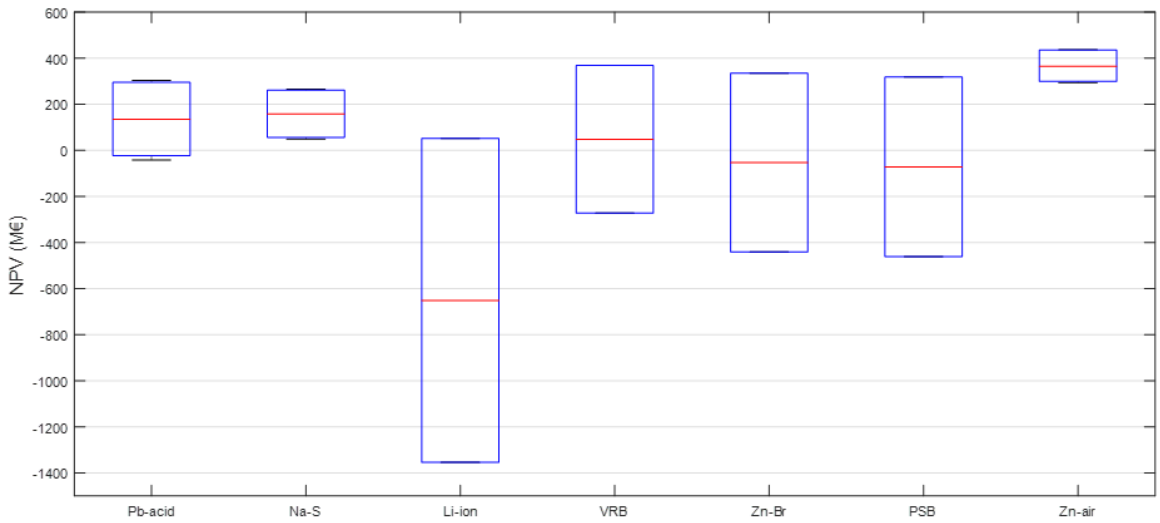

Figure 53. NPV for EES facilities participating in spinning reserve application.

8.6. Concluding Remarks

In this chapter, a methodology for the optimal planning of EES facilities involved in contingency-reserve applications has been presented. Based on a single-bus model the thermal generation of the power system of Cyprus has been optimally scheduled for the year 2017 without and with EES facilities. The UC optimization problem was conducted via a novel Lagrange Relaxation method with constraints and considering the impact of RES. The derived simulation results showed that improvements exist in profitable return credits when EES was integrated to retain energy storage for 5h. *TPC* is strongly affected by RES uncertainty and variability allowing different storage technologies to take place and enhance flexibility. Pb-acid, Zn-air, Na-S, Li-ion, VRB, Zn-Br and PSB batteries were selected to replace the deficit in spinning reserves and subjected to ablation analysis. The optimal size was determined to 143.94MW/498.94MWh based on the worst-case scenario. The ablation analysis performed on *NPV*, indicates that Zn-air offers the greatest potential in terms of performance and investment risk. Pb-acid and Na-S battery systems constitute feasible investments whereas Li-ion stands out of preferences since it possesses a negative mean value and is dominated by its still high capital cost. Finally, it is noted that the benefits derived from electricity storage would have increased, according to the availability of data regarding the emission cost, energy and reserve not served. This would allow an extension of the UC model to also incorporate these terms and enhance the profitable return reflected in security, reliability and emission avoidance cost.

9. Conclusions

This thesis has focused on advanced tools for enhancing the flexibility required by modern power systems. We have developed a novel approach based on Lagrange Relaxation framework for addressing the constrained unit commitment, considering the impact of renewable energy sources. The experimental evaluation of our approach showed that mathematical optimization principles can provide a persuasive and consistent mechanism for determining the appropriate generation schedules even for weak and isolated power networks. However, aiming to deal with future power needs in terms of system dimensionality and volatility, we have presented a radically innovative solution which is based on Bayesian optimization paradigm.

This approach relies on an effective Gaussian process algorithm enabling data-driven inference of the functional form of the underlying cost function, as well as the utilization of a state-of-the-art scheme for selecting the next function evaluation, namely an expected improvement-based acquisition function. This way, it possesses an effective means of alleviating the need of conventional methods to provide a parametric functional form for the optimized cost function. In addition, it provides the pathway for a solution that is intrinsically designed to converge in quite low number of function evaluations. We provided an experimental evaluation of our approach under a standard benchmark scenario, and we compared with three alternatives. As we observed, our proposed solution outperforms the alternatives in terms of the system costs, as well as the number of required function evaluations. These findings strongly corroborate our theoretical claims motivating this thesis.

The second topic of our study regarded the electricity storage. Developing a deep understanding of the various storage techniques and their performance characteristics, we performed both qualitative and quantitative assessments in order to adopt an appropriate methodology for selecting the best-fit candidates per application. All applications were modelled based on real-world requirements and preferences across the power system chain. To determine the best electricity storage technology, we deployed an algorithm capable of distinguishing the power-related and energy-related cost components. In this regard, a quick and useful metric for storage facility owners is provided, enabling the comparison between technologies that may possess different characteristics, such as response time, power rating,

suitable storage duration, round-trip efficiency, depth of discharge, self-discharge rate, cycling capability, lifespan times, capital and O&M costs, etc.

Finally, we have concluded this thesis by providing a comprehensive and consolidated demonstration of our integrated approach. The solution consists in finding both the optimal size of the intended EES facility and UC schedules based on actual annual data. The evolved formulation takes into account the variable renewable energy contribution, embedding a large number of real-world constraints regarding an isolated power network. The term of storage has been treated as an internal optimization task which its optimal sizing was found by balancing the benefits and cost. Identifying electrical energy storage as an approach enhancing the flexibility and reliability, we formulated and evaluated the selected facilities via a life-cycle cost analysis, based on the most realistic characteristics and cost metrics found in the literature. The derived simulation results showed that improvements exist in profitable return credits when storage was integrated.

9.1. PhD Thesis Contribution

The thesis introduced a number of contributions to the state of the art, focused on the operation of power systems, especially isolated systems, under high renewable penetration. Innovations were introduced in the solution to the unit commitment problem, in the electric energy storage systems assessment and in the use of electric energy storage to provide spinning reserve service to an isolated power system.

Regarding the unit commitment problem, the thesis presents two innovations: (a) the treatment of identical units in the framework of Lagrange Relaxation solution and (b) the development of a new, data driven, unit commitment solution method based on uncertainty aware machine learning, namely Bayesian optimization. Elaborating on mathematical optimization, we provide a novel approach that offers a high performance/low-cost unit commitment solution, retaining the ability to overcome non-convexity and non-linearity in the framework of Lagrange Relaxation. To account for the largely unaddressed challenge of the uncertain and volatile behavior of modern generation, we present a radically novel paradigm that is timely and highly relevant for the electric power industry in a decarbonized world. Our proposed approach is capable of processing the net load demand as an exogenous variable that must be satisfied, optimizing a stochastic function rather than a scalar objective. This way, it ensures exploration of global solutions to achieve optimality in contrast to

hourly, local estimations which, especially in the present of variable renewable generation, may lead to far away from optimal schedules.

Furthermore, the thesis provides a comprehensive assessment of electrical energy storage technologies competing in distinguished applications. This includes a thorough analysis of storage cost structure and life-cycle cost and an innovative multi-criteria decision method for the selection of the appropriate electricity storage system for a specific application, based on a ranking of the different technologies according to their characteristics. Finally, the integrated Lagrange Relaxation solution is combined with the life cycle cost analysis to determine the optimal sizing of electricity storage for spinning reserve provision in an isolated power system with high renewable penetration.

9.2. Future Directions

As for future directions for research, we indicate the consolidation of several consecutive hours into one stage. More extended works may also involve multi-bus formulations introducing the real power network losses and transmission constraints into the UC task. We strongly believe that by increasing the formulation complexity our novel approach might allow for even higher optimization performance. In addition, a more comprehensive UC formulation that accounts for the EES operation would be able to extract the full value of storage through the provision of multiple system services.

With the development of active power networks due to the intermittency of renewable energy and the randomness of the demand-side load, the operating uncertainty is becoming serious. At the same time, the means of controlling such networks are becoming more necessary to set the distributed generation as a decision variable, incentivise price-responsive prosumers and optimize the objectives of renewable generation utilization and user satisfaction. A wide variety of sustainable services and concepts are available to support the cooperation of flexible power sources and flexible loads, improving the predictability and manageability of various intermittent renewable energy sources. In this context, the optimal placement of electricity storage devices remains a robust challenge. New research directions may include formulations that take into account the geographical and topographical conditions. In combination with load demand and electricity-price forecasting in the presence of stochastic renewable generation, such models could provide optimal solutions regarding the expected equipment-upgrade deferral or network losses reduction.

References

[1] P. Nikolaidis and A. Poullikkas, “Sustainable Services to Enhance Flexibility in the Upcoming Smart Grids,” in *Sustaining Resources for Tomorrow*, 2020, pp. 245–274.

[2] R. a. Hites, “Persistent Organic Pollutants in the Great Lakes: An Overview,” *Handb. Environ. Chem.*, vol. 5, no. Part N, pp. 1–12, 2006.

[3] H. Guasch, A. Serra, N. Corcoll, B. Bonet, and M. Leira, “Metal Ecotoxicology in Fluvial Biofilms : Potential Influence of Water Scarcity,” *Hdb Env Chem*, no. October, pp. 41–53, 2010.

[4] T. N. Veziroğlu and S. Şahin, “21st Century’s energy: Hydrogen energy system,” *Energy Convers. Manag.*, vol. 49, no. 7, pp. 1820–1831, 2008.

[5] H. Lund, “Renewable energy strategies for sustainable development,” *Energy*, vol. 32, no. 6, pp. 912–919, 2007.

[6] P. Nikolaidis, “High Renewable Energy Integration through Optimal Unit Commitment and Electricity Storage in Weak Power Networks,” *Cyprus Univ. Technol.*, vol. Comprehens, no. November, pp. 1–61, 2017.

[7] A. Oberhofer and P. Meisen, “Energy Storage Technologies & Their Role in Renewable Integration,” *GENI Glob. Energy Inst.*, no. July, pp. 1–42, 2012.

[8] P. Poonpun and W. Jewell, “Analysis of the cost per kWh to store electricity,” *2008 IEEE Power Energy Soc. Gen. Meet. - Convers. Deliv. Electr. Energy 21st Century*, vol. 23, no. 2, pp. 529–534, 2008.

[9] Ecofys, “Energy Storage Opportunities and Challenges,” *Sustain. Energy Everyone*, vol. White Pape, pp. 1–61, 2014.

[10] B. Hodges and M. Sheriff, “Moving Energy Storage from Concept to Reality,” *Energy*, pp. 1–79, 2011.

[11] G. Allan, I. Eromenko, M. Gilmartin, I. Kockar, and P. McGregor, “The economics of distributed energy generation: A literature review,” *Renew. Sustain. Energy Rev.*, vol. 42, pp. 543–556, 2015.

[12] A. Poullikkas, “Sustainable options for electric vehicle technologies,” *Renew. Sustain. Energy Rev.*, vol. 41, pp. 1277–1287, 2015.

[13] E. Karden, S. Ploumen, B. Fricke, T. Miller, and K. Snyder, “Energy storage devices for future hybrid electric vehicles,” *J. Power Sources*, vol. 168, no. 1 SPEC. ISS., pp. 2–11, 2007.

[14] M. Farhoodnea, A. Mohamed, H. Shareef, and H. Zayandehroodi, “Power quality impacts of high-penetration electric vehicle stations and renewable energy-based generators on power distribution systems,” *Meas. J. Int. Meas. Confed.*, vol. 46, no. 8, pp. 2423–2434, 2013.

[15] X. Tan, Q. Li, and H. Wang, “Advances and trends of energy storage technology in Microgrid,” *Int. J. Electr. Power Energy Syst.*, vol. 44, no. 1, pp. 179–191, 2013.

[16] A. J. Wood, B. F. Wollenberg, and G. B. Sheblé, *POWER GENERATION, OPERATION, AND CONTROL*. New Jersey: John Wiley & Sons, 2014.

[17] D. Yang, W. Liao, Y. Wang, K. Zeng, and Q. Chen, “Data-Driven Optimization Control for Dynamic Reconfiguration of Distribution Network,” *Energies*, vol. 11, no. 10, p. 2628, 2018.

[18] A. I. Mahmutogullari, S. Ahmed, O. Cavus, and M. S. Akturk, “The Value of Multi-stage Stochastic Programming in Risk-averse Unit Commitment under Uncertainty,” *IEEE Trans. Power Syst.*, vol. PP, no. c, p. 1, 2018.

[19] Q. P. Zheng, J. Wang, and A. L. Liu, “Stochastic Optimization for Unit Commitment - A Review,” *IEEE Trans. Power Syst.*, vol. 30, no. 4, pp. 1913–1924, 2015.

[20] S. A. Kazarlis, A. G. Bakirtzis, and V. Petridis, “A genetic algorithm solution to the unit commitment problem,” *IEEE Trans. Power Syst.*, vol. 11, no. 1, pp. 83–92, 1996.

[21] G. B. Sheble and S. Member, “Altos, CA 94022,” *Electr. Eng.*, vol. 9, no. 1, pp. 128–135, 1994.

[22] N. P. Padhy, “Unit commitment - A bibliographical survey,” *IEEE Trans. Power Syst.*, vol. 19, no. 2, pp. 1196–1205, 2004.

[23] P. V. R. Krishna and S. Sao, “Price Based Unit Commitment Problem Under Deregulation,” *Int. J. Sci. Eng. Technol.*, vol. 184, no. 1, pp. 177–184, 2012.

[24] Y. G. Xie and H. D. Chiang, “A novel solution methodology for solving large-scale thermal unit commitment problems,” *Electr. Power Components Syst.*, vol. 38, no. 14, pp. 1615–1634, 2010.

[25] S. Patra, S. K. Goswami, and B. Goswami, “Differential evolution algorithm for solving unit commitment with ramp constraints,” *Electr. Power Components Syst.*, vol. 36, no. 8, pp. 771–787, 2008.

[26] M. Obi, S. M. Jensen, J. B. Ferris, and R. B. Bass, “Calculation of levelized costs of electricity for various electrical energy storage systems,” *Renew. Sustain. Energy Rev.*, vol. 67, pp. 908–920, 2017.

[27] X. Zhang, J. Xie, Z. Zhu, J. Zheng, H. Qiang, and H. Rong, “Smart grid cost-emission unit commitment via Co-evolutionary agents,” *Energies*, vol. 9, no. 10, pp. 1–13, 2016.

[28] C. Suazo-Martínez, E. Pereira-Bonvallet, and R. Palma-Behnke, “A simulation framework for optimal energy storage sizing,” *Energies*, vol. 7, no. 5, pp. 3033–3055, 2014.

[29] M. Tahanan, W. van Ackooij, A. Frangioni, and F. Lacalandra, “Large-scale Unit Commitment under uncertainty,” *4or*, vol. 13, no. 2, pp. 115–171, 2015.

[30] S. Y. Abujarad, M. W. Mustafa, and J. J. Jamian, “Recent approaches of unit commitment in the presence of intermittent renewable energy resources: A review,” *Renew. Sustain. Energy Rev.*, vol. 70, no. September 2016, pp. 215–223, 2017.

[31] S. Salam, “Unit Commitment Solution Methods,” *Eng. Technol.*, vol. 26, no. December, pp. 320–325, 2007.

[32] S. Y. Abujarad, M. W. Mustafa, and J. J. Jamian, “Recent approaches of unit commitment in the presence of intermittent renewable energy resources: A review,” *Renew. Sustain. Energy Rev.*, vol. 70, no. September 2016, pp. 215–223, 2017.

[33] T. Li and M. Shahidehpour, “Price-Based Unit Commitment : A Case of Lagrangian Constants :,” *IEEE Trans. Power Syst.*, vol. 20, no. 4, pp. 2015–2025, 2005.

[34] A. Rong, P. Luh, and R. Lahdelma, “Dynamic programming based algorithm for unit commitment of transmission constrained multi-site CHP systems,” *Proc. 2016 World Acad. Sci. Technol. Conf.*, vol. 10, no. 8, pp. 3180–3187, 2016.

[35] M. S. Nazir, F. D. Galiana, and A. Prieur, “Unit Commitment Incorporating Histogram Control of Electric Loads with Energy Storage,” *IEEE Trans. Power Syst.*, vol. 31, no. 4, pp. 2857–2866, 2016.

[36] H. Park, J. Lyu, Y. Kang, and J. Park, “Unit Commitment Considering Interruptible Load for Power System Operation with Wind Power,” *Energies*, vol. 7, no. 7, pp. 4281–4299, 2014.

[37] I. G. Marneris, P. N. Biskas, and A. G. Bakirtzis, “Stochastic and deterministic Unit Commitment considering uncertainty and variability reserves for high renewable integration,” *Energies*, vol. 10, no. 1, 2017.

[38] Z. Yang, K. Li, Q. Niu, and Y. Xue, “A comprehensive study of economic unit commitment of power systems integrating various renewable generations and plug-in electric vehicles,” *Energy Convers. Manag.*, vol. 132, pp. 460–481, 2017.

[39] H. S. Madraswala, “Modified genetic algorithm solution to unit commitment problem,” in *2017 International Conference on Nascent Technologies in Engineering, ICNTE 2017 - Proceedings*, 2017, no. 2, pp. 1–6.

[40] S. K. Garg, P. Konugurthi, and R. Buyya, “A linear programming-driven genetic algorithm for meta-scheduling on utility grids,” *Int. J. Parallel, Emergent Distrib. Syst.*, vol. 26, no. 6, pp. 493–517, 2011.

[41] W. Wang, C. Li, X. Liao, and H. Qin, “Study on unit commitment problem considering pumped storage and renewable energy via a novel binary artificial sheep algorithm,” *Appl. Energy*, vol. 187, pp. 612–626, 2017.

[42] F. A. C. C. Fontes, D. B. M. M. Fontes, and L. A. Roque, “An optimal control approach to the Unit Commitment problem,” *2012 IEEE 51st IEEE Conf. Decis. Control*, pp. 7069–7074, 2013.

[43] Z. Wang, M. Zoghi, D. Matheson, F. Hutter, and N. de Freitas, “Bayesian Optimization in a Billion Dimensions via Random Embeddings,” *J. Mach. Learn.*

Res., vol. 55, no. 1, pp. 361–387, 2012.

[44] O. Bousquet, U. von Luxburg, and G. Ratsch, *Advanced Lectures On Machine Learning: ML Summer Schools 2003, Canberra, Australia, February 2-14, 2003, Tubingen, Germany, August 4-16, 2003, Revised Lectures (Lecture Notes in Computer Science)*. Germany: Springer Berlin Heidelberg, 2004.

[45] P. Nikolaidis, S. Chatzis, and A. Poullikkas, "Optimal planning of electricity storage to minimize operating reserve requirements in an isolated island grid," *Energy Syst.*, no. 1, pp. 1–18, 2019.

[46] X. Feng and Y. Liao, "A new lagrangian multiplier update approach for lagrangian relaxation based unit commitment," *Electr. Power Components Syst.*, vol. 34, no. 8, pp. 857–866, 2006.

[47] P. Nikolaidis, S. Chatzis, and A. Poullikkas, "Renewable energy integration through optimal unit commitment and electricity storage in weak power networks," *Int. J. Sustain. Energy*, vol. 37, no. 10, pp. 1–17, 2018.

[48] P. Nikolaidis and A. Poullikkas, "Enhanced Lagrange Relaxation for the optimal unit commitment of identical generating units," *IET Gener. Transm. Distrib.*, vol. 1, no. 1, pp. 2–13, 2020.

[49] L. Acerbi and W. J. Ma, "Practical Bayesian Optimization for Model Fitting with Bayesian Adaptive Direct Search," *Adv. Neural Inf. Process. Syst.*, no. Nips, pp. 1–11, 2017.

[50] M. Rosenblatt, "A CENTRAL LIMIT THEOREM AND A STRONG MIXING CONDITION," in *Proceedings of the National Academy of Sciences of the United States of America*, 1956, vol. 42, no. 3, pp. 43–47.

[51] R. Salakhutdinov and G. Hinton, "Using Deep Belief Nets to Learn Covariance Kernels for Gaussian Processes," *Adv. Neural Inf. Process. Syst.*, no. Nips, pp. 1249–1256, 2008.

[52] A. D. Bull, "Convergence rates of efficient global optimization algorithms," *J. Mach. Learn. Res.*, vol. 12, pp. 2879–2904, 2011.

[53] E. Brochu, V. M. Cora, and N. de Freitas, "A Tutorial on Bayesian Optimization of

Expensive Cost Functions, with Application to Active User Modeling and Hierarchical Reinforcement Learning," *arXiv Prepr. arXiv1012.2599*, 2010.

[54] J. M. Hernández-Lobato, M. A. Gelbart, R. P. Adams, M. W. Hoffman, and Z. Ghahramani, "A General Framework for Constrained Bayesian Optimization using Information-based Search," *J. Mach. Learn. Res.*, vol. 17, pp. 5549–5601, 2015.

[55] M. A. Gelbart, J. Snoek, and R. P. Adams, "Bayesian Optimization with Unknown Constraints," *arXiv Prepr. arXiv1403.5607*, pp. 1–14, 2014.

[56] H. Quan, D. Srinivasan, A. M. Khambadkone, and A. Khosravi, "A computational framework for uncertainty integration in stochastic unit commitment with intermittent renewable energy sources," *Appl. Energy*, vol. 152, pp. 71–82, 2015.

[57] "Statistics and Machine Learning Toolbox ™ User ' s Guide R 2018 a How to Contact MathWorks." pp. 615–696, 2018.

[58] G. S. Georgiou, P. Nikolaidis, L. Lazari, and P. Christodoulides, "A Genetic Algorithm Driven Linear Programming for Battery Optimal Scheduling in nearly Zero Energy Buildings," in *2019 54th International Universities Power Engineering Conference (UPEC)*, 2019, pp. 1–6.

[59] F. Rahman, S. Rehman, and M. A. Abdul-Majeed, "Overview of energy storage systems for storing electricity from renewable energy sources in Saudi Arabia," *Renew. Sustain. Energy Rev.*, vol. 16, no. 1, pp. 274–283, 2012.

[60] M. Beaudin, H. Zareipour, A. Schellenberglabe, and W. Rosehart, "Energy storage for mitigating the variability of renewable electricity sources: An updated review 10.1016/j.esd.2010.09.007 : Energy for Sustainable Development | ScienceDirect.com," *Energy Sustain. Dev.*, vol. 14, no. 4, pp. 302–314, 2010.

[61] F. Díaz-González, A. Sumper, O. Gomis-Bellmunt, and R. Villafáfila-Robles, "A review of energy storage technologies for wind power applications," *Renew. Sustain. Energy Rev.*, vol. 16, no. 4, pp. 2154–2171, 2012.

[62] B. Ni and C. Sourkounis, "Control strategies for energy storage to smooth power fluctuations of wind parks," *Proc. Mediterr. Electrotech. Conf. - MELECON*, pp. 973–978, 2010.

[63] G. G. Soma, “Benefit assessment of energy storage for distribution network voltage regulation,” *CIRED 2012 Work. Integr. Renewables into Distrib. Grid. IET*, no. May, pp. 4–7, 2012.

[64] A. Lahyani, P. Venet, A. Guermazi, and A. Troudi, “Battery/Supercapacitors Combination in Uninterruptible Power Supply (UPS),” *IEEE Trans. Power Electron.*, vol. 28, no. 4, pp. 1509–1522, 2013.

[65] J. Baker, “New technology and possible advances in energy storage,” *Energy Policy*, vol. 36, no. 12, pp. 4368–4373, 2008.

[66] Teske Sven and oliver schäfer Sawyer Steve, *Energy [r]evolution*. greenpeace international, global wind energy Council solarPowereurope, 2015.

[67] P. Medina, A. W. Bizuayehu, J. P. S. Catalão, E. M. G. Rodrigues, and J. Contreras, “Electrical energy storage systems: Technologies’ state-of-the-art, techno-economic benefits and applications analysis,” *Proc. Annu. Hawaii Int. Conf. Syst. Sci.*, pp. 2295–2304, 2014.

[68] S. Sabihuddin, A. E. Kiprakis, and M. Mueller, “A numerical and graphical review of energy storage technologies,” *Energies*, vol. 8, no. 1, pp. 172–216, 2015.

[69] M. C. Argyrou, P. Christodoulides, and S. A. Kalogirou, “Energy storage for electricity generation and related processes: Technologies appraisal and grid scale applications,” *Renew. Sustain. Energy Rev.*, vol. 94, no. June, pp. 804–821, 2018.

[70] P. Nikolaidis and A. Poullikkas, “A comparative review of electrical energy storage systems for better sustainability,” *J. Power Technol.*, vol. 97, no. 3, pp. 220–245, 2017.

[71] R. M. Dell and D. A. J. Rand, “Energy storage, a key technology for global energy sustainability,” *J. Power Sources*, vol. 100, no. 1, pp. 2–17, 2001.

[72] P. Nikolaidis, “Transient behavior analysis of grounding grid in an installed photovoltaic park,” 2012.

[73] P. Nikolaidis, “Lightning protection of PV systems,” *Dep. Electr. Eng. Comput. Sci. Patrai*, 2012.

[74] P. Nikolaidis and A. Poullikkas, “Cost metrics of electrical energy storage technologies in potential power system operations,” *Sustain. Energy Technol. Assessments*, vol. 25, no. August 2017, pp. 43–59, 2018.

[75] J. P. Deane, B. P. Ó Gallachóir, and E. J. McKeogh, “Techno-economic review of existing and new pumped hydro energy storage plant,” *Renew. Sustain. Energy Rev.*, vol. 14, no. 4, pp. 1293–1302, 2010.

[76] J. K. Kaldellis, “Integrated electrification solution for autonomous electrical networks on the basis of RES and energy storage configurations,” *Energy Convers. Manag.*, vol. 49, no. 12, pp. 3708–3720, 2008.

[77] I. Hadjipaschalis, A. Poullikkas, and V. Efthimiou, “Overview of current and future energy storage technologies for electric power applications,” *Renew. Sustain. Energy Rev.*, vol. 13, no. 6–7, pp. 1513–1522, 2009.

[78] H. Chen, T. N. Cong, W. Yang, C. Tan, Y. Li, and Y. Ding, “Progress in electrical energy storage system: A critical review,” *Prog. Nat. Sci.*, vol. 19, no. 3, pp. 291–312, 2009.

[79] C. J. Yang and R. B. Jackson, “Opportunities and barriers to pumped-hydro energy storage in the United States,” *Renew. Sustain. Energy Rev.*, vol. 15, no. 1, pp. 839–844, 2011.

[80] “Capturing Grid Power 32,” no. august, pp. 32–41, 2009.

[81] B. Roberts, “Capturing grid power,” *IEEE Power Energy Mag.*, vol. 7, no. 4, pp. 32–41, 2009.

[82] A. I. Federal, “Executive Summary,” *IEC*, vol. White Pape, pp. 1–78, 1972.

[83] J. A. Suul, K. Uhlen, and T. Undeland, “Wind power integration in isolated grids enabled by variable speed pumped storage hydropower plant BT - 2008 IEEE International Conference on Sustainable Energy Technologies, ICSET 2008, November 24, 2008 - November 27, 2008,” pp. 399–404, 2008.

[84] J. Suul and K. Uhlen, “Variable speed pumped storage hydropower for integration of wind energy in isolated grids-case description and control strategies,” *Proc. NORPIE*, 2008.

[85] D. O. Akinyele and R. K. Rayudu, “Review of energy storage technologies for sustainable power networks,” *Sustain. Energy Technol. Assessments*, vol. 8, pp. 74–91, 2014.

[86] H. Lund and G. Salgi, “The role of compressed air energy storage (CAES) in future sustainable energy systems,” *Energy Convers. Manag.*, vol. 50, no. 5, pp. 1172–1179, 2009.

[87] H. Ibrahim, A. Ilinca, and J. Perron, “Energy storage systems-Characteristics and comparisons,” *Renew. Sustain. Energy Rev.*, vol. 12, no. 5, pp. 1221–1250, 2008.

[88] J. B. Greenblatt, S. Succar, D. C. Denkenberger, R. H. Williams, and R. H. Socolow, “Baseload wind energy: modeling the competition between gas turbines and compressed air energy storage for supplemental generation,” *Energy Policy*, vol. 35, no. 3, pp. 1474–1492, 2007.

[89] A. Cavallo, “Controllable and affordable utility-scale electricity from intermittent wind resources and compressed air energy storage (CAES),” *Energy*, vol. 32, no. 2, pp. 120–127, 2007.

[90] S. van der Linden, “Bulk energy storage potential in the USA, current developments and future prospects,” *Energy*, vol. 31, no. 15, pp. 3446–3457, 2006.

[91] X. Luo, J. Wang, M. Dooner, and J. Clarke, “Overview of current development in electrical energy storage technologies and the application potential in power system operation,” *Appl. Energy*, vol. 137, pp. 511–536, 2015.

[92] S. Zunft, C. Jakiel, M. Koller, and C. Bullough, “Adiabatic Compressed Air Energy Storage for the Grid Integration of Wind Power,” *Sixth Int. Work. Large-Scale Integr. Wind Power tTransmission Networks Offshore Wind.*, no. October, pp. 26–28, 2006.

[93] N. Hartmann, O. Vöhringer, C. Kruck, and L. Eltrop, “Simulation and analysis of different adiabatic Compressed Air Energy Storage plant configurations,” *Appl. Energy*, vol. 93, pp. 541–548, 2012.

[94] K. Bradbury, “Energy Storage Technology Review,” *A Br. Introd. to Batter.*, no. September, pp. 1–33, 2010.

[95] Y. M. Kim, J. H. Lee, S. J. Kim, and D. Favrat, “Potential and evolution of compressed air energy storage: Energy and exergy analyses,” *Entropy*, vol. 14, no. 8, pp. 1501–1521, 2012.

[96] C. Bullough *et al.*, “Advanced Adiabatic Compressed Air Energy Storage for the Integration of Wind Energy AA - CAES = Advanced Adiabatic - Compressed Air Energy Storage No fuel used / no CO 2 emissions at point of storage .,” *Proc. Eur. Wind energy Conf. EWEC*, vol. 22, no. November, pp. 1–8, 2012.

[97] R. P. Ag, “Adele–Adiabatic Compressed-Air Energy Storage for Electricity Supply,” *RWE Power AG, Essen/Koln*, pp. 953–956, 2010.

[98] D. J. Swider, “Compressed air energy storage in an electricity system with significant wind power generation,” *IEEE Trans. Energy Convers.*, vol. 22, no. 1, pp. 95–102, 2007.

[99] A. Goodwin and J. Derby, “Compressed air Batteries,” *Energ. Gr.*, pp. 2–4, 2011.

[100] J. J. Proczka, K. Muralidharan, D. Villela, J. H. Simmons, and G. Frantziskonis, “Guidelines for the pressure and efficient sizing of pressure vessels for compressed air energy storage,” *Energy Convers. Manag.*, vol. 65, pp. 597–605, 2013.

[101] S. M. Schoenung and W. Hassenzahl, “Characteristics and Technologies for Long- vs. Short-Term Energy Storage A Study by the DOE Energy Storage Systems Program SAND2001-0765,” *Sandia Natl. Lab. U.S. Dept. Energy*, no. March, p. 46 pp., 2001.

[102] P. J. Hall and E. J. Bain, “Energy-storage technologies and electricity generation,” *Energy Policy*, vol. 36, no. 12, pp. 4352–4355, 2008.

[103] R. G. Hull, J. R., Mulcahp, T. M., Uherka, K. L., Erck, R. A., & Abboud, “FLYWHEEL ENERGY STORAGE USING SUPERCONDUCTING MAGNETIC BEARINGS,” *Appl. Supercond.*, vol. 2, no. 7, pp. 449–455, 1995.

[104] A. A. K. Arani, H. Karami, G. B. Gharehpetian, and M. S. A. Hejazi, “Review of Flywheel Energy Storage Systems structures and applications in power systems and microgrids,” *Renew. Sustain. Energy Rev.*, vol. 69, no. September 2015, pp. 9–18, 2017.

[105] B. Bolund, H. Bernhoff, and M. Leijon, “Flywheel energy and power storage systems,” *Renew. Sustain. Energy Rev.*, vol. 11, no. 2, pp. 235–258, 2007.

[106] H. Liu and J. Jiang, “Flywheel energy storage-An upswing technology for energy sustainability,” *Energy Build.*, vol. 39, no. 5, pp. 599–604, 2007.

[107] I. Naxakis, P. Nikolaidis, and E. Pyrgioti, “Performance of an installed lightning protection system in a photovoltaic park,” in *2016 IEEE International Conference on High Voltage Engineering and Application (ICHVE)*, 2016, no. 2, pp. 2–5.

[108] M. H. WANG, “Application of Flywheel Energy Storage System to Enhance Transient Stability of Power Systems,” *Electr. Power Components Syst.*, vol. 33, no. 4, pp. 463–479, 2005.

[109] S. M. S. M. Lukic *et al.*, “Energy Storage Systems for Automotive Applications,” *Ind. Electron. IEEE Trans.*, vol. 55, no. 6, pp. 2258–2267, 2008.

[110] S. Vazquez, S. M. Lukic, E. Galvan, L. G. Franquelo, and J. M. Carrasco, “Energy Storage Systems for Transport and Grid Applications,” *IEEE Trans. Ind. Electron.*, vol. 57, no. 12, pp. 3881–3895, 2010.

[111] J. Cho, S. Jeong, and Y. Kim, “Commercial and research battery technologies for electrical energy storage applications,” *Prog. Energy Combust. Sci.*, vol. 48, pp. 84–101, 2015.

[112] K. C. Divya and J. Østergaard, “Battery energy storage technology for power systems-An overview,” *Electr. Power Syst. Res.*, vol. 79, no. 4, pp. 511–520, 2009.

[113] K. S. Ng, C. S. Moo, Y. C. Lin, and Y. C. Hsieh, “Investigation on intermittent discharging for lead-acid batteries,” *PESC Rec. - IEEE Annu. Power Electron. Spec. Conf.*, vol. 3839, no. October, pp. 4683–4688, 2008.

[114] A. Poullikkas, “A comparative overview of large-scale battery systems for electricity storage,” *Renew. Sustain. Energy Rev.*, vol. 27, pp. 778–788, 2013.

[115] Pavlos Nikolaidis and Andreas Poullikkas, “Secondary battery technologies: a static potential for power,” in *Energy Generation and Efficiency Technologies for Green Residential Buildings*, 2019, pp. 191–207.

[116] G. M. Ehrlich, *Lithium-Ion Batteries*. New York: McGraw-Hill, 2002.

[117] A. L. Salgado, A. M. O. Veloso, D. D. Pereira, G. S. Gontijo, A. Salum, and M. B. Mansur, "Recovery of zinc and manganese from spent alkaline batteries by liquid-liquid extraction with Cyanex 272," *J. Power Sources*, vol. 115, no. 2, pp. 367–373, 2003.

[118] W. H. Zhu, Y. Zhu, Z. Davis, and B. J. Tatarchuk, "Energy efficiency and capacity retention of Ni-MH batteries for storage applications," *Appl. Energy*, vol. 106, pp. 307–313, 2013.

[119] M. A. Fetcenko *et al.*, "Recent advances in NiMH battery technology," *J. Power Sources*, vol. 165, no. 2, pp. 544–551, 2007.

[120] A. K. Shukla, S. Venugopalan, and B. Hariprakash, "Nickel-based rechargeable batteries," *J. Power Sources*, vol. 100, no. 1–2, pp. 125–148, 2001.

[121] D. Larcher and J.-M. Tarascon, "Towards greener and more sustainable batteries for electrical energy storage.," *Nat. Chem.*, vol. 7, no. 1, pp. 19–29, 2015.

[122] B. L. Ellis and L. F. Nazar, "Sodium and sodium-ion energy storage batteries," *Curr. Opin. Solid State Mater. Sci.*, vol. 16, no. 4, pp. 168–177, 2012.

[123] S. J. Kazempour, M. P. Moghaddam, M. R. Haghifam, and G. R. Yousefi, "Electric energy storage systems in a market-based economy: Comparison of emerging and traditional technologies," *Renew. Energy*, vol. 34, no. 12, pp. 2630–2639, 2009.

[124] B. Scrosati and J. Garche, "Lithium batteries: Status, prospects and future," *J. Power Sources*, vol. 195, no. 9, pp. 2419–2430, 2010.

[125] J. G. Kim *et al.*, "A review of lithium and non-lithium based solid state batteries," *J. Power Sources*, vol. 282, pp. 299–322, 2015.

[126] I. Råde and B. A. Andersson, "Requirement for metals of electric vehicle batteries," *J. Power Sources*, vol. 93, no. 1–2, pp. 55–71, 2001.

[127] J. McDowall, P. Biensan, and M. Broussely, "Industrial lithium ion battery safety-What are the tradeoffs?," in *Telecommunications Energy Conference*, 2007, pp. 701–707.

[128] M. Skyllas-Kazacos, M. H. Chakrabarti, S. a. Hajimolana, F. S. Mjalli, and M. Saleem, “Progress in Flow Battery Research and Development,” *J. Electrochem. Soc.*, vol. 158, no. 8, p. R55, 2011.

[129] B. Dunn, H. Kamath, and J.-M. Tarascon, “Electrical Energy Storage for the Grid: A Battery of Choices,” *Science (80-.).*, vol. 334, no. 6058, pp. 928–935, 2011.

[130] M. DELUCHI, “Hydrogen vehicles: an evaluation of fuel storage, performance, safety, environmental impacts, and cost,” *Int. J. Hydrogen Energy*, vol. 14, no. 2, pp. 81–130, 1989.

[131] M. Momirlan and T. N. Veziroglu, “The properties of hydrogen as fuel tomorrow in sustainable energy system for a cleaner planet,” *Int. J. Hydrogen Energy*, vol. 30, no. 7, pp. 795–802, 2005.

[132] M. Momirlan and T. N. Veziroglu, “Current status of hydrogen energy,” *Renew. Sustain. Energy Rev.*, vol. 6, no. 1–2, pp. 141–179, 2002.

[133] P. Nikolaidis and A. Poullikkas, “A comparative overview of hydrogen production processes,” *Renew. Sustain. Energy Rev.*, vol. 67, pp. 597–611, 2017.

[134] S. Satyapal, J. Petrovic, C. Read, G. Thomas, and G. Ordaz, “The U.S. Department of Energy’s National Hydrogen Storage Project: Progress towards meeting hydrogen-powered vehicle requirements,” *Catal. Today*, vol. 120, no. 3-4 SPEC. ISS., pp. 246–256, 2007.

[135] D. K. Ross, “Hydrogen storage: The major technological barrier to the development of hydrogen fuel cell cars,” *Vacuum*, vol. 80, no. 10, pp. 1084–1089, 2006.

[136] S. G. Chalk and J. F. Miller, “Key challenges and recent progress in batteries, fuel cells, and hydrogen storage for clean energy systems,” *J. Power Sources*, vol. 159, no. 1 SPEC. ISS., pp. 73–80, 2006.

[137] J. D. Holladay, J. Hu, D. L. King, and Y. Wang, “An overview of hydrogen production technologies,” *Catal. Today*, vol. 139, no. 4, pp. 244–260, 2009.

[138] M. Ball and M. Wietschel, “The future of hydrogen - opportunities and challenges,” *Int. J. Hydrogen Energy*, vol. 34, no. 2, pp. 615–627, 2009.

[139] J. B. Goodenough, “Energy storage materials: A perspective,” *Energy Storage Mater.*, vol. 1, pp. 158–161, 2015.

[140] R. Shinnar, “The hydrogen economy, fuel cells, and electric cars,” *Technol. Soc.*, vol. 25, no. 4, pp. 455–476, 2003.

[141] J. Zheng, X. Liu, P. Xu, P. Liu, Y. Zhao, and J. Yang, “Development of high pressure gaseous hydrogen storage technologies,” *Int. J. Hydrogen Energy*, vol. 37, no. 1, pp. 1048–1057, 2012.

[142] ¨A.\ Züttel, “Materials for hydrogen storage,” *Mater. Today*, no. September, p. 24, 2003.

[143] B. Sakintuna, F. Lamari-Darkrim, and M. Hirscher, “Metal hydride materials for solid hydrogen storage: A review,” *Int. J. Hydrogen Energy*, vol. 32, no. 9, pp. 1121–1140, 2007.

[144] J. K. Kaldellis, D. Zafirakis, and K. Kavadias, “Techno-economic comparison of energy storage systems for island autonomous electrical networks,” *Renew. Sustain. Energy Rev.*, vol. 13, no. 2, pp. 378–392, 2009.

[145] A. Đukić and M. Firak, “Hydrogen production using alkaline electrolyzer and photovoltaic (PV) module,” *Int. J. Hydrogen Energy*, vol. 36, no. 13, pp. 7799–7806, 2011.

[146] A. Kashefi Kaviani, G. H. Riahy, and S. M. Kouhsari, “Optimal design of a reliable hydrogen-based stand-alone wind/PV generating system, considering component outages,” *Renew. Energy*, vol. 34, no. 11, pp. 2380–2390, 2009.

[147] M. J. Khan and M. T. Iqbal, “Analysis of a small wind-hydrogen stand-alone hybrid energy system,” *Appl. Energy*, vol. 86, no. 11, pp. 2429–2442, 2009.

[148] A. Khalilnejad and G. H. Riahy, “A hybrid wind-PV system performance investigation for the purpose of maximum hydrogen production and storage using advanced alkaline electrolyzer,” *Energy Convers. Manag.*, vol. 80, pp. 398–406, 2014.

[149] B. Panahandeh, J. Bard, A. Outzourhit, and D. Zejli, “Simulation of PV-wind-hybrid systems combined with hydrogen storage for rural electrification,” *Int. J. Hydrogen*

Energy, vol. 36, no. 6, pp. 4185–4197, 2011.

[150] M. ud din Mufti, S. A. Lone, S. J. Iqbal, M. Ahmad, and M. Ismail, "Super-capacitor based energy storage system for improved load frequency control," *Electr. Power Syst. Res.*, vol. 79, no. 1, pp. 226–233, 2009.

[151] D. Cericola, P. W. Ruch, R. Kötz, P. Novák, and A. Wokaun, "Simulation of a supercapacitor/Li-ion battery hybrid for pulsed applications," *J. Power Sources*, vol. 195, no. 9, pp. 2731–2736, 2010.

[152] A. Chu and P. Braatz, "Comparison of commercial supercapacitors and high-power lithium-ion batteries for power-assist applications in hybrid electric vehicles," *J. Power Sources*, vol. 112, no. 1, pp. 236–246, 2002.

[153] J. Cao, A. Emadi, and S. Member, "A New Battery / UltraCapacitor Hybrid Energy Storage System for Electric , Hybrid , and Plug-In Hybrid Electric Vehicles," *IEEE Trans. POWER Electron.*, vol. 27, no. 1, pp. 122–132, 2012.

[154] H. Gualous, D. Bouquain, A. Berthon, and J. M. Kauffmann, "Experimental study of supercapacitor serial resistance and capacitance variations with temperature," *J. Power Sources*, vol. 123, no. 1, pp. 86–93, 2003.

[155] N. C. Hoyt, J. S. Wainright, and R. F. Savinell, "Current Density Scaling in Electrochemical Flow Capacitors," *J. Electrochem. Soc.*, vol. 162, no. 6, pp. A1102–A1110, 2015.

[156] W. Buckles and W. V. Ilassenzahl, "Superconducting Magnetic Energy Storage," *IEEE Power Eng. Rev.*, no. November, pp. 16–29, 2000.

[157] Y. Mizuguchi *et al.*, "Novel BiS2 -based layered superconductor Bi4 O4 S3," *Preprint*, pp. 1–13, 2013.

[158] H. Hosono *et al.*, "Exploration of new superconductors and functional materials, and fabrication of superconducting tapes and wires of iron pnictides," *Sci. Technol. Adv. Mater.*, vol. 16, no. 3, p. 033503, 2015.

[159] P. Turner and L. Nottale, "A New Ab Initio Approach to the Development of High Temperature Superconducting Materials," *J. Supercond. Nov. Magn.*, 2016.

[160] J. Eyer and G. Corey, “Energy Storage for the Electricity Grid : Benefits and Market Potential Assessment Guide,” *Contract*, vol. 321, no. February, pp. 1–232, 2010.

[161] J. Zhu, M. Qiu, B. Wei, H. Zhang, X. Lai, and W. Yuan, “Design, dynamic simulation and construction of a hybrid HTS SMES (high-temperature superconducting magnetic energy storage systems) for Chinese power grid,” *Energy*, vol. 51, pp. 184–192, 2013.

[162] J. K. Kaldellis and D. Zafirakis, “Optimum energy storage techniques for the improvement of renewable energy sources-based electricity generation economic efficiency,” *Energy*, vol. 32, no. 12, pp. 2295–2305, 2007.

[163] Z. Yu, F. Haghighat, B. C. M. Fung, and H. Yoshino, “A decision tree method for building energy demand modeling,” *Energy Build.*, vol. 42, no. 10, pp. 1637–1646, 2010.

[164] G. K. F. Tso and K. K. W. Yau, “A study of domestic energy usage patterns in Hong Kong,” *Energy*, vol. 28, no. 15, pp. 1671–1682, 2003.

[165] Y. J. Zhang, C. Zhao, W. Tang, and S. H. Low, “Profit Maximizing Planning and Control of Battery Energy Storage Systems for Primary Frequency Control,” *IEEE Trans. Smart Grid*, vol. 3053, no. c, pp. 1–1, 2016.

[166] R. Latha, S. Palanivel, and J. Kanakaraj, “Frequency Control of Microgrid Based on Compressed Air Energy Storage System,” *Distrib. Gener. Altern. Energy J.*, vol. 27, no. 4, pp. 8–19, 2012.

[167] G. O. Suvire and P. E. Mercado, “DSTATCOM with Flywheel Energy Storage System for wind energy applications: Control design and simulation,” *Electr. Power Syst. Res.*, vol. 80, no. 3, pp. 345–353, 2010.

[168] C. Abbey and G. Joos, “Supercapacitor energy storage for wind energy applications,” *IEEE Trans. Ind. Appl.*, vol. 43, no. 3, pp. 769–776, 2007.

[169] D. Jovcic *et al.*, “High Voltage Direct Current Transmission : Converters, Systems, and DC Grids,” *CEUR Workshop Proc.*, vol. 1542, no. 3, pp. 33–36, 2011.

[170] P. F. Lyons *et al.*, “Design and analysis of electrical energy storage demonstration projects on UK distribution networks,” *Appl. Energy*, vol. 137, pp. 677–691, 2015.

[171] P. Modi, S. Singh, J. Sharma, and P. Pradhan, “Stability Improvement of Power System By Decentralized Energy,” *Electr. Eng.*, 2008.

[172] C. Ponce de León, A. Frías-Ferrer, J. González-García, D. A. Szánto, and F. C. Walsh, “Redox flow cells for energy conversion,” *J. Power Sources*, vol. 160, no. 1, pp. 716–732, 2006.

[173] G. K. F. Tso and K. K. W. Yau, “Predicting electricity energy consumption: A comparison of regression analysis, decision tree and neural networks,” *Energy*, vol. 32, no. 9, pp. 1761–1768, 2007.

[174] A. Azadeh, S. F. Ghaderi, S. Tarverdian, and M. Saberi, “Integration of artificial neural networks and genetic algorithm to predict electrical energy consumption,” *Appl. Math. Comput.*, vol. 186, no. 2, pp. 1731–1741, 2007.

[175] T. Kinjo, T. Senjyu, N. Urasaki, and H. Fujita, “Output levelling of renewable energy by electric double-layer capacitor applied for energy storage system,” *IEEE Trans. Energy Convers.*, vol. 21, no. 1, pp. 221–227, 2006.

[176] M. Korpaas, A. T. Holen, and R. Hildrum, “Operation and sizing of energy storage for wind power plants in a market system,” *Int. J. Electr. Power Energy Syst.*, vol. 25, no. 8, pp. 599–606, 2003.

[177] P. Denholm, E. Ela, B. Kirby, and M. Milligan, “The Role of Energy Storage with Renewable Electricity Generation,” *Contract*, vol. NREL/, no. January, pp. 1–53, 2010.

[178] Electric Power Research Institute, “Electricity Energy Storage Technology Options,” p. 170, 2010.

[179] D. J. Lee and L. Wang, “Small-signal stability analysis of an autonomous hybrid renewable energy power generation/energy storage system part I: Time-domain simulations,” *IEEE Trans. Energy Convers.*, vol. 23, no. 1, pp. 311–320, 2008.

[180] P. Mercier, R. Cherkaoui, and A. Oudalov, “Optimizing a battery energy storage system for frequency control application in an isolated power system,” *IEEE Trans. Power Syst.*, vol. 24, no. 3, pp. 1469–1477, 2009.

[181] B. Dursun and B. Alboyaci, “The contribution of wind-hydro pumped storage

systems in meeting Turkey's electric energy demand," *Renew. Sustain. Energy Rev.*, vol. 14, no. 7, pp. 1979–1988, 2010.

[182] J. Torreglosa, P. Garcia, L. Fernandez, and F. Jurado, "Predictive Control for the Energy Management of a Fuel Cell-Battery-Supercapacitor Tramway," *IEEE Trans. Ind. Informatics*, vol. 10, no. 1, pp. 1–1, 2013.

[183] S. Succar and R. Williams, "Princeton Environmental Institute PRINCETON UNIVERSITY Energy Systems Analysis Group Compressed Air Energy Storage : Theory , Resources , And Applications For Wind Power Acknowledgments," *Princet. Environ. Inst. Rep.*, vol. 8, no. April, p. 81, 2008.

[184] M. Klafki and E. S. K. Gmbh, "Status and Technical Challenges of Advanced Compressed Air Energy Storage (CAES) Technology Motivation for Large-Scale Energy Storage," *2009 Int. Work. Environ. Altern. Energy*, vol. Nov 10, pp. 1–8, 2009.

[185] W. J. Luo XI, "Overview of Current Development on Compressed Air Energy Storage," *Sch. Eng. Univ. Warwick*, vol. 3, no. 11, pp. 1–39, 2004.

[186] A. Kyriakopoulos, D. O. Sullivan, J. G. Hayes, J. Griffiths, and M. G. Egan, "Kinetic Energy Storage for High Reliability Power Supply Back-up," *APEC 07-Twenty-Second Annu. IEEE Appl. Power Electron. Conf. Expo.*, pp. 1158–1163, 2007.

[187] K. S. Gandhi, "Storage of Electrical Energy," *Indian Chem. Eng.*, vol. 52, no. 1, pp. 57–75, 2010.

[188] M. Kapsali and J. K. Kaldellis, "Combining hydro and variable wind power generation by means of pumped-storage under economically viable terms," *Appl. Energy*, vol. 87, no. 11, pp. 3475–3485, 2010.

[189] S. Papaefthimiou, E. Karamanou, S. Papathanassiou, and M. Papadopoulos, "Operating policies for wind-pumped storage hybrid power stations in island grids," *IET Renew. Power Gener.*, vol. 3, no. 3, p. 293, 2009.

[190] B. P. Roberts and S. Member, "Utility Energy Storage Applications," *Power Qual.*, vol. 11, no. 3, pp. 1–2, 2008.

[191] S. V. Papaefthymiou, E. G. Karamanou, S. A. Papathanassiou, and M. P. Papadopoulos, “A wind-hydro-pumped storage station leading to high RES penetration in the autonomous island system of Ikaria,” *IEEE Trans. Sustain. Energy*, vol. 1, no. 3, pp. 163–172, 2010.

[192] E. D. Castronuovo and J. A. P. Lopes, “Optimal operation and hydro storage sizing of a wind-hydro power plant,” *Int. J. Electr. Power Energy Syst.*, vol. 26, no. 10, pp. 771–778, 2004.

[193] A. I. N. Press, “Economics of electric energy storage for energy arbitrage and regulation in New York,” *Energy Policy*, vol. 35, pp. 2558–2568, 2007.

[194] J. S. Anagnostopoulos and D. E. Papantonis, “Simulation and size optimization of a pumped-storage power plant for the recovery of wind-farms rejected energy,” *Renew. Energy*, vol. 33, no. 7, pp. 1685–1694, 2008.

[195] D. Zafirakis and J. K. Kaldellis, “Economic evaluation of the dual mode CAES solution for increased wind energy contribution in autonomous island networks,” *Energy Policy*, vol. 37, no. 5, pp. 1958–1969, 2009.

[196] P. Denholm and R. Sioshansi, “The value of compressed air energy storage with wind in transmission-constrained electric power systems,” *Energy Policy*, vol. 37, no. 8, pp. 3149–3158, 2009.

[197] P. Denholm and R. M. Margolis, “Evaluating the limits of solar photovoltaics (PV) in electric power systems utilizing energy storage and other enabling technologies,” *Energy Policy*, vol. 35, no. 9, pp. 4424–4433, 2007.

[198] C. for E. S. Deloitte, “Electricity Storage Technologies , impacts , and prospects,” *Energy Solut.*, no. September, pp. 1–16, 2015.

[199] B. Nyamdash, E. Denny, and M. O’Malley, “The viability of balancing wind generation with large scale energy storage,” *Energy Policy*, vol. 38, no. 11, pp. 7200–7208, 2010.

[200] P. D. Brown, J. A. Peças Lopes, and M. A. Matos, “Optimization of pumped storage capacity in an isolated power system with large renewable penetration,” *IEEE Trans. Power Syst.*, vol. 23, no. 2, pp. 523–531, 2008.

[201] N. J. Schenk, H. C. Moll, J. Potting, and R. M. J. Benders, “Wind energy, electricity, and hydrogen in the Netherlands,” *Energy*, vol. 32, no. 10, pp. 1960–1971, 2007.

[202] C. Bueno and J. A. Carta, “Wind powered pumped hydro storage systems, a means of increasing the penetration of renewable energy in the Canary Islands,” *Renew. Sustain. Energy Rev.*, vol. 10, no. 4, pp. 312–340, 2006.

[203] A. O. Converse, “Seasonal Energy Storage in a Renewable Energy Sytsem,” *Proc. IEEE*, vol. 100, no. 2, 2012.

[204] M. Little, M. Thomson, and D. Infield, “Electrical integration of renewable energy into stand-alone power supplies incorporating hydrogen storage,” *Int. J. Hydrogen Energy*, vol. 32, no. 10–11, pp. 1582–1588, 2007.

[205] J. K. Kaldellis, M. Kapsali, and K. A. Kavadias, “Energy balance analysis of wind-based pumped hydro storage systems in remote island electrical networks,” *Appl. Energy*, vol. 87, no. 8, pp. 2427–2437, 2010.

[206] R. Amirante, E. Cassone, E. Distaso, and P. Tamburrano, “Overview on recent developments in energy storage: Mechanical, electrochemical and hydrogen technologies,” *Energy Convers. Manag.*, vol. 132, pp. 372–387, 2017.

[207] H. Zhao, Q. Wu, S. Hu, H. Xu, and C. N. Rasmussen, “Review of energy storage system for wind power integration support,” *Appl. Energy*, vol. 137, pp. 545–553, 2015.

[208] M. Daghi, M. Sedghi, A. Ahmadian, and M. Aliakbar-Golkar, “Factor analysis based optimal storage planning in active distribution network considering different battery technologies,” *Appl. Energy*, vol. 183, pp. 456–469, 2016.

[209] T. M. I. Mahlia, T. J. Saktisahdan, A. Jannifar, M. H. Hasan, and H. S. C. Matseelar, “A review of available methods and development on energy storage; Technology update,” *Renew. Sustain. Energy Rev.*, vol. 33, pp. 532–545, 2014.

[210] E. Hittinger, J. F. Whitacre, and J. Apt, “What properties of grid energy storage are most valuable?,” *J. Power Sources*, vol. 206, pp. 436–449, 2012.

[211] D. Zafirakis, K. J. Chalvatzis, G. Baiocchi, and G. Daskalakis, “The value of

arbitrage for energy storage: Evidence from European electricity markets," *Appl. Energy*, vol. 184, pp. 971–986, 2016.

[212] V. Jülch, "Comparison of electricity storage options using levelized cost of storage (LCOS) method," *Appl. Energy*, vol. 183, pp. 1594–1606, 2016.

[213] A. Berrada, K. Loudiyi, and I. Zorkani, "Valuation of energy storage in energy and regulation markets," *Energy*, vol. 115, pp. 1109–1118, 2016.

[214] M. S. Guney and Y. Tepe, "Classification and assessment of energy storage systems," *Renew. Sustain. Energy Rev.*, vol. 75, no. November 2016, pp. 1187–1197, 2017.

[215] D. Parra *et al.*, "An interdisciplinary review of energy storage for communities: Challenges and perspectives," *Renew. Sustain. Energy Rev.*, vol. 79, no. May 2016, pp. 730–749, 2017.

[216] P. Nikolaidis, S. Chatzis, and A. Poullikkas, "Renewable energy integration through optimal unit commitment and electricity storage in weak power networks," *Int. J. Sustain. Energy*, vol. 38, no. 4, pp. 398–414, 2018.

[217] P. Nikolaidis, S. Chatzis, and A. Poullikkas, "Life cycle cost analysis of electricity storage facilities in flexible power systems," *Int. J. Sustain. Energy*, vol. 6451, pp. 1–21, 2019.

[218] NREL, "Lifecycle Cost Analysis of Hydrogen Versus Other Technologies for Electrical Energy Storage," *Tech. Rep. NREL/TP-560-46719*, no. November, pp. 1–59, 2009.

[219] A. Joseph and M. Shahidehpour, "Battery storage systems in electric power systems," *2006 IEEE Power Eng. Soc. Gen. Meet.*, pp. 8--pp, 2006.

[220] S. M. Schoenung and W. V. Hassenzahl, "Long- vs . Short-Term Energy Storage Technologies Analysis," *Power Qual.*, vol. SAND2011-2, no. August, pp. 1–84, 2003.

[221] D. O. Akinyele and R. K. Rayudu, "Review of energy storage technologies for sustainable power networks," *Sustain. Energy Technol. Assessments*, vol. 8, pp. 74–91, 2014.

[222] K. Bradbury, L. Pratson, and D. Patiño-Echeverri, “Economic viability of energy storage systems based on price arbitrage potential in real-time U.S. electricity markets,” *Appl. Energy*, vol. 114, pp. 512–519, 2014.

[223] A. Dekka, R. Ghaffari, B. Venkatesh, and B. Wu, “A survey on energy storage technologies in power systems,” *2015 IEEE Electr. Power Energy Conf. Smarter Resilient Power Syst. EPEC 2015*, pp. 105–111, 2016.

[224] H. Kwon, J. K. Park, D. Kim, J. Yi, and H. Park, “A flexible ramping capacity model for generation scheduling with high levels of wind energy penetration,” *Energies*, vol. 9, no. 12, 2016.

[225] Y. Kuang *et al.*, “A review of renewable energy utilization in islands,” *Renew. Sustain. Energy Rev.*, vol. 59, pp. 504–513, 2016.

[226] R. Shirley and D. Kammen, “Renewable energy sector development in the Caribbean : Current trends and lessons from history,” *Energy Policy*, vol. 57, pp. 244–252, 2013.

[227] CERA, “ANNUAL REPORT OF CYPRUS ENERGY REGULATORY AUTHORITY www.cera.org.cy.” CERA, pp. 1–102, 2017.

[228] R. Dufo-López and J. L. Bernal-Agustín, “Techno-economic analysis of grid-connected battery storage,” *Energy Convers. Manag.*, vol. 91, pp. 394–404, 2015.

[229] C. A. Spanias, P. N. Nikolaidis, and I. Lestas, “Techno-Economic Analysis of the Potential Conversion of the Outdated Moni Power Plant to a Large Scale Research Facility,” in *5th International Conference on Renewable Energy Sources & Energy Efficiency*, 2016, pp. 208–220.